INVESTIGATING THE MECHANISMS OF CGRP-INDUCED VASORELAXATION IN RAT CORONARY ARTERIES

Lucy Anne Donovan

Keble College

University of Oxford

A thesis submitted for the degree of

Doctor of Philosophy

Trinity 2023

For my Dad

Abstract

It is vital that the heart is able to match blood distribution to the metabolic demands of the myocardium. This is achieved through the modulation of coronary artery tone, with the greatest changes in vascular resistance occurring in the microvasculature. Calcitonin gene-related peptide (CGRP) is the most potent endogenous vasodilator and has been shown to have cardioprotective effects. Despite this clinical relevance, the intracellular signalling pathways underlying CGRP-induced vasorelaxation and hyperpolarization in the coronary microvasculature have not been widely studied. This thesis aimed to further elucidate these signalling pathways in isolated rat coronary septal arteries using a combination of wire and pressure myography, electrophysiology, and immunohistochemistry. Following confirmation that CGRP was indeed a potent vasorelaxant in these vessels, the present investigation determined that there is a significant endothelium-dependent component to the CGRP response which relies primarily on nitric oxide (NO) synthesis and release. Further examination revealed that CGRP activates a Gβγ subunit-mediated pathway in both the endothelial cells (ECs) and vascular smooth muscle cells (VSMCs), rather than a Gαs subunit-mediated pathway as is widely reported in the literature. The present study is the first to study the effects of CGRP on vasorelaxation and hyperpolarization simultaneously in the coronary vasculature and demonstrated that stimulation with CGRP initiates hyperpolarization of the VSMCs. This suggests that NO acts to open EC and/or VSMC K^+ channels, including K_V7 channels. Finally, these investigations revealed that coronary resistance arteries do not receive sensory nerve innervation, but instead CGRP is stored in the vascular and endocardial ECs. This thesis, therefore, demonstrates that CGRP-induced vasorelaxation and hyperpolarization in the coronary microvasculature is endothelium-dependent and

offers a significant, novel mechanism by which blood flow is regulated in the heart. The present findings may have clinical implications for patients with coronary microvascular dysfunction and ischaemia and, as such, warrants future research to further consolidate the intracellular signalling pathways involved.

Acknowledgments

When I began my DPhil in 2018, I never anticipated quite how challenging yet rewarding this journey would be. I am immensely proud of everything I have learnt over the past 5 years, both as a scientist and as a person, and I have a lot of truly wonderful people to thank for this.

I would like to begin by expressing my deepest gratitude to the British Heart Foundation for funding my studentship. I am incredibly lucky to have been given this opportunity and I will forever be in their debt.

I could not have asked for better supervisors than Professor Kim Dora and Professor Christopher Garland. Since first visiting their lab in 2017, they have shown immeasurable generosity and brilliance, and I cannot thank them enough for their enthusiasm and encouragement at every step of the journey. Being a member of their research group has honestly been the opportunity of a lifetime.

Thank you to my colleagues, past and present: Hanson Ng, Katie Banecki, Lily Wallis, Dr JinHeng Lin, Dr Lauren Phillips, Dr Will Stockdale, Dr Hamish Lemmey, and Dr Lludmyla Borysova. Their guidance, solidarity, and humour made even the toughest days enjoyable. A special thank you to H for making me smile every day and whom I utterly adore.

I am beyond grateful to my friends who are, without a doubt, my greatest achievement. Selina and Sophie, whose friendship is the closest thing in my life to magic; Ollie and

Shona, who will remain lifelong friends; my Juxon housemates (Flavia, Yas, Clelia, Kadi, and Mev), for the laughter and the therapy; my friends from OUHC and Vincent's Club (they know who they are), being a part of these communities has been one of the best things to happen to me. My friends inspire me, they build me up and humble me in equal measure, and I am very fond of all of them.

Thank you to my family for always showing a genuine interest in my work, even though they have little idea what I'm talking about. I know they are proud of me and that means the world.

Finally, the most heartfelt thank you to my parents, Samantha and Simon Donovan. They have shown unwavering support throughout my education, but they have taught me what a book never could: perseverance, diligence, and optimism, without which I would never have succeeded. Although my Dad did not get to see this thesis completed, I know that he will be with me as I start my next adventure.

Publications

Wallis, L., Donovan, L., Johnston, A., Phillips, L. C., Lin, J., Garland, C. J., & Dora, K. A. (2023). Tracking endothelium-dependent NO release in pressurized arteries. Front Physiol, 14, 1108943.

Douglas, G., Mehta, V., Zen, A. A. H., Akoumianakis, I., Goel, A., Rashbrook, V. S., Trelfa, L., Donovan, L., Drydale, E., Chuaiphichai, S., Antoniades, C., Watkins, H., Kyriakou, T., Tzima, E., & Channon, K. M. (2019). A key role for the novel coronary artery disease gene JCAD in atherosclerosis via shear stress mechanotransduction. Cardiovascular Research. 116(11):1863-1874

Conference Communications

Donovan, L. Dora, K. A. Importance of nitric oxide in CGRP-induced vasorelaxation in rat coronary arteries. Oral presentation given at: CGRP 2022; 11-12 April 2022; virtual.

Donovan, L. Dora, K. A. Unravelling the intracellular signalling pathways in CGRP-induced vasorelaxation in rat coronary arteries. Oral presentation given at: BHF 4Y PhD Programme Student Conference; 29 June 2022; Leeds, UK.

Donovan, L. Dora, K. A. Unravelling the intracellular signalling pathways in CGRP-induced vasorelaxation in rat coronary arteries. Oral presentation given at: Europhysiology 2022; 16-18 September 2022, Copenhagen, Denmark.

Donovan, L. Garland, C. J., Dora, K. A. Unravelling the intracellular signalling pathways in CGRP-induced vasorelaxation in rat coronary arteries. Oral presentation given at: APSA-ASCEPT 2022; 29 November - 2 December 2022, Perth, Australia.

Donovan, L. Garland, C. J., Dora, K. A. Unravelling the intracellular signalling pathways in CGRP-induced vasorelaxation in rat coronary arteries. Selected for poster presentation at: American Physiology Summit; 20-23 April 2023; Long Beach, CA, USA.

Contents

Figures

Tables

Abbreviations

ACh	Acetylcholine
AM	Adrenomedullin
Akt	Phospholipase B
cAMP	Cyclic adenosine monophosphate
AMY	Amylin
ATP	Adenosine trisphosphate
BK_{Ca}	Large-conductance Ca^{2+}-activated K^{+} channels
CAD	Coronary artery disease
CFR	Coronary flow reserve
CGRP	Calcitonin gene-related peptide
CLR	Calcitonin-like receptor
CMVD	Coronary microvascular disease
CSX	Cardiac X syndrome
CT	Calcitonin
CTR	Calcitonin receptor
DMSO	Dimethyl sulfoxide
EC	Endothelial cell
EDH	Endothelium-dependent hyperpolarization
EDHF	Endothelium-dependent hyperpolarizing factor
EDRF	Endothelium-dependent relaxing factor
EEC	Endocardial endothelial cell
Em	Membrane potential

eNOS	Endothelial nitric oxide synthase
sGC	Soluble guanylate cyclase
cGMP	Cyclic guanosine monophosphate
GPCR	G protein-coupled receptor
HNO	Nitroxyl
IEL	Internal elastic lamina
IK_{Ca}	Intermediate-conductance Ca^{2+}-activated K^+ channels
IP_3	Inositol trisphosphate
IPA-NO	Isopropylamine NONOate
K_{ATP}	ATP-sensitive K^+ channel
K_{IR}	Inwardly rectifying K^+ channel
K_V	Voltage-gated K^+ channel
L-NAME	L-N^G-nitro arginine methyl ester
LAD	Left anterior descending
MEGJ	Myoendothelial gap junction
MEJ	Myoendothelial junction
NO	Nitric oxide
NOS	Nitric oxide synthase
NPY	Neuropeptide Y
PBS	Phosphate-buffered saline
PE	Phenylephrine
PGI_2	Prostacyclin
PKA	Protein kinase A
PLC	Phospholipase C
RAA	Right atrial appendage

RAMP	Receptor activity-modifying protein
RCP	Receptor component protein
RT-PCR	Reverse transcription polymerase chain reaction
SEM	Standard error mean
SK_{Ca}	Small-conductance Ca^{2+}-activated K^+ channels
SNAP	S-nitroso-*N*-acetyl-DL-penicillamine
SP	Substance P
TRP	Transient receptor potential
VSMC	Vascular smooth muscle cell

CHAPTER 1: INTRODUCTION

1.1 Properties of resistance vessels

Resistance vessels are small diameter arteries and arterioles (<~400 μm) that constitute the region of the vascular tree where the greatest changes in vascular resistance occur. In this way, they contribute significantly to the regulation of blood flow to tissues and organs. To ensure that blood supply matches the metabolic demands of the surrounding tissue, these arteries can dynamically adapt vascular resistance. This process is regulated by several intrinsic and extrinsic factors. It is understood that resistance vessels can contribute to the pathogenesis of many cardiovascular diseases; therefore, the signalling pathways underlying the regulation of vascular resistance have been studied extensively.

1.1.1 Structure of resistance arteries

Resistance arteries, like most blood vessels, consist of 3 histologically distinct layers: the *tunica intima*, the *tunica media*, and the *tunica adventitia* (Pugsley & Tabrizchi, 2000) (Figure 1.1.1). The *tunica intima* consists of a single layer of longitudinally arranged endothelial cells (ECs) which line the inside of the vessel. The *tunica media* surrounds the ECs and is comprised of multiple layers of vascular smooth muscle cells (VSMCs) and elastic fibres. The VSMCs are arranged in concentric rings, perpendicular to the ECs and direction of blood flow. Between the *tunica intima* and *tunica media* is the internal elastic lamina (IEL), a fenestrated sheet of elastin that forms a barrier between the two layers. Finally, the outer layer, the *tunica adventitia,* is primarily composed of the connective tissue, fibroblasts, and perivascular nerves. This layer provides support and structure to the vessel, but it may also influence vascular function (Gutterman, 1999).

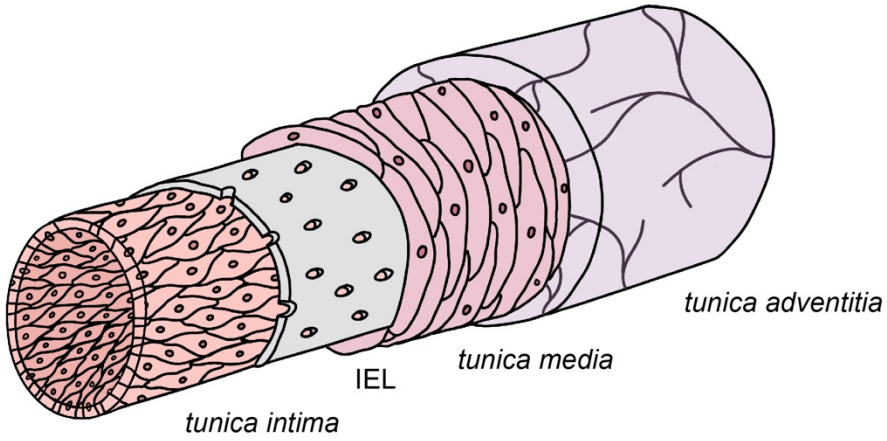

Figure 1.1.1 Structure of a resistance artery. The innermost layer, the *tunica intima*, consists of a layer of ECs arranged longitudinally. The internal elastic lamina (IEL) is a fenestrated sheet of elastin. The *tunica media* is formed from multiple layers of VSMCs arranged in concentric rings. The outermost layer, the *tunica adventitia*, is comprised of connective tissue, fibroblasts, and perivascular nerves.

1.1.2 Myoendothelial junctions

Resistance arteries regulate local blood flow, and this process requires complex communication between the endothelium and smooth muscle. Myoendothelial junctions (MEJs) have been implicated in the facilitation of bidirectional signalling between VSMCs and ECs (Straub et al., 2014). MEJs were first observed by Moore and Ruska (1956) in canine coronary arteries where electron microscopy images revealed projections from the endothelium that extended through the fenestrations of the IEL to make physical contact with the VSMCs. It is understood that myoendothelial gap junctions (MEGJs), located at the MEJs, provide the coupling mechanism that allows the transfer of electrical and chemical signals between the endothelium and smooth muscle (Dora et al., 1997; Emerson & Segal, 2000). Sandow and Hill (2000) demonstrated that MEGJs are more prevalent in smaller, distal rat mesenteric vessels compared to the larger, proximal vessels; this correlates with the relative importance of endothelium-dependent hyperpolarization (EDH) which confers a more significant contribution to vasorelaxation in small diameter arteries. As such, MEJs form a signalling microdomain that allows for heterocellular communication which is likely to play a critical role in the regulation of vascular resistance.

1.2 Regulation of coronary microvascular resistance

While the larger arteries in the heart are important for delivering the blood necessary for each beat, the microcirculation is where the greatest changes in vascular resistance occur; therefore, these vessels are ultimately responsible for regulating blood distribution in the heart. It is essential that the heart can match the local blood supply to the metabolic demands of the myocardium. For this to occur, coronary microvascular resistance must be constantly adapted through adjustments in the level of vascular tone. This process can be regulated by metabolic, myogenic, endothelial, and neurohumoral mechanisms.

1.2.1 Myogenic tone

The myogenic response was originally described by Bayliss (1902) as the observed vasoconstriction of a blood vessel in response to an increase in intraluminal pressure. This property is intrinsic to resistance arteries and allows them to respond dynamically to changes in blood pressure which helps limit blood flow and prevent damage to the capillary bed. Myogenic tone refers to the resting contractile state of the smooth muscle at a given pressure, which confers a diameter from which an artery can dilate and constrict in response to changes in intraluminal pressure or vasoactive mediators. This is important in determining the basal coronary vascular tone and coronary flow reserve (CFR). The precise mechanisms underlying the development of myogenic tone are still not fully understood, but it is known that the release of vasoactive factors from both the endothelium and nerves, as well as local metabolites, can increase or decrease the level of smooth muscle tone and thus alter vascular resistance.

The contractile activity is associated with VSMC depolarization, resulting from Ca^{2+} and Na^{2+} influx and Cl^- efflux, and the subsequent phosphorylation of Ca^{2+}-dependent myosin light chain which leads to the generation of tension (Brozovich et al., 2016; Davis & Hill, 1999; Meininger & Davis, 1992). The development of myogenic tone, but not the depolarization, can be prevented by L-type voltage-gated Ca^{2+} channel inhibition which indicates that these channels provide the main mechanism of Ca^{2+} entry (Potocnik et al., 2000). The exact mechanism by which the VSMCs sense changes in pressure, however, is yet to be elucidated. Transient receptor potential (TRP) channels have been implicated in the myogenic response, with several studies proposing that these channels may contribute to the ability of resistance arteries to detect changes in pressure (Sharif-Naeini et al., 2008). A study by Welsh et al. (2002) demonstrated that TRPC6 antisense-treatment inhibited vasoconstriction induced by increases in intravascular pressure in intact cerebral arteries by 70-80%. Interestingly, experiments conducted by Mederos y Schnitzler et al. (2008) indicated that TRPC6 channels are not mechanosensitive as they failed to activate ion channels in isolated inside-out membrane patches from TRPC6-expressing HEK293 cells when a pressure of -10 cm H_2O was applied. TRPC6-dependent ion currents were activated, however, when TRPC6 was co-expressed with the angiotensin 1 receptor (AT_1R) and these currents could be reduced by AT_1R inhibition with losartan. The same response was also seen when TRPC6 was co-expressed with a range of other $G_{q/11}$-coupled receptors, including the H_1 histamine receptor (H_1R) and muscarinic receptor (M_5R). Furthermore, losartan attenuated pressure-induced myogenic tone development in isolated cannulated rat cerebral arteries (Mederos y Schnitzler et al., 2008). It was concluded that TRPC6 receptors are not gated by membrane stretch themselves but are instead activated downstream from mechanical activation of $G_{q/11}$-coupled receptors. These findings support previous work in cardiomyocytes where it was

discovered that AT_1R can be activated independently of angiotensin by mechanical stress (Zou et al., 2004). Pharmacological inhibition and molecular suppression of P2Y4 and P2Y6 pyrimidine receptors, which are also $G_{q/11}$-coupled, were shown to diminish myogenic tone in cannulated, pressurised cerebral parenchymal arteries (Brayden et al., 2012). Further investigations into the role of the ion channels and G protein-coupled receptors (GPCRs) implicated in the myogenic response is critical for understanding this fundamental property of the microvasculature and may result in clinically relevant insights, especially as it likely that the precise mechanism differs between vascular beds.

1.2.2 Endothelial-dependent vasodilation

The endothelium was historically assumed to be an inert anti-coagulation barrier; however, the work by Furchgott and Zawadski (1980) revealed that it is in fact crucial to vascular function following the observation that intentional removal of the endothelium in rabbit thoracic aorta abolished ACh-induced vasorelaxation. The endothelium has a critical role in regulating vascular tone through the production of endothelium-derived relaxing factors (EDRFs), including nitric oxide (NO) and prostacyclin (PGI_2), and the generation of endothelium-dependent hyperpolarization (EDH).

In 1987, it was proposed by both Furchgott and Ignarro that NO may be the unknown signalling molecule, or EDRF, released from ECs (Ignarro et al., 1987; Moncada & Higgs, 2006). NO is synthesised in ECs by endothelial nitric oxide synthase (eNOS) from L-arginine and oxygen. eNOS can be activated by either Ca^{2+}-dependent or -independent pathways. On one hand, agonists, such as acetylcholine (ACh), can bind to G_q-coupled receptors on the EC plasma membrane, which initiates the phospholipase C (PLC)-inositol trisphosphate (IP_3) signalling pathway. This results in Ca^{2+} release from the

sarcoplasmic reticulum (SR) which binds to calmodulin, which in turn binds to eNOS and stimulates NO production. On the other hand, eNOS can be activated by phosphorylation through alternate signalling cascades by protein kinases, including protein kinase A (PKA) and B (Akt), independently from intracellular Ca^{2+} mobilisation (Fleming et al., 1997; Fulton et al., 1999). NO diffuses from the ECs into the VSMCs, resulting in soluble guanylate cyclase (sGC) activation and subsequent cyclic guanosine monophosphate (cGMP) synthesis. This activates protein kinase G (PKG) which, through phosphorylation of multiple targets, leads to vasorelaxation of the smooth muscle. The discovery that NO activates sGC was first reported by Murad, who observed that nitroglycerin caused cGMP formation by emitting NO (Arnold et al., 1977). This work, along with that of Furchgott and Ignarro, culminated in The Nobel Prize 1998 for identifying a new principle by which NO, a gas, acts as a signalling molecule in the cardiovascular system.

PGI_2 is produced in the endothelium by cyclooxygenase and is the primary metabolite of arachidonic acid. It is known to inhibit platelet aggregation and cause vasorelaxation (Moncada & Vane, 1979). Shimokawa et al. (1988) demonstrated PGI_2-induced vasorelaxation in isolated pig coronary arteries, which was attenuated when the endothelium was removed. PGI_2 exerts its vasorelaxant effects by binding to G_s-coupled receptors on the VSMCs, initiating the cyclic adenosine monophosphate (cAMP)-PKA pathway. It appears, however, that PGI_2 does not contribute significantly to endothelium-derived vasorelaxation, with Shimokawa et al. (1996) observing a negligible contribution to vasorelaxation in the rat aorta and both proximal and distal mesenteric arteries compared to NO and EDH.

NO production does not account for the entirety of endothelium-dependent vasorelaxation in resistance arteries. Bolton et al. (1984) provided the first evidence that endothelium-dependent vasorelaxation to carbachol in guinea-pig mesenteric arteries was accompanied by hyperpolarization of the VSMCs. When the endothelium of these vessels was removed, carbachol caused a modest depolarization rather than hyperpolarization, and vasorelaxation was abolished. This endothelium-dependent hyperpolarization (EDH) has since been observed in several vascular beds and is not affected by inhibition of NO- or PGI_2-induced vasorelaxation but can instead be attributed to the opening of K^+ channels (Chen et al., 1988; Waldron & Garland, 1994a). It is now understood that EDH is the result of an increase in EC intracellular Ca^{2+} activating Ca^{2+}-sensitive K^+ channels: IK_{Ca} and SK_{Ca} (Waldron & Garland, 1994b). The resulting K^+ efflux from the ECs acts as an EDH factor which hyperpolarizes VSMCs by activating smooth muscle inwardly rectifying K^+ (K_{IR}) and Na^+/K^+-ATPase channels (Edwards et al., 1998). Other diffusible factors that are released by the endothelium and initiate VSMC hyperpolarization have been proposed, including epoxyeicosatrienoic acids (EETs) and hydrogen peroxide (H_2O_2), but their role in EDH has been questioned (Luksha et al., 2009). The MEGJs have also been implicated in EDH, following the observation by Yamamoto et al. (1999) that ACh failed to produce hyperpolarization in the VSMCs if the gap junctions were blocked. In this way, the hyperpolarization generated in the ECs can also spread to adjacent VSMCs through MEGJs (Garland & Dora, 2017).

It has been suggested that the relative importance of EDRFs vary with vessel calibre, vascular bed, and species. In both rat and human arteries, it was demonstrated that the contribution of nitric oxide (NO) was greater in larger vessels, whereas the role of EDHF was more prominent in smaller vessels (Garland et al., 1995; Shimokawa et al., 1996;

Urakami-Harasawa et al., 1997). This observation is unsurprising since MEGJs are more abundant in smaller vessels (Sandow & Hill, 2000). The heterogenous contribution of NO in the coronary vascular bed was also observed by Jones et al. (1995) in canines *in vivo*, where NOS inhibition with L-NAME resulted in vasoconstriction of small arteries but vasorelaxation of arterioles. This indicates that vasorelaxation of small resistance arteries primarily relies on EDH in contrast with large arteries where NO confers the dominant effect; however, the clinical implications of this observation are yet to be confirmed.

1.2.3 Endothelial modulation of vascular tone

There is evidence that the endothelium also has intrinsic mechanisms that regulate the level of VSMC contraction, without needing direct stimulation from vasoactive substances. Garcia et al. (1997) was the first to investigate myogenic tone in rat coronary resistance arteries with isolated, pressurised septal arteries. These vessels developed spontaneous tone which increased following removal of the endothelium, indicating that the endothelium is actively modulating the level of myogenic tone under basal conditions. As discussed previously, MEGJs allow for bidirectional signalling via the transfer of current and small molecules, such as Ca^{2+} and IP_3 between the VSMCs and ECs. Dora et al. (1997) demonstrated in the hamster cheek pouch that the vasoconstrictors phenylephrine (PE) and KCl, which do not have a direct effect on the endothelium, caused an increase in EC intracellular Ca^{2+} alongside the expected increase in VSMC intracellular Ca^{2+}. It was proposed that Ca^{2+} may transfer from VSMCs to ECs via MEGJs. To further support this hypothesis, they showed that inhibition of NOS with L-NAME caused an increase in the level of vasoconstriction to PE and KCl. This finding suggested that the increase in EC intracellular Ca^{2+} initiates NO production and release from the endothelium, which limits vasoconstriction. This phenomenon is known as

myoendothelial feedback, whereby resistance arteries have an intrinsic regulatory feedback mechanism to limit vascular resistance (Lemmey et al., 2020).

1.2.4 Influence of perivascular nerves

Resistance arteries are innervated by perivascular nerves which can modulate vascular resistance through the local release of vasoactive substances. These nerves are primarily afferent sensory-motor C fibres and efferent sympathetic fibres. The cell bodies are found in the dorsal root ganglia and in the paravertebral sympathetic chains and other sympathetic ganglia, respectively. The perivascular nerves form a plexus around the arteries, the density of which is greater in smaller, resistance arteries compared to larger, conduit arteries, further emphasising a potential role in the regulation of vascular tone (Yokomizo et al., 2015).

The density of sympathetic nerve fibres is greater than sensory nerve fibres (Yokomizo et al., 2015). The neurotransmitters released by the sympathetic nerves typically cause vasoconstriction: noradrenaline (NA), which constricts mainly via α_1-adrenoceptors on VSMCs; adenosine 5'-triphosphate (ATP), which activates P2X and P2Y receptors on VSMCs; and neuropeptide Y (NPY), which activates Y_1 receptors on VSMCs (Aalkjaer et al., 2021). Some vessels also receive innervation from parasympathetic nerve fibres which release ACh, ATP, vasoactive intestinal peptide (VIP), and NO; however, parasympathetic innervation is largely absent in resistance arteries (Storkebaum & Carmeliet, 2011).

The sensory nerves are known to release calcitonin gene-related peptide (CGRP) (Brain et al., 1985; Rosenfeld et al., 1983) and substance P (SP) (Barja et al., 1983; Wharton et

al., 1986). A study by Kawasaki et al. (1988) demonstrated that electrical field stimulation of the isolated perfused rat mesenteric vascular bed, following sympathetic nerve inhibition, resulted in vasodilation. This vasodilation was abolished if the vessels were pre-treated with capsaicin, a transient receptor potential vanilloid 1 (TRPV1) agonist that depletes sensory nerves of CGRP and SP. The vasodilation to SP perfusion was minimal compared to that observed in response to CGRP, and immunohistochemistry revealed numerous CGRP-like immunoreactive nerve fibres but significantly fewer SP-like immunoreactive nerve fibres; therefore, it appears that CGRP release from sensory nerves may contribute to the regulation of vascular resistance.

1.2.5 Coronary microvascular dysfunction

In the past, clinical studies focused on larger, epicardial coronary arteries in patients with coronary artery disease (CAD) as these arteries are easier to visualise on angiograms and more accessible for therapeutic interventions. It is now widely understood that abnormalities in the structure and function of the coronary microvasculature, termed coronary microvasculature dysfunction (CMVD), may underlie several pathological conditions, and is associated with adverse clinical outcomes (Godo et al., 2021; Pries & Reglin, 2017). For example, almost half of patients with angina have non-obstructive coronary artery disease (ANOCA), which is associated with CMVD in two-thirds of cases (Perera et al., 2022; Sara et al., 2015). This is particularly prevalent in women; it has been suggested that approximately one-half of women with chest pain in the absence of obstructive CAD have CMVD (Reis et al., 2001). Despite the clinical need, our knowledge of the underlying pathophysiology is very limited and is likely to be heterogenous; therefore, furthering our understanding into the regulation of coronary

resistance arteries may provide us with vital insights into the pathogenesis of CMVD and future therapeutic strategies.

1.3 Calcitonin gene-related peptide

Following its discovery in the rat hypothalamus by Amara et al. (1982), the presence of CGRP was confirmed in both the central and peripheral nervous system (Rosenfeld et al., 1983). It is a member of the calcitonin (CT) family of peptides and acts through an atypical receptor. As a regulatory neuropeptide, it has numerous important biological effects in both health and disease.

1.3.1 CGRP synthesis and storage

α-CGRP is a 37-amino acid neuropeptide produced *via* alternative splicing of the *CALCA/CALC1* gene transcripts (Amara et al., 1982). CT can also be produced from the *CALCA* gene, but this predominantly occurs in the C cells of the thyroid gland or atrial cardiomyocytes (Moreira et al., 2020)(Figure 1.3.1). Another structurally similar isoform, β-CGRP, is encoded by a separate gene, *CALCB/CALC2* (Amara et al., 1985). Despite these two distinct isoforms sharing >90% homology and having similar biological roles, β-CGRP expression is largely concentrated in the enteric nervous system (Mulderry et al., 1988); therefore, the α-CGRP isoform is the primary focus in cardiovascular research and in this study.

Despite the *CALCA* gene being one of the earliest studied examples of alternative RNA processing, the mechanisms that determine this process are yet to be elucidated (Lou & Gagel, 1998). Furthermore, it is still unclear how CGRP synthesis is regulated within the nervous system. Donnerer and Stein (1992) used an *in vivo* unilateral paw inflammation model to demonstrate a significant increase in both CGRP content and axonal transport

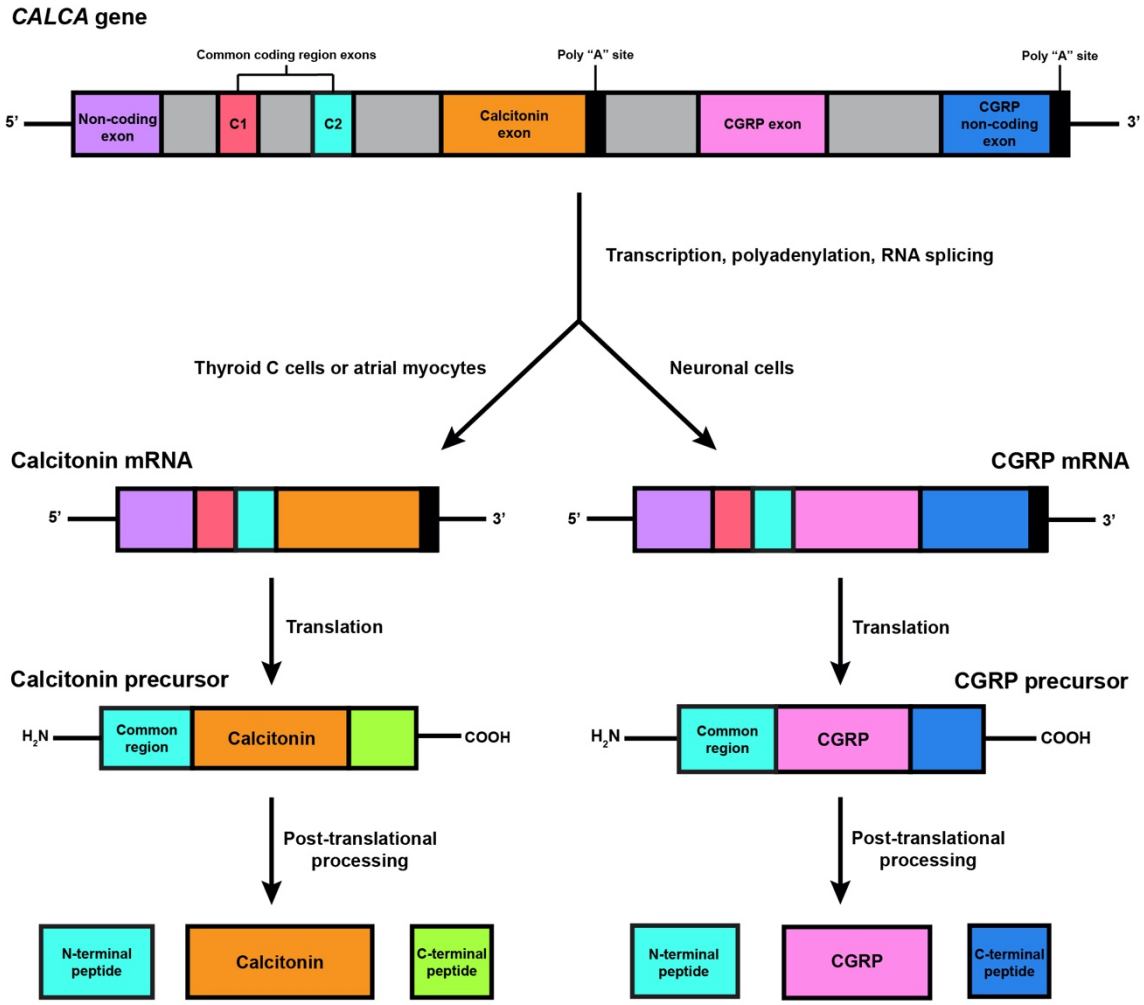

Figure 1.3.1 CGRP and CT synthesis from the *CALCA* gene. The *CALCA* gene undergoes alternative splicing to produce CT, in thyroid cells or atrial myocytes, or CGRP in neuronal cells.

in the sciatic nerve innervating the inflamed paw compared to the contralateral side, alongside increased CGRP content in the dorsal root ganglia. Other studies have reported that nerve growth factor (NGF) can stimulate an increase in CGRP mRNA and protein expression in the dorsal root ganglia of spontaneously hypertensive rats (SHR) (Supowit et al., 2001).

CGRP is distributed throughout the central and peripheral nervous system but is predominantly localised to sensory neurons, primarily unmyelinated C fibres or thinly myelinated Aδ fibres, where it is often colocalised with SP (Gibbins et al., 1985). The discovery that CGRP was contained in the perivascular nerves innervating blood vessels was particularly notable, as it provided a link between the peptide and the cardiovascular system. CGRP localisation in the perivascular nerves has been demonstrated in several vascular beds, including coronary (Gulbenkian et al., 1993; Lundberg et al., 1985; Wharton et al., 1988), mesenteric (De Mey et al., 2008a; Kawasaki et al., 1988; Le et al., 2020), and cerebral (Uddman et al., 1985; Uddman et al., 1986) It has also been shown to be circulating in the plasma of healthy human subjects, but plasma levels are in the low picomolar range (Girgis et al., 1985). Evidence has also emerged that implicates other non-neuronal sources of CGRP. CGRP expression has been detected in the ECs of rat carotid body, femoral, and mesenteric arteries, the thoracic aorta, and cultured human umbilical vein ECs (HUVECs) (Cai et al., 1993; Doi et al., 2001; Ozaka et al., 1997; Ye et al., 2007). Using light and immunoelectron microscopy, both Ozaka et al. (1997) and Doi et al. (2001) were able to visualise CGRP in the rough endoplasmic reticulum (rER) and Weibel-Palade bodies within ECs, and the latter study was also able to detect prepro-CGRP mRNA. Together, these findings indicate that CGRP can be both synthesised and stored in the ECs. Furthermore, CGRP expression has been reported in adipocytes,

keratinocytes, and certain immune cells, including B-lymphocytes and macrophages (Russell et al., 2014).

1.3.2 CGRP release

Following its synthesis, CGRP is stored in the sensory nerve terminals within large dense-core vesicles (Matteoli et al., 1988), which can be released following depolarization via Ca^{2+}-dependent exocytosis. A study by Zaidi et al. (1985) was the first to demonstrate CGRP release from perivascular nerves where depolarization of the nerve terminals with capsaicin, a TRPV1 agonist, caused a 15-fold increase in CGRP plasma levels. The release of CGRP following TRPV1 activation has since been reported extensively, using either capsaicin (Franco-Cereceda et al., 1987b; Franco-Cereceda et al., 1989; Luo et al., 2008; Varela-Lopez et al., 2021; Wharton et al., 1986) or other TRPV1 activators, including heat stress (Luo et al., 2008; Ye et al., 2007), low pH (Geppetti et al., 1991), and anandamide (Zygmunt et al., 1999). On the other hand, Kawasaki et al. (1998) proposed that angiotensin (ANG) can attenuate CGRP release from perivascular nerves after showing that N-acetyltetradecapeptide renin substrate, ANGI, and ANGII inhibited CGRP-induced vasodilation in the perfused mesenteric vascular bed. This effect could be reversed with the ANGII receptor (AT) inhibitor [Sar^1, Ile^8]AngII, but they did not differentiate between AT1 and AT2 receptor subtypes. AngII modulation of CGRP release was only observed in SHR and not in wild-type rats, indicating that CGRP release may be disrupted in disease. As such, further research into the precise mechanisms of CGRP release in both physiological and pathophysiological conditions are necessary.

1.3.3 CGRP metabolism

A study investigated the pharmacokinetics of CGRP in humans by continuously infusing CGRP into the cubital vein of one arm for 105 minutes, and taking blood samples at regular time intervals before, during, and after CGRP infusion from the other arm (Kraenzlin et al., 1985). It was calculated that the plasma half-life of CGRP is 6.9 minutes and 26.4 minutes for the first phase and slow decay phase, respectively. Despite this short half-life, there is a lack of thorough evidence regarding the metabolism of CGRP following its release, but several removal mechanisms have been proposed. The work by Katayama et al. (1991) supported a shared removal mechanism for both CGRP and SP by demonstrating (using high-performance liquid chromatography, HPLC) that neutral endopeptidase (NEP) cleaved both proteins. It was observed that CGRP was cleaved approximately 88-fold slower than SP, with 80% of CGRP being degraded after 2 hours. This suggests that NEP only confers a weak physiological effect on CGRP; however, it could still have a role in modulating CGRP activity, especially as NEP has been shown to be present in rat mesenteric ECs (Tamburini et al., 1989). Endothelin-converting enzyme-1 (ECE-1), present in early endosomes, has also been implicated in the degradation of CGRP. Padilla et al. (2007) observed in human embryonic kidney (HEK) cells expressing CLR-RAMP1 complexes that, following incubation with CGRP, CGRP was trafficked to early endosomes where it co-localised with ECE-1. Using HPLC, it was then demonstrated that ECE-1 degraded CGRP into fragments that were unable to rebind CLR-RAMP1. Finally, there has also been evidence published by Sams-Nielsen et al. (2001) suggesting that CGRP reuptake may occur at perivascular nerve terminals. Repeated administration of capsaicin to the guinea-pig basilar artery 3 times in a row resulted in a successive and significantly reduced vasodilation response each time, indicating CGRP depletion from the sensory nerves. After the third capsaicin challenge,

the CGRP-depleted arteries were incubated with 100 nM CGRP. This led to a significant reappearance of the vasodilatory response to the subsequent fourth capsaicin challenge, indicating that the nerve terminals were reloaded with the exogenous CGRP. This rescue of capsaicin-induced vasodilation with exogenous CGRP incubation was not observed when CGRP 8-37 was present during the CGRP incubation period. It was thus concluded that presynaptic CGRP receptors may play a role in CGRP reuptake into perivascular nerve terminals. Further investigation into the mechanisms of CGRP degradation and reuptake may lead to novel therapeutic targets to either increase or reduce the biological activity of CGRP.

1.4 Calcitonin family of peptides and their receptors

CGRP belongs to the calcitonin family of peptides: calcitonin (CT), α-CGRP, β-CGRP, adrenomedullin (AM), adrenomedullin 2 (AM_2, or intermedin), and amylin (AMY). These 6 peptides are all expressed in humans, rats, and mice. Apart from α-CGRP and β-CGRP, the CT family of peptides have limited sequence homology but are instead structurally related through the possession of a disulphide-bonded N terminus, which has α-helical tendencies, and a C-terminus with a β-turn and C-terminal amide (Hay et al., 2018). These peptides vary in their sites of production and expression, as well as their biological actions, which is summarised in Table 1.4.1.

1.4.1 Pharmacology

There are 2 GPCRs for the CT family of peptides: the CT receptor (CTR) and the CT receptor-like receptor (CLR). These are both class B GPCRs; the C-terminus of the peptide binds to the extracellular domain of the receptor and the N-terminus of the peptide binds to the transmembrane domain of the receptor, termed the two-domain model (Hay et al., 2018). CTR and CLR associate with receptor activity-modifying proteins (RAMPs) to form 7 distinct functional receptors. There are 3 RAMPs, each with an extracellular N-terminus, cytoplasmic C-terminus, and a single transmembrane domain. McLatchie et al. (1998) was the first to discover that RAMPs determine the specificity of CLR using *Xenopus* oocytes, and that RAMPs are required to transport CLR to the plasma membrane. It is now known that CLR associated with RAMP1, RAMP2, and RAMP3 forms CGRP, AM, and AM_2 receptors, respectively (McLatchie et al., 1998). The CT receptor can be expressed alone to bind calcitonin, but

Table 1.4.1: Summary of expression and biological actions of the calcitonin family of peptides

Peptide	Localisation	Function	References
Calcitonin	Thyroid C cells	Reduce plasma Ca^{2+}, promote bone formation	Hay et al. (2018)
α-CGRP	Central and peripheral nervous system, primarily sensory neurons	Vasodilator, nociception	Hay et al. (2018)
β-CGRP	Enteric nervous system, pituitary gland, immune cells	Vasodilator, nociception	Russell et al. (2014)
Adrenomedullin	Widespread expression, e.g.: vascular ECs	Vasodilator, maintains vascular integrity	Kita and Kitamura (2022)
Adrenomedullin 2/Intermedin	Widespread expression, e.g.: vascular ECs	Vasodilator (peripherally), increases sympathetic activity (centrally), increases prolactin release	Hong et al. (2012)
Amylin	Pancreatic β-cells	Suppresses glucagon release, reduces food intake and gastric emptying	Hay et al. (2015)

it can also associate with the same RAMPs to form AMY_1, AMY_2, and AMY_3 receptors, respectively (Rees et al., 2022) (Figure 1.4.1). The CLR receptor heterodimers also interact with another intracellular accessory protein, the receptor component protein (RCP). Evans et al. (2000) established the role for RCP by performing experiments on control or RCP-antisense NIH3T3 cells, which express CGRP receptors. It was revealed that neither CGRP receptor density nor affinity was altered by diminished RCP expression, but CGRP-induced cAMP responses were significantly reduced. The interaction between CLR and RCP was also confirmed *in vivo* using guinea-pig cerebellum, where the two proteins co-immunoprecipitated. Together, these findings indicate that RCP is not a chaperone protein like the RAMPs, but instead directly interacts to CLR to couple the receptor to intracellular signal transduction pathways.

1.4.2 CGRP receptor heterogeneity

Historically, it was believed that there were 2 CGRP receptor subtypes: the CGRP1 and CGRP2 receptor. The heterogeneity in CGRP receptors was proposed by Dennis et al. (1989) following the observation that the CGRP antagonist, CGRP 12-37, inhibited the inotropic and chronotropic actions of CGRP in guinea-pig atria but did not antagonise CGRP-induced inhibition of the twitch response in isolated rat vas deferens. On the other hand, the rat vas deferens was more sensitive to the CGRP agonist, $Cys(ACM)^{2,7}$-hαCGRP than the guinea-pig atria, suggesting that these tissues display different CGRP receptor subtypes. For several years, studies using CGRP receptor antagonists appeared to support CGRP receptor heterogeneity (Poyner et al., 2002). A later study by Hay et al. (2005), where cells were transfected with the CT receptor alone or in combination with different RAMPs, revealed that the AMY_1 receptor may be activated by CGRP. This finding, along with other investigations that confirmed CGRP could act at the receptors

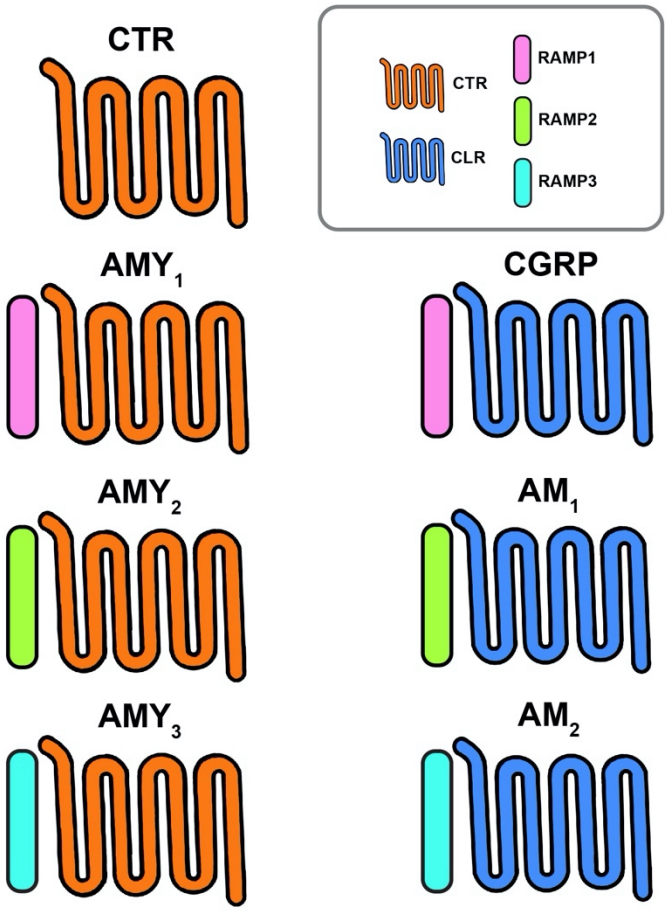

Figure 1.4.1 Components of the CT family of receptors. CTR can be expressed alone to bind CT, or it can associate with RAMP1, RAMP2, or RAMP3 to form AMY_1, AMY_2, and AMY_3 receptors, respectively. CLR associated with RAMP1, RAMP2, and RAMP3 forms CGRP, AM, and AM_2 receptors, respectively.

of the other peptides in the CT family when applied pharmacologically, led to the existence of the CGRP2 receptor being rebutted (Hay et al., 2008). As such, the complex nature of the CT peptide family pharmacology must be taken into consideration to ensure specificity of agonists and antagonists, and that observed responses to an exogenously administered peptide are being attributed to the correct receptor.

1.5 Vascular effects of CGRP

Fisher et al. (1983) was the first to report that systemically administered CGRP had hypotensive effects in rats. It was later identified as a vasodilator in a seminal study by Brain et al. (1985), where it was observed that CGRP induced vasodilation of microvessels in rabbit skin, human skin, and the hamster cheek pouch *in vivo* as well as causing vasorelaxation of rat aortic strips *in vitro*. These responses were seen at femtomolar concentrations of CGRP, making it the most potent endogenous vasodilator. CGRP has also been shown to have positive inotropic and chronotropic effects (Franco-Cereceda et al., 1987a; Gennari et al., 1990), further establishing a significant role for the peptide in the cardiovascular system.

1.5.1 CGRP receptor expression

Several studies have confirmed the presence of mRNA for the CGRP receptor components, CLR and RAMP1, in different vascular beds including rat mesenteric (Le et al., 2020), human left anterior descending (LAD) coronary (Hasbak et al., 2003b), rat pulmonary (Qing et al., 2001), and human cerebral (Sams et al., 2000). Immunohistochemical studies have confirmed the expression of CLR and RAMP1 protein in both the VSMCs and ECs of the rat and murine mesenteric arteries (Boerman & Segal, 2016; Sheykhzade et al., 2017) and human epicardial and intramyocardial coronary arteries (Chan et al., 2010; Hagner et al., 2001), but in rat middle cerebral arteries protein expression has only been detected in the VSMCs (Erdling et al., 2017). While CGRP receptor expression appears to be widespread throughout the vascular system, there is likely to be heterogeneity in expression depending on vascular bed and vessel calibre.

1.5.2 CGRP signalling in vascular smooth muscle cells

The consensus in the literature is that CGRP receptors are Gαs-coupled; their activation stimulates adenylate cyclase, resulting in cAMP accumulation and the subsequent activation of PKA (Aiyar et al., 1999; Edvinsson et al., 1985; Gray & Marshall, 1992a; Kubota et al., 1985). PKA phosphorylates several downstream targets resulting in, for example: reduced intracellular Ca^{2+}, a decreased affinity of myosin light chain kinase for Ca^{2+}-calmodulin, and the opening of K^+ channels (Argunhan & Brain, 2022; Sohn et al., 2020). In this way, CGRP causes relaxation and hyperpolarization of the smooth muscle and, ultimately, vasodilation (Figure 1.5.1). In particular, K_{ATP} channels have been implicated in CGRP-induced vasodilation (Kitazono et al., 1993; Nelson et al., 1990b; Wellman et al., 1998), although other studies have suggested a role for K_{Ca} channels (Sheykhzade & Berg Nyborg, 2001) and K_V7 channels (Chadha et al., 2014; Stott et al., 2018). More recently, studies have reported that the Gβγ subunit may contribute to CGRP-induced vasodilation (Meens et al., 2012; Stott et al., 2018), but the precise signalling pathway is yet to be elucidated.

1.5.3 CGRP signalling in the vascular endothelial cells

It is widely believed that CGRP also activates the Gαs-mediated cAMP-PKA pathway in the ECs, with CGRP-induced adenylate cyclase production being observed in bovine aortic endothelial cells (BAECs) (Crossman et al., 1990; Russell et al., 2014). There is substantial evidence indicating that CGRP causes NO production (Argunhan & Brain, 2022), although direct measurements of NO generation in response to CGRP are challenging in intact arteries. Instead, several studies have demonstrated that endothelium removal or NO inhibition attenuates CGRP-induced vasodilation, including rat aorta

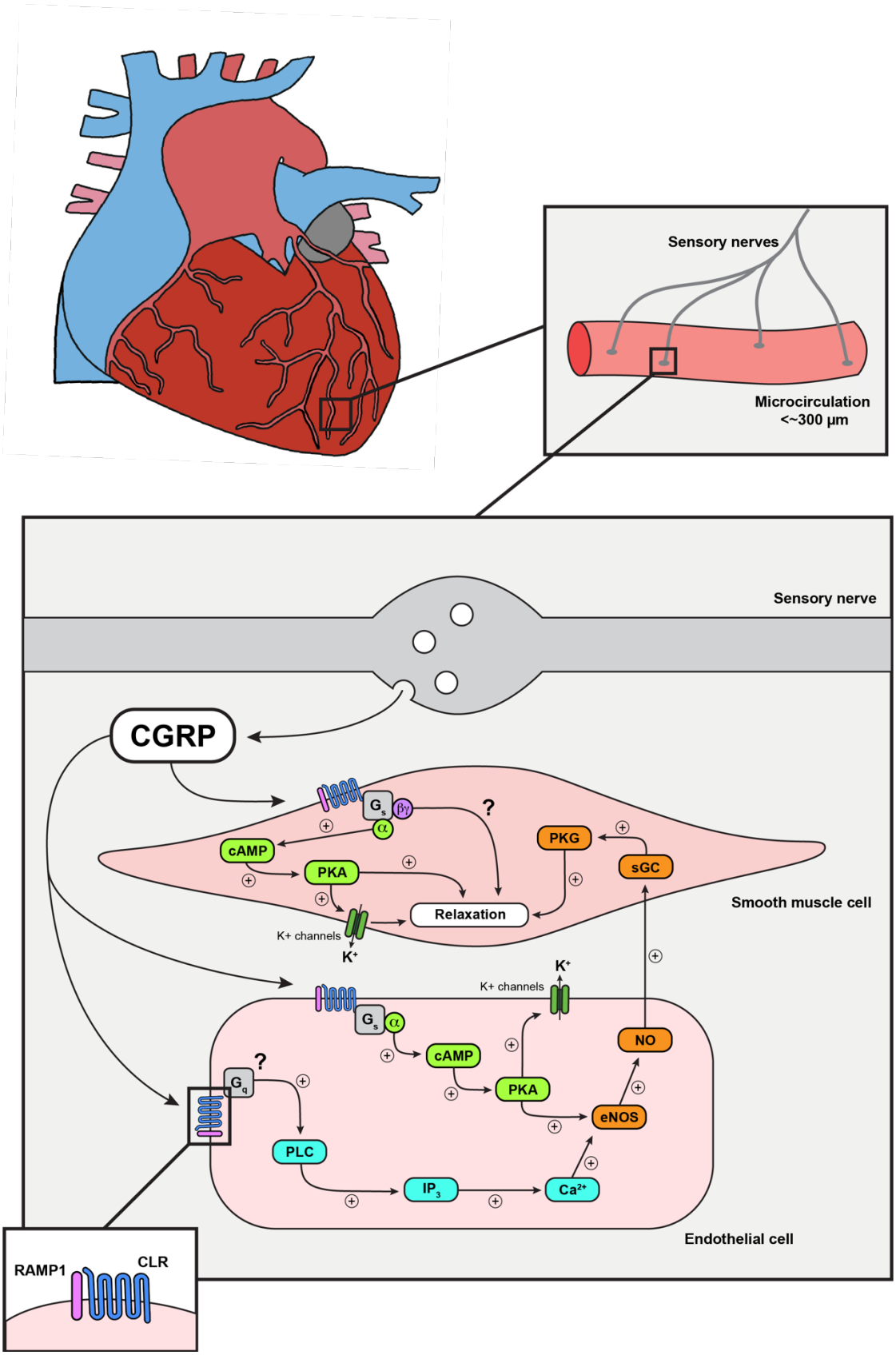
Sensory nerves
Microcirculation
<~300 µm
Sensory nerve
CGRP
cAMP
PKA
PKG
sGC
Relaxation
Smooth muscle cell
K+ channels
K+
NO
eNOS
PLC
IP3
Ca2+
Endothelial cell
RAMP1
CLR

Figure 1.5.1 Proposed signalling pathways underlying CGRP-induced vasorelaxation. CGRP released from sensory nerves activates the $G\alpha_s$-mediated cAMP-PKA pathway. In VSMCs, this results in vasorelaxation via several mechanisms, including activation of K^+ channels. In the ECs, this pathway initiates NO synthesis and release. Activation of the PLC-IP_3 pathway may play a role in the ECs, which stimulates NO release via an increase in intracellular Ca^{2+}. A $G\beta\gamma$ subunit-mediated pathway has been implicated in CGRP-induced vasorelaxation, but the precise signalling pathway is unknown.

(Grace et al., 1987; Gray & Marshall, 1992a, 1992b; Kubota et al., 1985), rat mesenteric arteries (Iwatani et al., 2008), and mouse mesenteric arteries (Norton et al., 2021). In contrast, other investigations saw no effect of endothelium removal on the CGRP response in rat intramural coronary arteries (Sheykhzade & Nyborg, 1998), porcine coronary arteries (Yoshimoto et al., 1998), and human pial and MMAs (Jansen-Olesen et al., 2003). This indicates that the relative importance of the endothelium in CGRP-induced vasodilation varies between species and vascular bed, as well as with vessel diameter.

Norton et al. utilised electrophysiological techniques in isolated endothelial tubes to investigate the effects of CGRP on EC membrane potential. They reported hyperpolarization of the VSMCs and ECs in response to CGRP in both mouse pulmonary (Norton & Segal, 2018) and mesenteric (Norton et al., 2021) arteries. In the pulmonary endothelial tubes, CGRP-induced hyperpolarization was abolished with either a PKA inhibitor, PKI, or the K_{ATP} channel inhibitor, glibenclamide. By contrast, CGRP-induced hyperpolarization in mesenteric endothelial tubes was not attenuated by glibenclamide, but was instead inhibited by K_{Ca} channel blockers, charybdotoxin and apamin, in combination. This implicates endothelial K^+ channels in CGRP-induced vasodilation and hyperpolarization, similarly to the VSMCs; however, these data suggest that there is differential K^+ activation not only between vascular beds, but also between cell types.

A study by Drissi et al. (1998) demonstrated an increase in intracellular Ca^{2+} in human bone OHS-4 cells in response to CGRP. This increase in Ca^{2+} was insensitive to the $G_{i/o}$ inhibitor, pertussis toxin, but was reduced by an anti-PLC-β1 antibody. These data indicate that CGRP may also activate the $G_{q/11}$-mediated PLC-IP_3 signalling pathway;

however, this is yet to be demonstrated in the vasculature. If this were to occur in vascular cells, it is likely that this pathway would be activated in ECs rather than VSMCs, as a rise in intracellular Ca^{2+} in VSMCs is associated with vasoconstriction, the opposite to the observed response. It has been reported that the Gβγ subunit can also activate PLC, providing further evidence that CGRP receptor may couple to several G proteins and activate multiple signalling pathways (Camps et al., 1992; Walker et al., 2010) (Figure 1.5.1).

1.6 Clinical implications of CGRP

In more recent years, it has emerged that CGRP has significant pathophysiological functions alongside its physiological effects. Most notably, it has been shown to have a role in migraines and has become a key therapeutic target in treatment strategies. There is also growing evidence that CGRP has cardioprotective effects, and it has been implicated in several cardiovascular diseases.

1.6.1 The role of CGRP in migraine

Migraine is a complex, neurobiological disorder characterised by recurrent episodes of severe headache alongside numerous other symptoms, including sensitivity to light and nausea (Goadsby et al., 2009). A study in England reported that 7.6% of males and 18.3% of females suffered with migraine, with most having an attack at least once per month. If these results are projected to the entire UK population, it is estimated that 5.85 million people aged 16-65 suffer with migraines, equating to approximately 190,000 migraine attacks each day and 25 million days of work or school being lost each year (Steiner et al., 2003). Migraine is thus a prevalent and debilitating condition that imposes a burden on patients, healthcare systems, and the economy.

The precise mechanisms underlying migraine are unclear, but it is believed that the pain arises from afferent sensory nerves, in particular the trigeminal nerve and nerve fibres (Rees et al., 2022). These fibres innervate the cerebral blood vessels and originate from the trigeminal ganglion; the ganglion and nerve fibres are known to contain CGRP (Goadsby et al., 2009; Uddman et al., 1985). CGRP was first implicated in migraine by Goadsby et al. (1990), who found that CGRP was elevated in the cranial circulation, but

not the peripheral circulation, in all migraine patients in the study compared to a control group. This occurred regardless of whether they suffered with classic (with aura) or common (without aura) migraine, although CGRP levels were greater in patients with classic migraine. No elevation was observed in other neuropeptide levels, including SP, NPY, and VIP. They went on to establish that activation of the trigeminalvascular system by stimulation of the trigeminal ganglion caused local cerebral vasodilation which was paired with an increase in CGRP levels in the jugular vein in cats. Administration of the serotonin (5-HT) receptor agonists used to treat migraines, sumatriptan and dihydroergotamine, reversed the elevated CGRP levels in both cats and humans (Goadsby & Edvinsson, 1993). These results not only confirm the significance of the trigeminalvascular system in migraine, but also determine that it can be antagonised to prevent CGRP release and potentially reduce symptom onset. Furthermore, a double-blind crossover study in migraine patients demonstrated that CGRP infusion caused an onset of headache in all patients in the treatment group, compared to only one patient in the placebo group, further establishing a causative role for CGRP (Lassen et al., 2002).

The disease-specific pharmacological treatment for migraine patients was previously restricted to the triptans, which are limited due to their cardiovascular effects whereby they cause vasoconstriction. For several years, work has carried out to develop CGRP antagonists with the hope that they may provide a more effective treatment strategy for migraine. The first selective non-peptide CGRP receptor antagonist, BIBN4096BS (olcegepant), was shown to prevent vasodilation upon stimulation of the trigeminal nerve in the marmoset (Doods et al., 2000). Although it appeared to have promising results in clinical trials and did not affect heart rate or blood pressure, it could only be administered by intravenous injection due to its large molecular weight. This was not viable for use by

migraine patients who would require immediate administration at symptom onset; therefore, there has been extensive work carried out by pharmaceutical companies to develop an orally available CGRP antagonist (Russell et al., 2014).

An alternative method of antagonising CGRP is to use function-blocking CGRP monoclonal antibodies. Zeller et al. (2008) used two rat blood flow models to measure electrically stimulated vasodilation in the mediodorsal skin (assessed using a Doppler skin probe) or MMA (assessed using a closed cranial window model) and showed that intravenous administration of anti-CGRP antibodies into the femoral artery inhibited vasodilation in the skin and MMA to the same extent as CGRP antagonists. Although the onset of action was slower with the anti-CGRP antibodies, their inhibitory effects lasted for at least 7 days and had no effects on systemic blood pressure or heart rate. These findings indicated that function-blocking CGRP antibodies could provide an effective preventative treatment for migraine patients. To date, there are a several FDA-approved CGRP receptor antagonists and antibodies now available for migraine treatment (Cohen et al., 2022). These include Aimovig (erenumab), the first FDA-approved therapeutic antibody that targets a GPCR (King et al., 2019), and ZAVZPRET (zavegepant), the first and only CGRP receptor antagonist nasal spray (Croop et al., 2022; Lipton et al., 2023).

1.6.2 Cardioprotective effects of CGRP

There is widespread evidence that CGRP can protect the myocardium from damage in several cardiovascular disease states. Firstly, Franco-Cereceda et al. (1989) found that 5-30 minutes of ischaemia in a Langendorff-perfused guinea-pig heart resulted in a significantly elevated CGRP-like immunoreactivity outflow in the perfusate that could be prevented either by using a Ca^{2+}-free Tyrode's solution or capsaicin pre-treatment. As

well as ischaemia inducing CGRP release, there is also evidence indicating that CGRP has a key role in ischaemic preconditioning. A study by Wolfrum et al. (2005) reported that CGRP infusion prior to 30-minute coronary artery occlusion in rats reduced the subsequent infarct size by 57%. Interestingly, a reduced infarct size was also observed in animals that underwent remote preconditioning by occlusion of the mesenteric artery, which occurred alongside an increase in plasma CGRP levels. These effects could all be attenuated by the CGRP receptor antagonist, CGRP 8-37 (Wolfrum et al., 2005). Consequently, this suggests that exogenous CGRP confers cardioprotective effects during ischaemia/reperfusion (I/R), and endogenous CGRP can mediate remote preconditioning to have similar protective effects on the heart. Although the mechanisms involved are not fully understood, Sekiguchi et al. (1994) reported that CGRP 8-37 had no effect on the diameter of coronary microvessels during acute myocardial ischaemia in canine hearts *in vivo*; therefore, the CGRP released during ischaemia may not be exerting its cardioprotective effects by acting on the coronary vasculature. It does appear, however, that ischaemia can dysregulate CGRP signalling in the vasculature, as it was observed that CGRP-induced vasodilation in the distal LAD coronary artery was attenuated in an I/R rat model compared to a sham group (Kristiansen et al., 2017).

Interestingly, although CGRP is the most potent vasodilator, its role in hypertension is unclear. CGRP levels have been reported to be elevated, reduced, or the same in human patients with hypertension, and CGRP knockout (KO) mice either have significantly raised or unchanged blood pressure depending on the strain (Kee et al., 2018). There is evidence, however, suggesting that CGRP may have a protective role in hypertension. CGRP administration has been found to attenuate the rise in systolic blood pressure in several rat models of hypertension (Fujioka et al., 1991; Kumar et al., 2019). Deng et al.

(2003) showed that CGRP plasma levels, dorsal root ganglia CGRP mRNA levels, and density of CGRP immunoreactive nerve fibres in the mesenteric artery were all increased in a two-kidney, one-clip hypertensive rat model. Furthermore, treatment with either CGRP 8-37, to antagonise CGRP receptors, or capsaicin, to deplete the sensory nerve fibres of CGRP, resulted in a further increase in blood pressure. It thus appears that CGRP has a compensatory contribution in hypertension, and that the loss of CGRP can lead to progression of the disease.

It is also believed that CGRP may provide a compensatory mechanism in heart failure. As discussed previously, CGRP has positive inotropic and chronotropic effects on the heart and, as such, it is understood that CGRP release from sensory nerves in the heart contributes to cardiac homeostasis. Li et al. (2010) demonstrated that plasma CGRP levels and dorsal root ganglia mRNA levels were reduced in an isoprenaline-induced rat cardiac remodelling model. By administrating a TRPV1 activator, rutaecarpine, CGRP production was increased, and cardiac remodelling was reversed. These results indicate that the pathological cardiac remodelling, which ultimately leads to heart failure, may be associated to dysfunctional CGRP release from the sensory nerves and treatments that aim to stimulate CGRP production could have therapeutic benefits in reversing the remodelling process. In fact, Gennari et al. (1990) reported an improvement in ventricular contractility in 5 patients with congestive heart failure following β-CGRP infusion. Similar results were also observed in a pressure overload heart failure model, which was induced in either CGRP KO or wild-type mice by transverse aortic constriction. The CGRP KO mice displayed greater adverse cardiac remodelling and dysfunction than the wild-type mice, as well as increased fibrosis, inflammation, and cell death (Li et al., 2013). These studies contribute to the overwhelming evidence that CGRP has a

cardioprotective role in several cardiovascular diseases, with reductions in CGRP production or release leading to exacerbated disease phenotypes.

1.7 Thesis aims and objectives

Investigations into the regulation of vascular resistance in the coronary microvasculature are limited despite growing evidence that dysfunctions in these vessels are found in most cardiovascular diseases. CGRP is a potent and clinically relevant endogenous vasodilator, yet there is still uncertainty surrounding the precise signalling pathways underlying CGRP-induced vasodilation, particularly in small coronary arteries. It is understood that CGRP confers cardioprotection in several diseases and has been shown to be a successful therapeutic target in migraine; therefore, improving our understanding of the actions of CGRP in the coronary vasculature may have important clinical and therapeutic implications.

This thesis aims to explore the intracellular signalling mechanisms that contribute to CGRP-induced vasodilation in rat intramuscular coronary septal arteries. Since studying the microvasculature *in vivo* is challenging due to limitations in imaging techniques, this study utilises *ex vivo* myography experiments, alongside immunohistochemical and fluorescent imaging techniques, to study isolated arteries.

The objectives of the following chapters are as follows:

1. To characterise the effects of CGRP on isolated, septal arteries
2. To determine the relative importance of the endothelium in CGRP-induced vasodilation
3. To investigate the contribution of the vascular smooth muscle, specifically in CGRP-induced hyperpolarization
4. To explore the site and mechanism of CGRP synthesis and release

CHAPTER 2: MATERIALS AND METHODS

2.1 Animals and Tissue Preparation

All animal procedures were conducted in accordance with the University of Oxford local ethical guidelines, the ARRIVE guidelines, and the UK Home Office Animal (Scientific Procedures) Act, 1986.

Wild-type male Wistar rats (6-8 weeks, 200-300 g; Charles River, UK or Germany) were used in the present investigations. Animals were housed in individually ventilated cages under a 12:12 h light:dark cycle at 20-22 °C. Standard chow and water were available *ad libitum*. Rats were killed in accordance with UK legislation as specified by Schedule 1 of the Animals (Scientific Procedures) Act by increasing concentration of CO_2 and confirmed with cervical dislocation. The heart and mesentery were excised and placed in ice-cold Krebs-buffered solution (see Section 2.9).

2.1.1 Isolation of mesenteric artery

The mesenteric arcade was pinned out in a Sylgard-coated dissection dish containing ice-cold Krebs-buffered solution. Third-order mesenteric arteries were carefully isolated from adhering connective tissue following removal of surrounding perivascular fat and the parallel mesenteric vein (Figure 2.1.1).

2.1.2 Isolation of the coronary septal artery

The excised heart was pinned down in a Sylgard-coated dissection dish containing ice-cold Krebs-buffered solution. The wall of the left atrium and right ventricle was partially removed to allow the interventricular septal artery to be carefully isolated from the adhering connective tissue and cardiomyocytes (**Figure 2.1.2**).

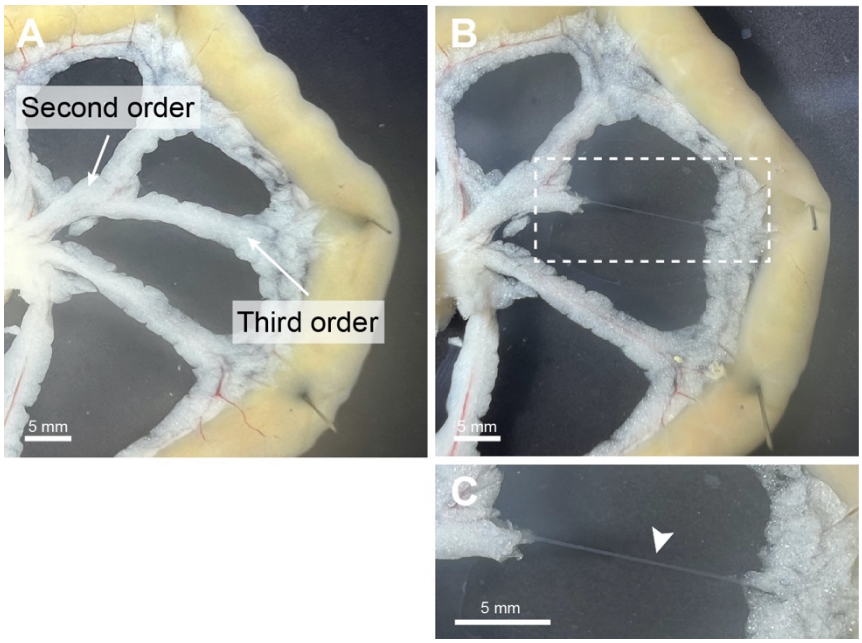

Figure 2.1.1 Rat mesenteric artery dissection. (**A**) Pinned mesenteric arcade detailing the location of the second and third order arteries. (**B** and **C**) Third order artery following removal of surrounding adipose tissue, adhering connective tissue, and parallel mesenteric vein. The dashed box (B) represents the region of magnification (C), and the arrowhead indicates the artery to be studied.

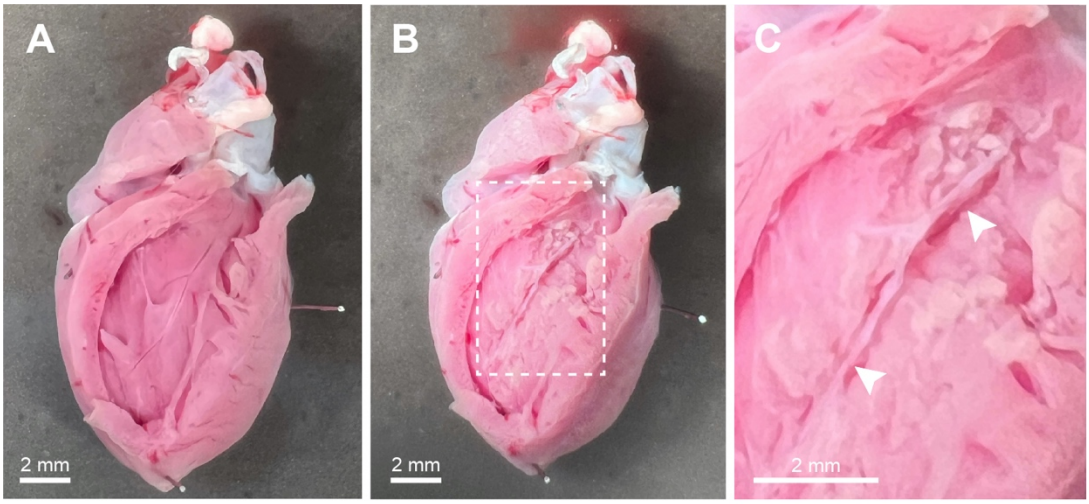

Figure 2.1.2 Rat coronary septal artery dissection. (**A**) Pinned heart following partial removal of the wall of the left atrium and right ventricle to reveal the interventricular septum. (**B** and **C**) Septal artery following removal of adhering connective tissue and cardiomyocytes. The dashed box (B) represents the region of magnification (C), and the arrowheads indicate the artery segments to be studied.

2.2 Wire myography

Bohr and Goulet (1961) first introduced a technique to directly record tension from isolated vascular smooth muscle under isometric conditions: the length of the muscle remains constant as contraction or relaxation is produced. This technique was refined in smaller vessels by Bevan and Osher (1972), who secured the tissue using two platinum wires passed through the lumen and stretched between two supporting plates, one attached to a micrometer and the other attached to a strain gauge. Mulvany and Halpern (1976) advanced this experimental method further by designing the Mulvany-Halpern myograph, which utilises two metal jaws to secure the vessel. One jaw is attached to a micrometer that allows the vessel to be stretched at known increments, and the other is attached to a force transducer which allows tension to be measured. By gradually increasing the internal circumference of the vessel and recording the corresponding wall tension, they were able to fit an exponential curve. In this way, the vessel could be normalised to determine an optimal resting wall tension that would not mask changes in active wall tension, and the experiment would be performed with the artery at the corresponding internal circumference.

2.2.1 Mounting of arteries in a wire myograph

Isolated artery segments (~2 mm) were mounted luminally using two 25 µm diameter gold-plated tungsten wires in a 5 mL chamber of a Mulvany-Halpern wire myograph (Danish Myo Technology Organ Bath Model 700MO or 610M) in Krebs-buffered solution (See Section 2.9) gassed with 21% O_2, 5% CO_2, and balance N_2. With the aid of a microscope, the length of the arteries was then measured (mm). The artery was allowed to equilibrate for 30 minutes while the chamber was warmed to 37°C. Changes in tension

(mN) were recorded at 10 Hz using a PowerLab/4SP data acquisition system (ADInstruments, New Zealand) and LabChart software (v8.1.17, AD Instruments). The arteries were normalised to a resting tension equivalent to that generated at 90% of the diameter of the vessel at 70 mm Hg (mesenteric) or 80 mmHg (coronary) (Figure 2.2.1).

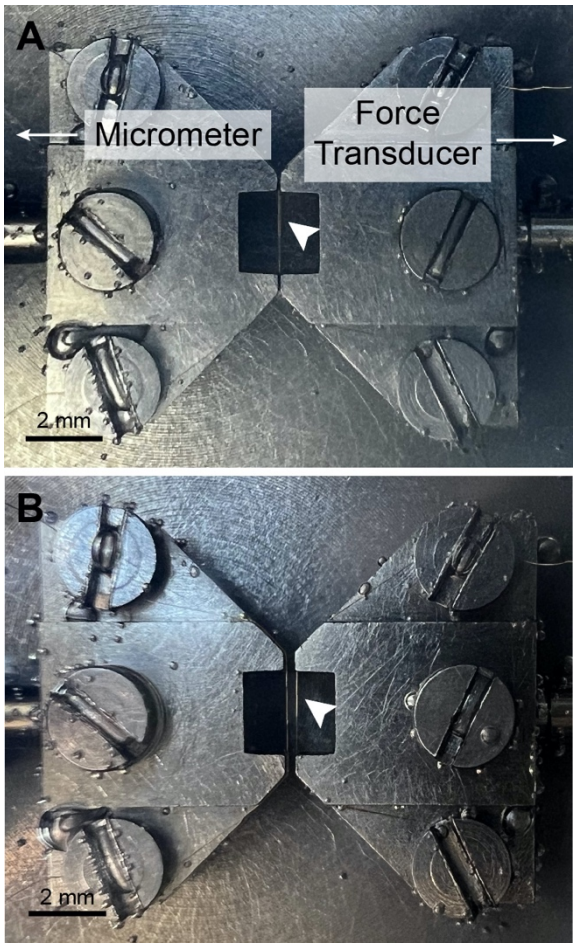

Figure 2.2.1 Wire myograph apparatus. (**A** and **B**) Mesenteric artery mounted in a wire myograph without (A) and with (B) applied normalised tension. One jaw is attached to a micrometer that allows vessel tension to be adjusted, and the other jaw is attached to a force transducer that allows tension to be measured.

2.2.2 Studying mesenteric arteries under isometric conditions

Arteries were allowed to equilibrate at their optimal resting tension for 30 minutes. Artery contractility was assessed by constriction to phenylephrine (PE, 1–3 μM) and the endothelium was assessed by relaxation to acetylcholine (ACh, 10 nM–1 μM). Only arteries that demonstrated robust and sustained contraction to PE and >95% relaxation to 100 nM ACh were considered viable. To study vasorelaxation, arteries were precontracted with a submaximal concentration of PE. Arteries were not exposed to multiple inhibitors, unless where indicated, nor washed out after their addition to eliminate the possibility of irreversible effects influencing other results.

2.2.3 Studying coronary septal arteries under isometric conditions

Arteries were allowed to equilibrate at their optimal resting tension for 60 minutes. Artery viability was assessed by the development of spontaneous myogenic tone followed by endothelium-dependent relaxation to ACh (10 nM–1 μM). Only arteries that developed >0.5 mN/mm spontaneous myogenic tone and relaxed >95% to 100 nM ACh were considered viable. If sufficient myogenic tone was not obtained, artery contractility was assessed by constriction to PE (1–5 μM) and the endothelium was assessed by relaxation to ACh (10 nM – 1 μM). Only arteries that demonstrated robust and sustained contraction to PE and >95% relaxation to 100 nM ACh were considered viable. To study vasorelaxation, arteries were not precontracted with PE unless where indicated. When necessary, ECs were removed with a hair and successful removal was confirmed by <10% relaxation to 1 μM ACh. Arteries were not exposed to multiple inhibitors, unless where indicated, or washed out after their addition to eliminate the possibility of irreversible effects influencing other results.

2.2.4 Analysis of mesenteric artery tension recordings

Each data point represents the mean tension over a 10 second period. For each relaxation response, the maximum tension was that obtained during precontraction to PE and the minimum tension was taken as the baseline tension prior to precontraction:

$$Vasorelaxation\ (\%) = \frac{Tension\ at\ peak\ response - Maximum\ tension}{Minimum\ tension - Maximum\ tension} \times 100$$

2.2.5 Analysis of coronary septal artery tension recordings

Each data point represents the mean tension over a 10 second period. For each relaxation response, the maximum tension was taken as the level of myogenic tone immediately prior to addition of the test agent, and the minimum tension was achieved with 1 μM nifedipine at the end of the experiment:

$$Vasorelaxation\ (\%) = \frac{Tension\ at\ peak\ response - Maximum\ tension}{Minimum\ tension - Maximum\ tension} \times 100$$

2.3 Pressure myography

The experimental method for studying isolated, cannulated small arteries was designed by Duling et al. (1981). The protocol aims to maintain the vessels in a physiological state as close to that *in vivo*, and so arteries are studied under isobaric conditions: the pressure within the vessels remains constant but the vessel diameter is able to change. In this way, changes in vessel diameter can be measured in response to different reagents and intraluminal pressures.

2.3.1 Artery cannulation and pressurisation

Following isolation, mesenteric and coronary septal artery segments (~2 mm) were transferred to a 2 mL confocal imaging chamber (RC-27; Warner Instruments, USA). Each end of the artery was cannulated with a glass micropipette (inner diameter, ~80 μm; outer diameter, ~130 μm) and secured with 11-0 Ethilon nylon sutures (Ethicon, USA). The chamber was secured to the stage of an inverted microscope (IX 70; Olympus, UK), attached to a confocal scanning unit (FV500 or FV1000; Olympus), with a heating platform (PH-6; Warner Instruments, USA) connected to a temperature controller (TC-324C; Warner Instruments, USA). Arteries were continually superfused at a rate of 2 mL/min with Krebs-buffered solution (See Section 2.9) warmed to 36.6–37.2°C and gassed with 21% O_2, 5% CO_2, and balance N_2. One pipette was attached to a pressure head which could be adjusted to alter the intraluminal pressure of the artery. The intraluminal pressure was gradually increased to 70 mmHg (mesenteric) or 80 mmHg (coronary), longitudinally stretching the artery with each pressure step. Whilst pressurised, an inline three-way tap was closed to check for artery deflation to ensure that no side-branches were present in the artery and that the sutures had been adequately

secured. Arteries were visualised using a 10× objective (NA 0.3; Olympus, Japan) and images were recorded at 1 Hz. Changes in artery diameter were recorded using FluoView software (v5.0; Olympus, Japan) (Figure 2.3.1).

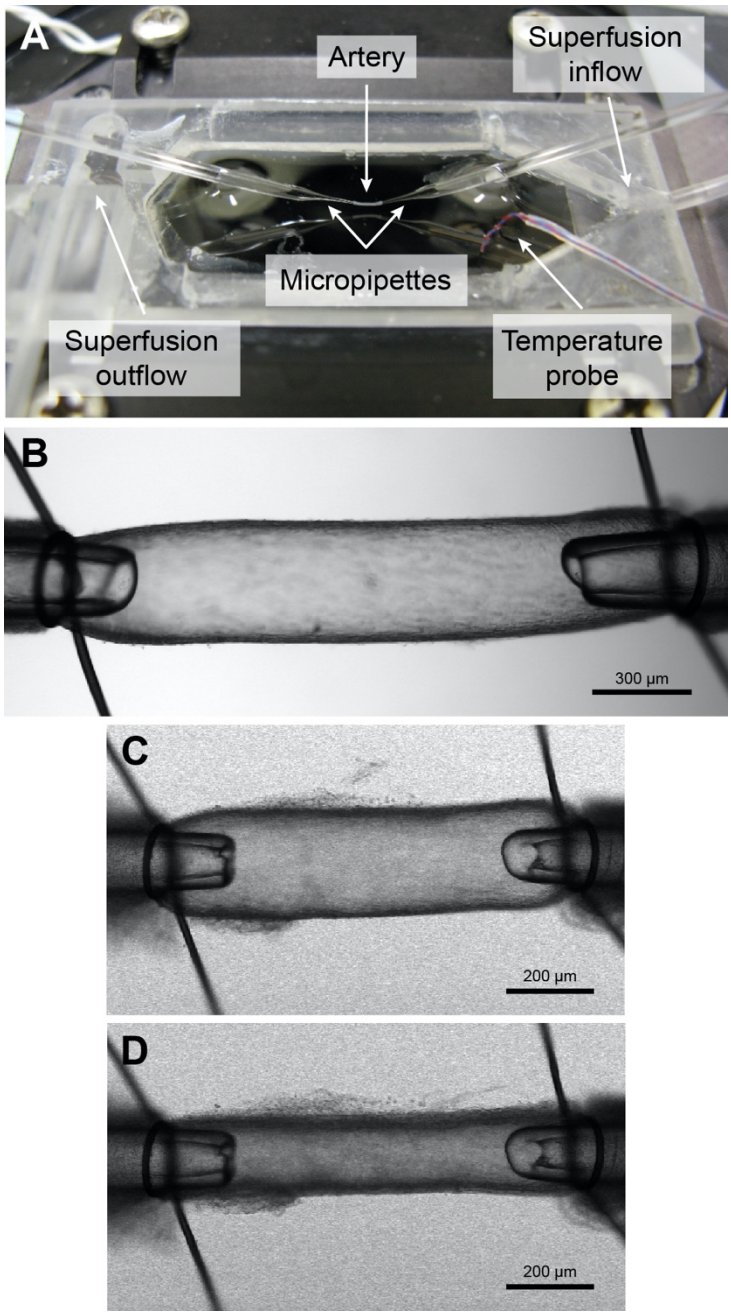

Figure 2.3.1 Pressure myography apparatus and pressurised arteries. (**A**) Imaging chamber with artery mounted on two micropipettes. (**B**) Cannulated and pressurised mesenteric artery. (**C** and **D**) Cannulated and pressurised coronary septal artery before (B) and after (C) developing myogenic tone at 80 mmHg.

2.3.2 Studying mesenteric arteries under isobaric conditions

If no leaks were detected, arteries were allowed to equilibrate for 30 minutes. Artery contractility was assessed by constriction to PE (1–3 μM) and the endothelium was assessed by vasodilation to ACh (10 nM–1 μM). Only arteries that demonstrated robust and sustained contraction to PE and >95% vasodilation to 100 nM ACh were considered viable. The superfusion was stopped immediately prior to adding agents to the chamber. To study vasodilation, arteries were precontracted with a submaximal concentration of PE.

2.3.3 Studying coronary septal arteries under isobaric conditions

If no leaks were detected, arteries were allowed to equilibrate for 60 minutes. Artery viability was assessed by the development of spontaneous myogenic tone followed by endothelium-dependent relaxation to ACh (10 nM–1 μM). Only arteries that developed >20% myogenic tone and >95% vasodilation to 100 nM ACh were considered viable. The superfusion was stopped immediately prior to adding agents to the static bath.

2.3.4 Analysis of mesenteric artery diameter recordings

The outer diameter was measured using VasoTracker Offline Diameter Analyser (v1.1.0, VasoTracker UK) (Lawton et al., 2019). Each data point represents the mean diameter over 10 seconds. For each vasodilation response, the minimum diameter was that obtained during precontraction to PE and the maximum diameter was taken as the passive diameter prior to precontraction:

$$Vasodilation(\%) = \frac{Diameter\ at\ peak\ response - Minimum\ diameter}{Passive\ diameter - Minimum\ diameter} \times 100$$

2.3.5 Analysis of coronary septal artery diameter recordings

The inner diameter was measured using VasoTracker Offline Diameter Analyser (v1.1.0, VasoTracker UK) (Lawton et al., 2019). The outer diameter was not measured because residual cardiomyocytes on the outside of the artery interfered with detection of the outer wall. Each data point represents the mean diameter over 10 seconds. Myogenic tone is calculated as a percentage decrease from the passive diameter (without myogenic tone):

$$Myogenic\ tone\ (\%) = \frac{Passive\ diameter - Diameter\ with\ myogenic\ tone}{Passive\ diameter} \times 100$$

For each vasodilation response, the minimum diameter was taken as the level of myogenic tone immediately prior to addition of the test agent and the maximum diameter was achieved with 1 μM nifedipine at the end of the experiment:

$$Vasodilation(\%) = \frac{Diameter\ at\ peak\ response - Minimum\ diameter}{Passive\ diameter - Minimum\ diameter} \times 100$$

2.4 Immunohistochemistry

2.4.1 Immunostaining of pressurised arteries

Arteries mounted for pressure myography experiments (See Section 2.3) can be fixed and stained for proteins of interest. Pressurised arteries were fixed *in situ* by adding 4% paraformaldehyde aqueous solution (PFA; J61899.AK; Thermo Scientific) to the chamber for 60 minutes at room temperature before being washed with 0.01 phosphate-buffered saline (PBS; P3813; Sigma). Arteries were then blocked for 90 minutes by luminal pumping of blocking buffer containing 1% bovine serum albumin (A3059; Sigma), 0.5% Triton X-100 (T8532; Sigma), and 0.05% Tween20 (P2287; Sigma) diluted in PBS. Blocking buffer was also added to the chamber. Arteries were incubated with the primary antibodies overnight at 4°C. The following day, arteries were washing in PBS and incubated with the secondary antibodies and Hoechst 33342 (10 µg/mL) for 2 hours at room temperature, before being washed in PBS again. Antibodies and Hoechst were diluted in blocking buffer.

2.4.2 Immunostaining of arteries mounted in the wire myograph

Arteries mounted in the wire myograph were checked for EC and VSMC function. Subsequently they were fixed *in situ* by adding 4% PFA to the chamber for 60 minutes at room temperature, before being washed with PBS. Fixed arteries were cut open laterally and removed from the wire myograph. Arteries were then blocked for 90 minutes with blocking buffer and incubated with the primary antibodies overnight at 4°C. The following day, arteries were washed in PBS and incubated with the secondary antibodies and Hoechst 33342 (10 µg/mL) for 2 hours at room temperature, before being washed in PBS again. Antibodies and Hoechst were diluted in blocking buffer. After staining, the

arteries were carefully opened and placed flat on glass slides in mounting medium (VECTASHIELD, H-1000; Vector Laboratories Inc., USA), with the EC layer facing up. Coverslips were lowered on top and sealed (CoverGrip, 23005; Biotium).

2.4.3 Immunostaining of endocardial endothelial cells

Myocardial strips were isolated from the right atrial appendage and left ventricle of the heart as described previously by Borysova et al. (2021). The strips were gently stretched and pinned into a Petri dish and were fixed with 4% paraformaldehyde aqueous solution to the chamber for 60 minutes at room temperature, before being washed with PBS. Myocardial strips were then blocked for 90 minutes with blocking buffer and incubated with the primary antibodies overnight at 4°C. The following day, strips were washed in PBS and incubated with the secondary antibodies and Hoechst 33342 (10 μg/mL) for 2 hours at room temperature, before being washed in PBS again. Antibodies and Hoechst were diluted in blocking buffer. After staining, the myocardial strips were placed on glass slides in mounting medium (VECTASHIELD HardSet, H-1400; Vector Laboratories, USA) with the endocardial endothelial cell (EEC) layer facing up. Coverslips were lowered on top and sealed (CoverGrip, 23005; Biotium).

2.4.4 Imaging immunohistochemistry preparations

Arteries were excited at 405, 488, 543, and 635 nm using sequential scans. The emitted fluorescence was acquired through a 40× water immersion objective (NA 1.15; WD 0.25 mm; 1024 × 1024-pixel clip box; Olympus, Japan) using a laser scanning confocal microscope (FV1200; Olympus). Arteries were imaged at 2–3× digital zoom. Scans were Kalman line arranged. Sequential z-stacks through the artery wall were acquired at 0.5

μm intervals using FluoView Software (FV10-ASW 3.0; Olympus) and reconstructed in Imaris Software (v8.0.2; Bitplane, USA).

2.5 Calcium Imaging

Pressure myography can be used in combination with fluorescence microscopy, such as Ca^{2+} imaging, which would be challenging to perform *in vivo*. Ca^{2+} imaging allows us to measure the Ca^{2+} dynamics within the ECs and VSMCs of isolated arteries.

2.5.1 Loading of arteries with Ca^{2+} indicator

The ECs of pressurised septal arteries were selectively loaded by intraluminally pumping filtered Krebs-buffered solution containing the Ca^{2+} indicator, Oregon Green 488 BAPTA-1 AM (10 μM; O6807, Invitrogen), and 0.0025% pluronic™ F-127 as described previously (Bagher et al., 2012). The total level of DMSO was 0.7%. ECs were loaded for ~20 minutes until a clear signal was observed. Excess indicator was washed from the vessel lumen, and the loaded dye was left to de-esterify and equilibrate for 30 minutes. EC Ca^{2+} activity was imaged at 40× (40×/1.15W, UApo N340 objective; Olympus) using an inverted microscope (IX81; Olympus) attached to a linescan confocal microscope (FV1000; Olympus). Images were acquired at a frequency of 3 Hz in a 640 × 128-pixel clip box at 1-1.8× zoom. To prevent movement artefacts, the L-type voltage-gated Ca^{2+} channel blocker, 1 μM nifedipine, was added to the superfusion to keep the artery dilated.

2.5.2 Analysis of Ca^{2+} fluorescence measurements

Whole-cell Ca^{2+} activity was analysed offline using MetaMorph (v7.7.4.0; Molecular Devices). Only cells that responded to ACh were analysed. Ca^{2+} activity is expressed as F/F_0 where F and F_0 are both taken as a 10 second average ~2 minutes after treatment and at baseline, respectively. Each data point represents the mean fluorescence intensity of at least 3 cells per artery.

2.6 Cu_2FL2E

NO-sensitive fluorescent dyes can be utilised to measure NO synthesis and release. Lim (2007) developed a transition-metal complex for detecting NO release in cultured cells, CuFl, which is prepared by adding a fluorescein derivative to copper(II) chloride. This NO-dye was advanced for use in biological systems by McQuade et al. (2010) through the development of Cu_2FL2E: a cell-trappable probe that does not diffuse out of cells, allowing for its use in experiments where intact tissue must be continually perfused.

2.6.1 Cu_2FL2E preparation

FL2E (0.5 mg; 07-0291; STREM Chemicals, UK) was dissolved in DMSO to make a stock solution of 1 mM FL2E. This was aliquoted and stored at −80°C as per the product sheet. When thawed, the solution was kept chilled in the dark and used as quickly as technically feasible; any unused dye was discarded. A 1 μM working solution was prepared by adding 1 mM FL2E stock to 2 mM $CuCl_2$. Each FL2E molecule has the potential to bind two Cu^{2+} ions (hence Cu_2), and each of the Cu^{2+} ions can be displaced by NO to form FL2E-NO (or FL2A-NO inside cells once de-esterifed) and increase dye fluorescence; therefore, when NO binds, Cu^{2+} becomes free in solution. Due to this, a working ratio of 1 FL2E : 2 Cu^{2+} was used. For experiments in intact arteries, 2.5 μl/mL pluronic™ F-127 was added to the Cu_2FL2E working solution (20% pluronic in DMSO). The total level of DMSO was 0.3%, which the laboratory has proven is the maximum amount that can be used before stimulating EC Ca^{2+} (unpublished).

2.6.2 Cell-free experiments

These experiments were performed in a 2 mL chamber (RC-27; Warner Instruments, USA) secured to the stage of an inverted microscope (IX 70; Olympus, UK). The chamber contained either PBS (~25 °C) or Krebs-buffered solution (~37°C). The solution was visualised 200 µm above the coverslip using an Olympus 20× water immersion objective (NA 0.17; WD 0.70 mm; 512 × 512-pixel clip box) and linescan confocal microscope (FV300 or FV500) with FluoView software (Olympus, Japan). Images were acquired at a frequency of 0.45 Hz. Cu_2FL2E was excited at 488 nm with emitted light detected at ≥ 505 nm. The Cu_2FL2E dye was added to the chamber, mixed, and left to equilibrate for 2 minutes. Once the signal was stable, the NO donor, S-Nitroso-N-acetyl-DL-penicillamine (SNAP), was added and acquisition continued for ~10 minutes.

2.6.3 Analysis of cell-free experiments

Data were analysed using MetaMorph software (v 7.7.4.0; Molecular Devices). The whole image field was defined as the region of interest (ROI) and used to generate time courses of Cu_2FL2E fluorescence. The maximum fluorescence (F_{Peak}/F_0) was calculated by dividing the maximal fluorescence intensity value (F_{Peak}) by the 30 second average before SNAP was added (F_0).

2.6.4 Cu_2FL2E loading into pressurised arteries

Isolated mesenteric arteries were mounted in a pressure myography chamber (See Section 2.3.1). To prevent movement artefacts, the L-type voltage-gated Ca^{2+} blocker, 1 µM nifedipine, was added to the superfusion to keep the artery dilated. Cu_2FL2E was added to the chamber, mixed, and left to load from the outside of the artery until there was a clear signal, above the background autofluorescence. Once this was achieved, the

superfusion was turned on for 10 minutes to wash the NO-dye away from the artery, as any residual NO-dye would respond to SNAP in the chamber. SNAP (10 or 100 μM) was then added to the chamber for 10 minutes. The artery wall was imaged using a 40× water immersion objective (40×/1.15W, UApo N340 objective; Olympus) using an inverted microscope (IX81; Olympus) attached to a linescan confocal microscope (FV1000; Olympus), obtaining 13.5 μm z-stacks in 2 μm steps (18.921s/stack). Each image plane was 640 × 256 pixels. Cu_2FL2E was excited at 488 nm with emitted light detected at 505–550 nm. Each line was the average of two scans (line Kalman). The transmitted light signal was also recorded.

2.6.5 Cu_2FL2E loading into en-face arteries

In the dissecting dish, cleaned arteries were partially cut transversely to make an opening in the lumen. Curved Vannas micro-scissors (World Precision Instruments, USA) were used to cut longitudinally through the wall along one side, leaving a flat, rectangular-shaped artery with ECs on one side and adventitia on the other. The flat section of artery was isolated from the rest of the tissue and transferred to a 5 mL imaging chamber (Danish Myo Technology, Confocal Cardiac Myograph) containing chilled Krebs-buffered solution as described previously (Borysova et al., 2021). The artery was secured at each end by two micro-clamps (Fine Science Tools, USA) and stretched to resemble its physiological length *in vivo*. Arteries were loaded and imaged following the same protocol as pressurised arteries (See Section 2.6.4).

2.7 Electrophysiology

The use of sharp glass microelectrodes, as described by Garland and McPherson (1992), allows for the VSMC membrane potential (E_m) of intact arteries to be recorded. This technique utilises isolated arteries mounted in the wire myograph, which enables the isometric tension and E_m to be recorded simultaneously. In this way, we can observe how changes in electrical activity correspond to changes in tension in response to vasoactive agents.

2.7.1 Preparation of arteries

Rat coronary septal arteries were mounted in a 10 mL wire myograph chamber, as described in Chapters 2.2.1 and 2.2.3. It was important to carefully remove all connective tissue and cardiomyocytes, as excess tissue on the outside of the artery interferes with impalement and maintaining a stable recording.

2.7.2 Preparation of microelectrodes

Borosilicate glass capillaries with an internal filament (30-0044; Harvard Apparatus, USA) were pulled using a pre-defined programme on a pipette puller (model P-1000; Sutter Instruments, USA). The electrodes were backfilled with 2 M KCl, inserted into an electrode holder, and attached to the head-stage of the electrophysiology rig. The electrode was tested to ensure that the tip impedance was between ~60 MΩ; if the tip impedance was not suitable, the temperature and/or pull force on the pipette puller were adjusted and a new electrode was pulled. The sharp microelectrodes were made on the day of use by Professor Christopher Garland.

2.7.3 Intracellular recording of smooth muscle cells

The electrode was advanced in 1.5 μm increments towards the mounted artery using a Burleigh Inchworm motor and 6000 Series controller (Burleigh, USA). An impalement of a single smooth muscle cell was considered successful if a rapid deflection towards the resting V_m was observed, near -50 mV, and if this remained stable for a minimum of 30 s. V_m was recorded through a pre-amplifier (Neurolog System; Digitimer Ltd, UK) linked to a MacLab Data Acquisition System (Model 4e; AD Instruments). This technique was performed by Professor Christopher Garland.

2.8 RNAscope™

2.8.1 Preparation of arteries

Intact, septal arteries were fixed for 60 minutes with 4% PFA while mounted in the wire myography (see Section 2.2.1). After this initial fixing, arteries were washed in PBS, removed from the wires, before being fixed overnight in 4% PFA at 4°C. Fixed arteries were then washed twice in 0.1% PBS-T (0.1% Tween-20 in PBS) for 5 minutes each. Arteries were dehydrated in a methanol (Sigma, UK) gradient (methanol diluted in PBS-T; 25%, 50% 75% and 100% × 2 for 10 minutes each). Once in 100% methanol, arteries can be stored at -20°C for up to 6 months.

2.8.2 RNAscope™ protocol

To detect the hybridisation signal, RNAscope™ Multiplex Fluorescent Detection Reagents v2 (ACD, USA), utilising the TSA Vivid 520 and TSA Vivid 570 fluorophores respectively (Perkin Elmer, USA), were applied. Arteries were rehydrated using the same methanol gradient and washed twice in 0.1% PBS-T. Arteries were treated with hydrogen peroxide (ACD, USA) at room temperature for 10 minutes before being washed with PBS-T. This was followed by digestion with RNAscope™ protease plus at 40°C for 10 minutes before arteries were washed with 0.2× saline-sodium citrate (SSC; Sigma, UK) 5 minutes x 3. Following protease treatment, arteries were incubated with the RNAscope™ Rn-*Calca*-C2 (317511-C2, ACD, USA*)* and Rn-*Ppib*-C3 (recommended positive control; 313921-C3, ACD, USA) probes, for approximately 5 hours at 40°C and overnight at room temperature. Arteries were then washed with 0.2× SSC. Probe signals were amplified by incubation with AMP1, AMP2 and AMP3 at 40 °C

for 50, 50 and 20 minutes respectively, with 0.2× SSC washes after each. Following this, RNAscope™ HRP-C2, for the *Calca* probe, was applied for 20 minutes at 40°C before the addition of TSA Vivid 520, with 0.2× SSC washes between and after fluorophore addition. HRP blocker was then applied for 20 minutes at 40°C followed by a 0.2× SSC. This was then repeated with RNAscope™ HRP-C3, for the *Ppib* probe, and TSA Vivid 570, followed by HRP blocker before a final 0.2× SSC wash. Arteries were then stained for ZO-1 using the immunohistochemistry protocol described in Section 2.4.2, except Triton-X was removed from the blocking buffer, and images as described in Section 2.4.4.

2.9 Solutions and Drugs

During tissue collection, dissection, and myography experiments, Krebs-buffered solution was used containing (in mM): 118 NaCl, 25 NaHCO3, 3.6 KCl, 1.2 MgSO4(7H2O), 1.2 KH2PO4, 11 glucose, and 1.25 CaCl, and gassed with 21% O_2, 5% CO_2, and balance N_2.

Drug and compound stock solutions were diluted in Krebs-buffered solution. The total level of DMSO in the myography chambers never exceeded 0.3%, which the laboratory has proven is the maximum amount that can be used before stimulating EC Ca^{2+} (unpublished). Arteries were allowed at least 15 minutes between experiments to recover. All inhibitors were incubated with the tissue for at least 15 minutes prior to experimentation and until myogenic tone had plateaued when relevant.

Details of drugs and compounds used in the current investigations are given in Table Table 2.9.1.

Table 2.9.1 Details of drugs and compounds used in the current investigations.

Drug/Compound	Product Code	Supplier	[Stock] (mM)	Stock Solvent
Acetylcholine	A6625	Sigma, UK	10	Milli-Q
BIBN4096BS	4561	Tocris, UK,	10	DMSO
CGRP	1161	Tocris, UK	0.1	Milli-Q
CGRP 8-37	1169	Tocris, UK	0.3	Milli-Q
Gallein	3090	Tocris, UK	50	DMSO
Glibenclamide	G0639	Sigma, UK	10	DMSO
Isoprenaline	I5627	Sigma, UK	100	Milli-Q
IPA-NO	Custom-made	Gift from K. M. Miranda, University of Arizona	10	NaOH
L-NAME	N5751	Sigma, UK	100	Milli-Q
Levcromakalin	1378	Tocris, UK	1	DMSO
Linopirdine	1999	Tocris, UK	10	Milli-Q
Nifedipine	N7634	Sigma, UK	10	Ethanol
Phenylephrine	P6126	Sigma, UK	10	Milli-Q
Retigabine	90221	Sigma, UK	10	DMSO
SNAP	ab120014	Abcam, UK	100	DMSO

2.10 Statistical Analyses

All myography and electrophysiology data were analysed identically with methods determined prior to data collection; therefore, data randomisation and blinding were not necessary in these current investigations. Furthermore, lack of randomisation and blinding were unlikely to skew results as multiple arteries from one animal were used for different treatment protocols.

All data analysis was completed *post-hoc* using Microsoft Excel (v16; Microsoft, USA) and GraphPad Prism (v9.4.0, GraphPad Software Inc.; San Diego, USA). All data are summarised as mean ± SEM of *n* arteries, where *n* denotes biological replicates. All datasets have sample sizes greater than or equal to 5, unless specified. All datasets are unpaired (non-repeated measures between treatments), unless specified.

Concentration-response curves were fitted using variable slope nonlinear regression. Normality was assessed using a Shapiro-Wilk test. Parametric analysis was performed if all datasets passed the normality test. Parametric data were analysed using a paired/unpaired t-test. Non-parametric data were analysed using a Mann-Whitney (paired) or Wilcoxon (unpaired) test. Concentration-response curves were analysed using mixed-effects analysis with Sidak's multiple comparisons test. $P < 0.05$ was considered statistically significant.

CHAPTER 3: EFFECTS OF CGRP ON ISOLATED RAT MESENTERIC AND CORONARY ARTERIES

3.1 Introduction

CGRP has been shown to cause a potent vasorelaxation in several vascular beds. It has been well-documented that the vasodilator activity of several agonists varies depending on the vascular bed, as well as the size of the vessel (Lüscher et al., 1990). It is likely that this is also true for CGRP; some have reported that the sensitivity to CGRP is greater in small coronary vessels (Gupta et al., 2006; Sheykhzade & Berg Nyborg, 1998), while others argue that CGRP has a greater effect on epicardial arteries compared to the smaller, resistance arteries in the myocardium (Ludman et al., 1991; Sekiguchi et al., 1994). While CGRP-induced vasorelaxation in the rat mesenteric vascular bed is particularly well-characterised (De Mey et al., 2008b; Han et al., 1990; Kawasaki et al., 1988; Marshall et al., 1986), the existing data for the effects of CGRP on coronary vessels and its underlying signalling pathways mainly utilise the aorta or larger, epicardial vessels, such as the LAD coronary artery, as these are more readily accessible. While these investigations are undoubtedly important, it is becoming increasingly clinically relevant to study the smaller vessels of the coronary microvasculature, and the fact that CGRP-induced vasorelaxation appears to change with vessel calibre means that the physiology of the microcirculation should not be inferred from larger coronary vessels.

It is challenging to directly study the coronary microvasculature *in vivo* as current imaging techniques have poor resolution. As such, studies utilising *ex vivo* techniques with isolated, intact arteries are fundamental for progressing our understanding of how coronary microvessels are modulated and the underlying signalling mechanisms. Wire myography has been used extensively to study the effects of CGRP on isolated vessels from various vascular beds but, as discussed above, only a few have investigated small,

coronary arteries in this way (Labruijere et al., 2013; Prieto et al., 1991; Sheykhzade & Berg Nyborg, 1998; Sheykhzade & Berg Nyborg, 2001). On the other hand, despite more closely resembling the physiological state of the artery *in vivo*, pressure myography is rarely used in the study of the microvasculature. Edvinsson et al. (2007) used this technique to investigate CGRP-induced vasodilation in the middle cerebral artery but the effects of CGRP on intact, pressurised coronary microvessels has never been studied. Furthermore, it has been reported that the effects of CGRP vary depending on the stimulus used for pre-constriction (Prieto et al., 1991; Sheykhzade & Berg Nyborg, 2001). Although it has been shown that coronary arteries will develop spontaneous myogenic tone *ex vivo* (Dora et al., 2022a; Dora et al., 2022b; Garcia et al., 1997; Takeda et al., 2019), as they would physiologically *in vivo*, there do not appear to be any studies that have relied on myogenic tone to provide a baseline level of contraction when investigating the vasodilatory effects of CGRP.

The presence of the components of the CGRP1 receptor (CLR, RAMP1, and RCP) have been confirmed in human coronary arteries using RT-PCR (Gupta et al., 2006; Hasbak et al., 2003a) and immunohistochemical techniques (Chan et al., 2010; Hagner et al., 2001); however, this has not been demonstrated in rat small coronary arteries using these techniques. An obvious limitation when studying the individual components of the CGRP1 receptor is that their presence, either at the mRNA or protein level, does not necessarily mean they associate to confer a functional role. As a result, studies have aimed to characterise the CGRP1 receptor using pharmacological techniques, utilising specific CGRP1 receptor antagonists. One such antagonist is the C-terminal fragment, CGRP 8-37, first described by Chiba et al. (1989). It has been widely used in CGRP1 receptor characterisation studies (Poyner, 1992), including in rat intramural (Sheykhzade &

Nyborg, 1998) and porcine coronary arteries (Foulkes et al., 1991). The limitations of peptide compounds, including weak membrane permeability and poor *in vivo* stability, led to the development of small molecule CGRP1 receptor antagonists that may have therapeutic potential for the treatment of migraines. Doods et al. (2000) first described the use of BIBN4096BS as a high affinity and selective non-peptide CGRP1 antagonist. Studies have demonstrated that BIBN4096BS is more selective than CGRP 8-37 for CLR/RAMP1 over CLR/RAMP2 (Hay et al., 2002), indicating that it may be a more effective antagonist experimentally as well as therapeutically. It has been shown that BIBN4096BS is effective in inhibiting CGRP-induced vasorelaxation in mouse aorta and mesenteric arteries (Grant et al., 2004) as well as human coronary, cerebral and subcutaneous arteries (Edvinsson et al., 2002b; Sheykhzade et al., 2004) where it has been utilised to investigate CGRP1 receptor expression in these vascular beds.

3.1.1 Aims and hypotheses

It was hypothesised that CGRP would be a potent vasodilator in both the rat mesenteric and septal arteries. It was necessary to characterise this response before further investigations; therefore, the aims of the present study were as follows:

i. Characterise the effects of CGRP in isolated rat mesenteric and septal arteries in both the wire and pressure myograph.
ii. Characterise the CGRP1 receptor antagonists, CGRP 8-37 and BIBN4096BS, in these vessels.

3.2 Materials and Methods

3.2.1 Wire myography

Mesenteric and septal arteries were prepared for wire myography chambers, as described in Section 2.2. In wire myography experiments, arteries were normalised to a resting tension equivalent to that generated at 90% of the diameter of the vessel at 70 mmHg (mesenteric) and 80 mmHg (septal).

3.2.2 Pressure myography

Mesenteric and septal arteries were prepared for pressure myography experiments, as described in Section 2.3. In pressure myography experiments, intraluminal pressure was set at 70 mmHg (mesenteric) or 80 mmHg (septal).

3.2.3 Inhibitors

The following drugs were used in this chapter to inhibit their respective targets, at concentrations which have been previously shown to be effective but were further optimised for use in the present study: 1–3 μM CGRP 8-37 to inhibit CGRP1 receptors (Hasbak et al., 2003a) and 10 nM–1 μM BIBN4096BS to inhibit CGRP1 receptors (Edvinsson et al., 2002b).

3.3 Results

3.3.1 CGRP causes vasorelaxation of rat mesenteric arteries under isometric conditions

Cumulative CGRP concentration-response curves (0.1 pM–10 nM) were conducted in isolated rat mesenteric arteries mounted in the wire myograph. Arteries were pre-constricted with a sub-maximal concentration of PE (1–3 μM). CGRP caused a slowly developing, potent vasorelaxation that did not tend to plateau (Figure 3.3.1A). For this reason, each concentration was added for 2 minutes and values for relaxation were taken at this time point. Using this defined protocol, CGRP had an EC_{50} of 6.4 pM ($logEC_{50}$ = -11.4 ± 0.3; *n* = 7–12; Figure 3.3.1B).

3.3.2 CGRP causes vasodilation of rat mesenteric arteries under isobaric conditions

Cumulative CGRP concentration-response curves (0.1 pM–10 nM) were carried out using mesenteric arteries which had been cannulated and pressurised. Arteries were pre-constricted with a sub-maximal concentration of PE (1–3 μM). CGRP caused a dose-dependent vasodilation with EC_{50} 0.6 pM ($logEC_{50}$ -11.9 ± 0.3; *n* = 10; Figure 3.3.1B-C, which was not significantly different to that observed in arteries mounted in the wire myograph ($logEC_{50}$ -11.4 ± 0.3; *n* = 10–12; Figure 3.3.1B).

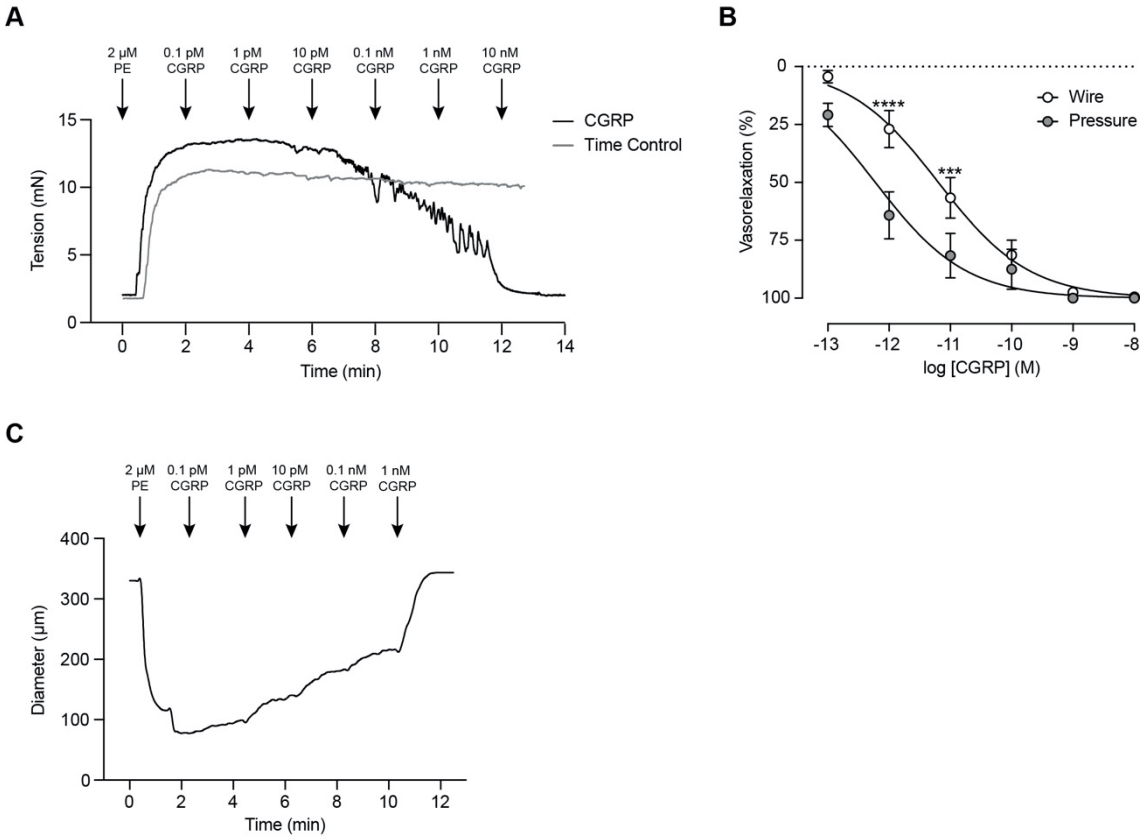

Figure 3.3.1 Effect of CGRP in mesenteric arteries. (**A**) Representative trace showing the effects of cumulative CGRP administration on tension compared to a paired time control following PE pre-constriction. CGRP was added at 2-minute intervals. (**B**) Cumulative concentration-response curves summarising relaxation to CGRP under isometric (wire) and isobaric (pressure) conditions. (**C**) Representative trace showing the effects of cumulative CGRP administration at 2-minute intervals on artery outer diameter. Data are means ± SEM; $n = 7–12$; ***$P < 0.0005$, ****$P < 0.0001$ compared to wire at the same concentration using mixed-effects analysis with Sidak's multiple comparisons test.

3.3.3 CGRP causes vasorelaxation of rat septal arteries under isometric conditions

Cumulative CGRP concentration-response curves (0.1 pM–10 nM) were conducted in isolated rat septal arteries mounted in the wire myograph. Arteries were either pre-constricted with a sub-maximal concentration of PE (1–5 μM) or concentration-response curves were carried out from myogenic tone (1.5 ± 0.1 mN/mm; n = 58; Figure 3.3.2A). CGRP caused a pronounced, concentration-dependent vasorelaxation from PE (EC_{50} 1.0 nM, $logEC_{50}$ -9.1 ± 0.1; n = 10–14) and from myogenic tone (EC_{50} 51 pM, $logEC_{50}$ -10.2 ± 0.2; n = 3–7; Figure 3.3.2B-C). However, pre-constriction with PE caused a significant and approximate 30-fold rightward shift in the CGRP response compared to that observed from myogenic tone. This shift appeared to be specific to CGRP, as vasorelaxation to ACh from PE pre-constriction (EC_{50} 11.1 nM) was identical to vasorelaxation from myogenic tone (EC_{50} 8.9 nM) and was not investigated further. Overall, the CGRP response in the septal arteries was significantly right shifted compared to the CGRP response in the mesenteric arteries, both from myogenic tone (P = 0.0037) and PE pre-constriction (P < 0.0001; Figure 3.3.2D). As a result, only arteries with myogenic tone were used to generate CGRP concentration-response curves in rat septal arteries for the remainder of this project.

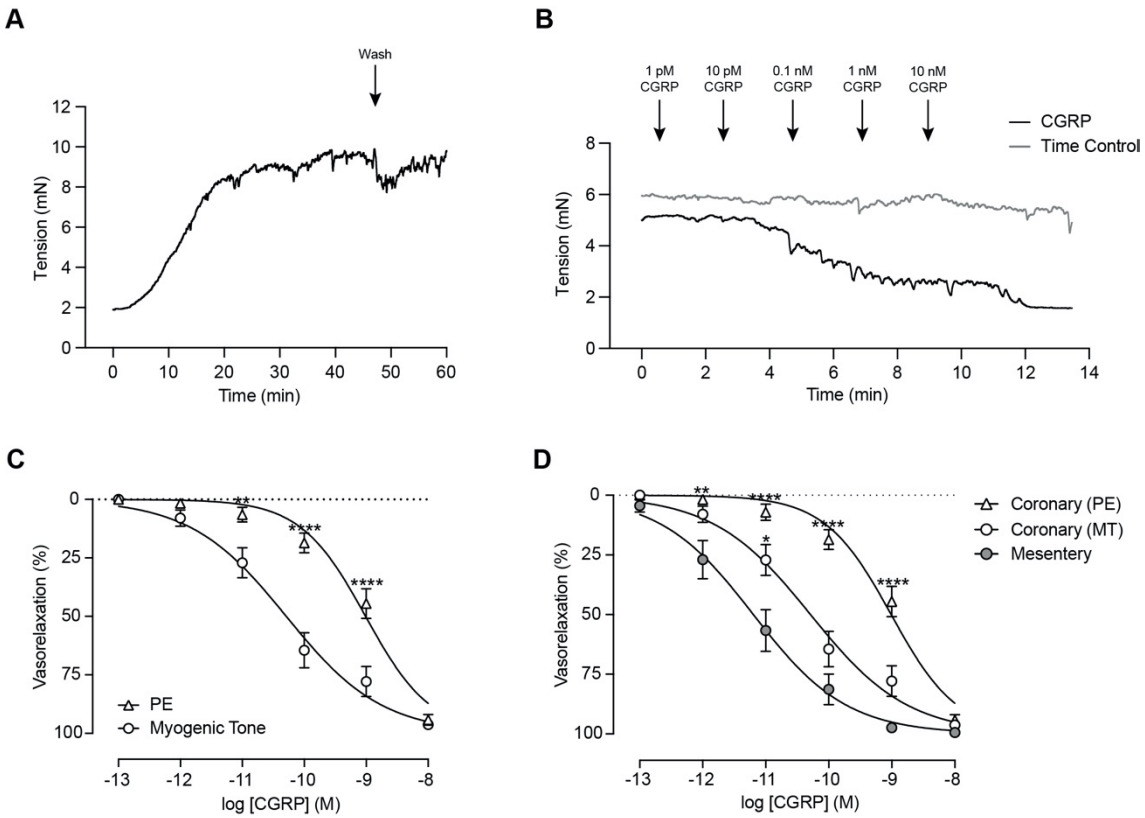

Figure 3.3.2 Effect of CGRP in septal arteries under isometric conditions. (**A**) Representative trace showing the development of spontaneous myogenic tone. The arrow indicates where the Krebs-buffered solution in the chamber was replaced. (**B**) Representative trace showing the effects of cumulative CGRP administration on tension from myogenic tone compared to a paired time control. CGRP was added at 2-minute intervals. (**C**) Cumulative concentration-response curves summarising relaxation to CGRP either from myogenic tone or following PE pre-constriction. (**D**) Cumulative concentration-response curves summarising relaxation to CGRP in mesenteric arteries, following PE pre-constriction, and in coronary septal arteries, either from myogenic tone or following PE pre-constriction. Data are means ± SEM; n = 3–14. *$P < 0.05$, **$P < 0.01$, ****$P < 0.0001$ compared to myogenic tone (C) or mesentery (D) at the same concentration using mixed-effects analysis with Sidak's multiple comparisons test.

3.3.4 CGRP causes vasodilation of rat septal arteries under isobaric conditions

Cumulative CGRP concentration-response curves (0.1 pM–10 nM) were carried out on septal arteries which had been cannulated, pressurised, and allowed to develop myogenic tone (32.9% ± 5.1, n = 5). CGRP causes a dose-dependent vasodilation with EC_{50} 0.7 nM ($logEC_{50}$ -9.2 ± 0.2; *n* = 6; Figure 3.3.3A-B). Interestingly, there was a significant and greater than 10-fold rightward shift compared to the CGRP-induced vasorelaxation from myogenic tone observed in septal arteries mounted in the wire myograph ($logEC_{50}$ -10.2 ± 0.2; *n* = 6-7; Figure 3.3.3B).

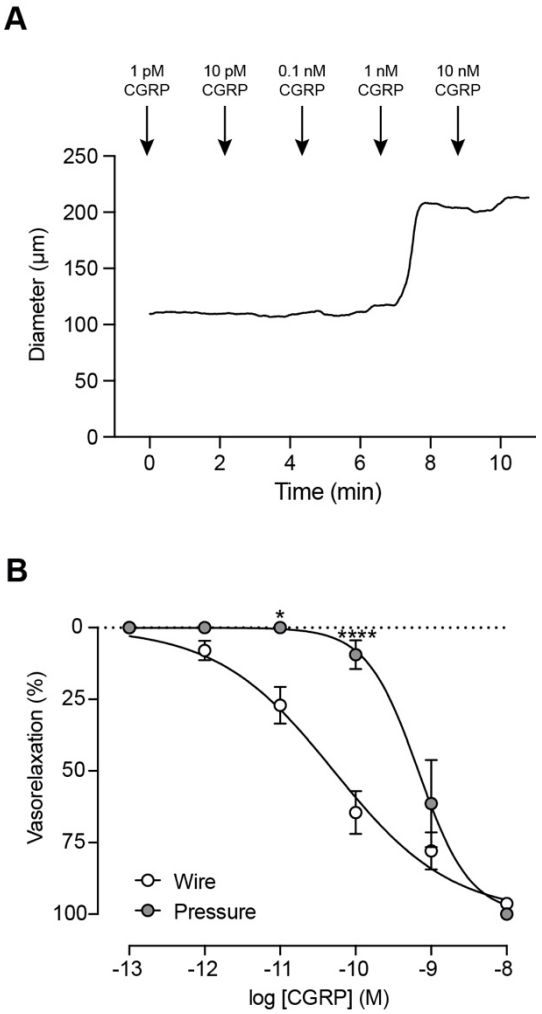

Figure 3.3.3 Effect of CGRP in septal arteries under isobaric conditions. (**A**) Representative trace showing the effects of cumulative CGRP administration on artery inner diameter from myogenic tone. CGRP was added at 2-minute intervals. (**B**) Cumulative concentration-response curves summarising relaxation to CGRP under isometric (wire) and isobaric (pressure) conditions. Data are means ± SEM; n = 3–6. *P < 0.05, ****P < 0.0001 compared to wire at the same concentration using mixed-effects analysis with Sidak's multiple comparisons test.

3.3.5 CGRP 8-37 inhibits CGRP-induced vasorelaxation in rat mesenteric and septal arteries

To confirm that exogenous CGRP was specifically binding to and activating the CGRP1 receptor, mesenteric and septal arteries were pre-incubated with CGRP1 receptor peptide antagonist, CGRP 8-37. We determined that 1 μM was an appropriate concentration to use, as 3 μM CGRP 8-37 did not result in a more pronounced inhibition of the CGRP response (n = 2–12; Figure 3.3.4A) and the pIC_{50} is reported to be 6.75 ± 0.12 in bovine cerebral vessels (Moreno et al., 2002). 1 μM CGRP 8-37 significantly inhibited CGRP-induced vasorelaxation in the mesenteric arteries, reducing relaxation to 0.1 nM CGRP from 89.4 ± 8.1% to 18.8 ± 12.3%, and relaxation to 1 nM CGRP from 97.5 ± 1.0 % to 33.2 ± 8.1% (n = 9–12; Figure 3.3.4B). In the septal arteries, 1 μM CGRP 8-37 also significantly inhibited CGRP-induced vasorelaxation, reducing relaxation to 1 nM CGRP from 77.9 ± 6.4% to 1.7 ± 1.7% and relaxation to 10 nM CGRP from 96.3 ± 1.3% to 20.8 ± 7.8% (n = 5–7; Figure 3.3.5A-B). As an observation, and while not significant, incubation with CGRP 8-37 tended to increase myogenic tone (n = 5; Figure 3.3.5C). In summary, these data indicate that exogenous CGRP is indeed activating the CGRP1 receptor and suggest that CGRP-induced vasorelaxation in the septal arteries is equally sensitive to inhibition by CGRP 8-37, yet the response to CGRP itself is less potent.

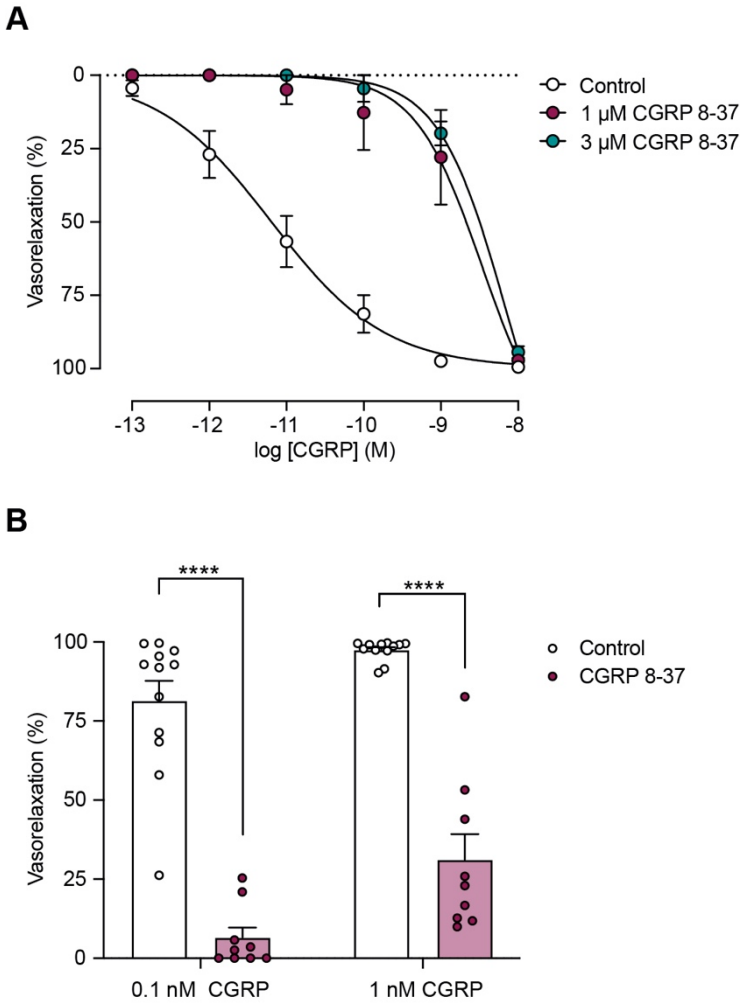

Figure 3.3.4 Effect of CGRP 8-37 on CGRP-induced vasorelaxation in mesenteric arteries. (**A**) Cumulative concentration-response curves summarising relaxation to CGRP in the absence and presence of 1 μM or 3 μM CGRP 8-37. Control data adapted from Figure 3.3.1. Treated data represents paired experiments. (**B**) Bar graph summarising relaxation to CGRP in the absence and presence of 1 μM CGRP 8-37. Control data adapted from Figure 3.3.1. Data are means ± SEM; $n = 2–12$. ****$P < 0.0001$ compared to control using Mann-Whitney test.

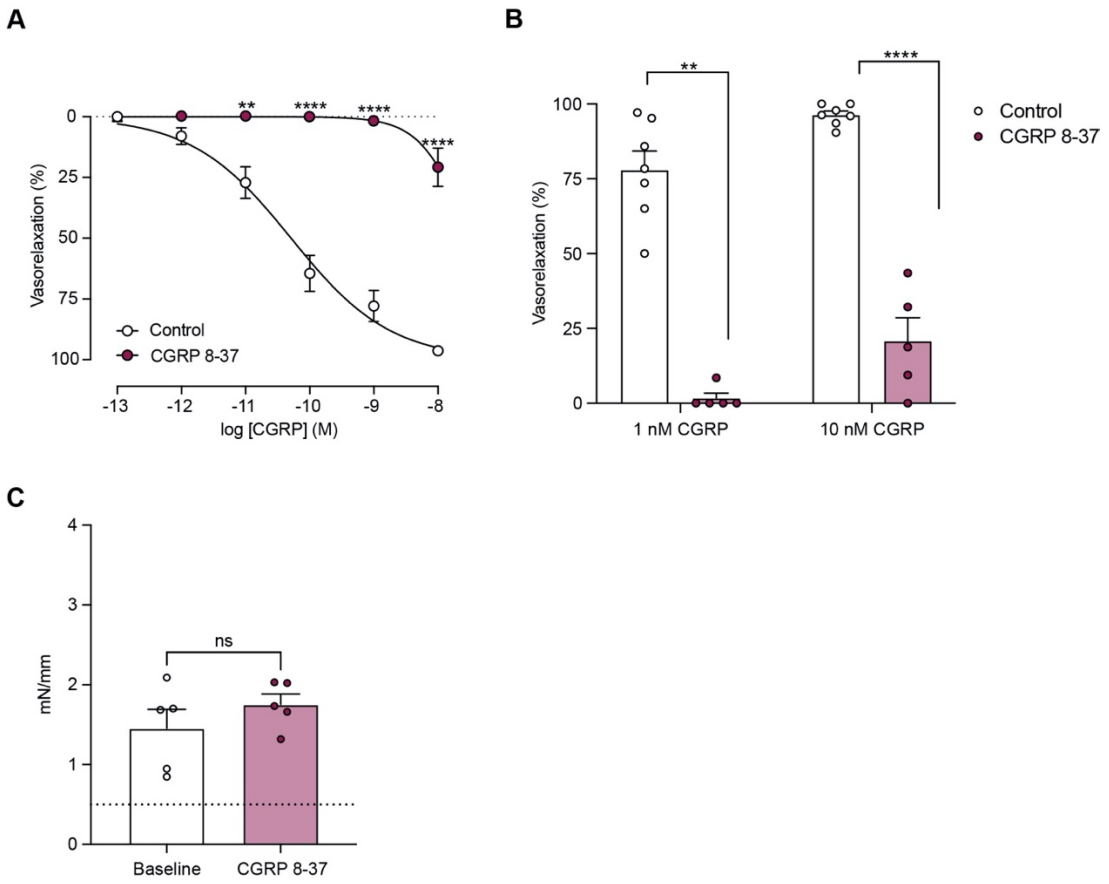

Figure 3.3.5 Effect of CGRP 8-37 on CGRP-induced vasorelaxation in septal arteries. Cumulative concentration-response curves (**A**) and bar graph (**B**) summarising relaxation to CGRP in the absence and presence of 1 μM CGRP 8-37. Control data adapted from Figure 3.3.2. (**C**) Bar graph summarising the level of myogenic tone in the absence and presence of 1 μM CGRP 8-37. Data represents paired experiments. The dotted line represents the minimum mN/mm required to consider an artery as being myogenically active. Data are means ± SEM; n = 5–7. **$P < 0.005$, ****$P < 0.0001$ compared to control using mixed-effects analysis with Sidak's multiple comparisons test (A), Mann-Whitney test (B), or paired t test (C).

3.3.6 BIBN4096BS inhibits CGRP-induced vasorelaxation in rat mesenteric and septal arteries

We also investigated the effect of the small molecule non-peptide antagonist, BIBN4096BS, on CGRP-induced vasorelaxation. First, mesenteric arteries were pre-incubated with a range of BIBN4096BS concentrations (1 nM–1 μM). It is worth noting that only 3 concentrations of CGRP were tested, with the aim of providing an index of effectiveness of antagonism by BIBN4096BS. Inhibition of the CGRP response was observed at concentrations of 10 nM–1 μM BIBN4096BS in a concentration-dependent manner (n = 3–5; Figure 3.3.6A). From these data, we decided to use 0.1 μM BIBN4096BS in further investigations as this caused a parallel, >10-fold rightward shift of the CGRP concentration-response curve. In the mesenteric vessels, 0.1 μM BIBN4096BS significantly inhibited CGRP-induced vasorelaxation, with the response to 0.1 nM CGRP being reduced from 81.4 ± 6.4% to 0.3 ± 0.3% and the response to 1 nM CGRP being reduced from 97.5 ± 0.9% to 9.2 ± 2.5% (n = 3–12; Figure 3.3.6B). In the septal arteries, BIBN4096BS caused a potent and significant inhibition of CGRP-induced vasorelaxation, with the response at 1 nM CGRP being reduced from 77.9 ± 6.4% to 2.1 ± 2.1 % and the response to 10 nM CGRP being reduced from 96.3 ± 1.3% to 14.5 ± 2.7% (n = 5–7; Figure 3.3.7A-B). The same observation was made with BIBN4096BS which tended to, but did not significantly, increase myogenic tone (n = 7; Figure 3.3.7C). These findings confirm that BIBN4096BS is an effective antagonist in these arteries and, similarly to CGRP 8-37, CGRP-induced vasorelaxation in both the mesenteric and septal arteries is equally sensitive to inhibition by BIBN4096BS. Furthermore, we are confident that the exogenous rat CGRP used in the present study is binding to and activating the CGRP1 receptor as expected.

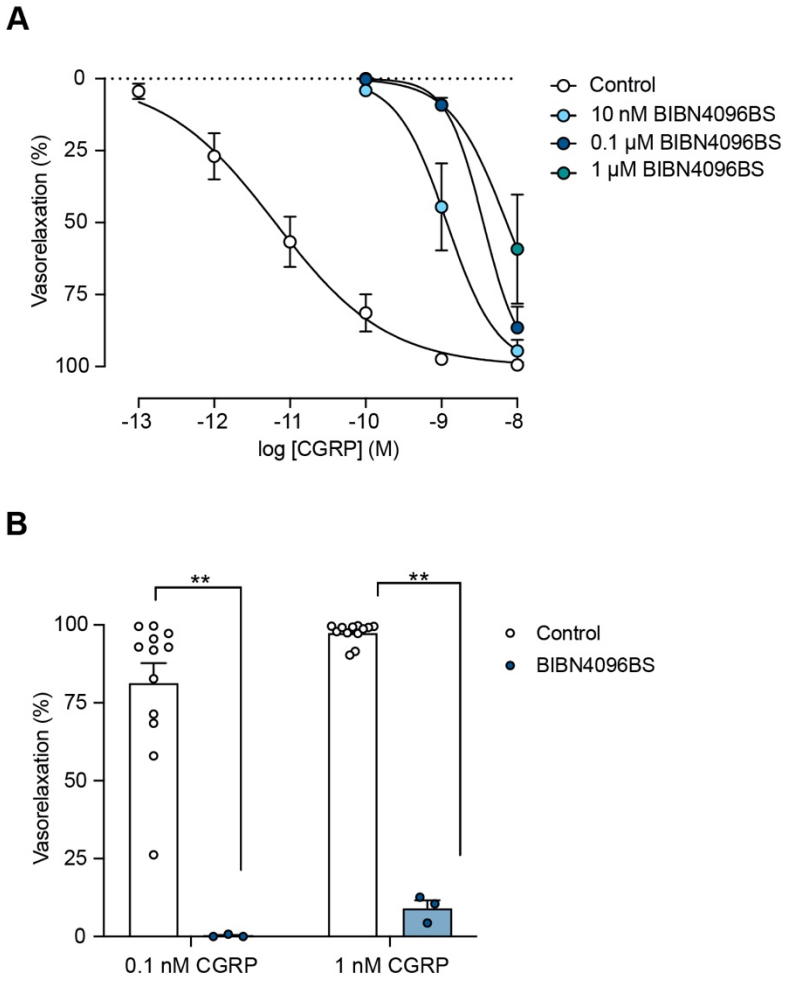

Figure 3.3.6 Effect of BIBN4096BS on CGRP-induced vasorelaxation in mesenteric arteries. (**A**) Cumulative concentration-response curves summarising relaxation to CGRP in the absence and presence of 10 nM, 0.1 µM, and 1 µM BIBN4096BS. (**B**) Bar graph summarising relaxation to CGRP in the absence and presence of 0.1 µM BIBN4096BS. Control data adapted from Figure 3.3.1. Data are means ± SEM; n = 3–12. **$P < 0.005$ compared to control using Mann-Whitney test.

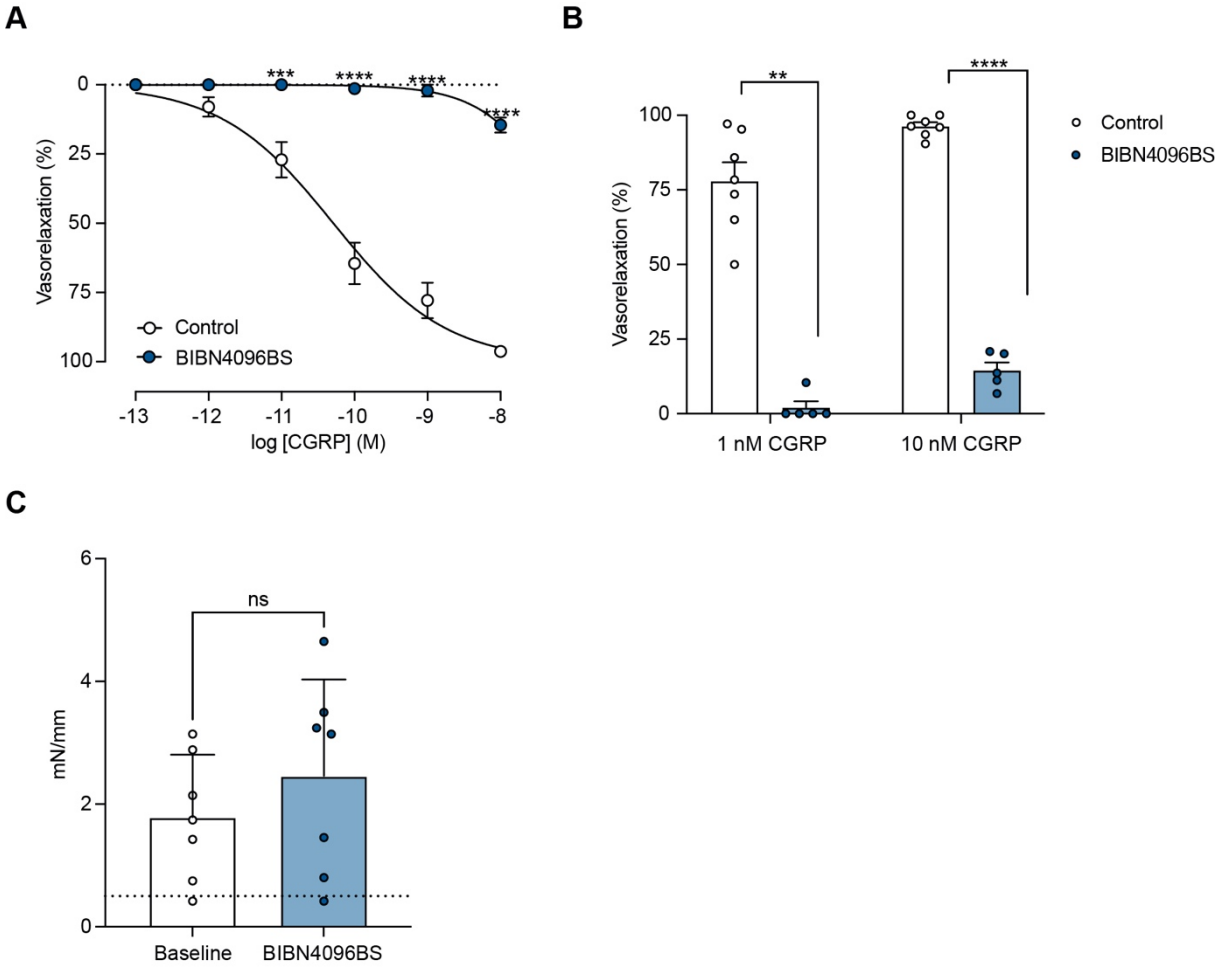

Figure 3.3.7 Effect of BIBN4096BS on CGRP-induced vasorelaxation in septal arteries. Cumulative concentration-response curves (**A**) and bar graph (**B**) summarising relaxation to CGRP in the absence and presence of 0.1 μM BIBN4096BS. Control data adapted from Figure 3.3.2. (**C**) Bar graph summarising the level of myogenic tone in the absence and presence of 0.1 μM BIBN4096BS. Data represents paired experiments. The dotted line represents the minimum mN/mm required to consider an artery as being myogenically active. Data are means ± SEM; n = 5–7. ***$P < 0.0005$, ****$P < 0.0001$ using mixed-effects analysis with Sidak's multiple comparisons test (A), Mann-Whitney and unpaired t test (B), or paired t test (C).

3.4 Discussion

The present study aimed to characterise the response to CGRP in isolated rat mesenteric and septal arteries, as well the CGRP1 receptor antagonists, CGRP 8-37 and BIBN4096BS. These data support the hypothesis that CGRP is a potent vasodilator in both mesenteric and septal arteries and confirm that both antagonists are effective at inhibiting the CGRP response in these vessels.

We observed a gradual but potent relaxation to CGRP in both the mesenteric and septal arteries. As the response to CGRP was slow, in comparison to the rapid relaxation response to agonists such as ACh, we developed a protocol where 2 minutes was left between the addition of each concentration; all further investigations will follow this protocol. Analysis of the CGRP-response in mesenteric vessels was challenging at the lower concentrations of CGRP because it was often unclear whether changes in tension or diameter were in response to CGRP or due to fade of the PE pre-constriction. Although time controls were conducted, data interpretation at these lower concentrations often required a degree of subjectivity, whereas this was not the case in the coronary arteries where pre-constriction to PE or myogenic tone was well-maintained. Interestingly, the CGRP response observed in the cannulated, pressurised septal arteries was significantly right shifted compared to the vessels mounted in the wire myograph. The opposite was true in the mesenteric arteries, where the CGRP response in the pressurised vessels was significantly left shifted compared to those mounted in the wire myograph. It appears that this observation is due to differences between vascular beds rather than methodology, although this was not investigated further.

We found that PE significantly attenuated CGRP-induced vasorelaxation in the septal arteries, compared to when concentration-response curves were conducted from myogenic tone. Several studies have commented on the effects of pre-constrictors on CGRP-induced vasorelaxation. Prieto et al. (1991) found that the relaxation to CGRP was greater in proximal coronary arteries sub-maximally contracted with prostaglandin $F_{2\alpha}$ ($PGF_{2\alpha}$) than those maximally contracted, although no difference was seen in distal coronary arteries. Many studies use KCl to pre-constrict vessels, but Shoji et al. (1987) observed that pre-constriction with 50 mM KCl prevented vasorelaxation to CGRP in porcine coronary arteries. This is unsurprising as K^+ channels have been widely implicated in the CGRP response and increasing the external [K^+] will inhibit their activation. These findings emphasise that the pre-constricting agent used must be taken into careful consideration when conducting these experiments. Using our methodology, the septal arteries routinely develop spontaneous myogenic tone; this not only provides a more accurate representation of the physiological state of the arteries *in vivo*, but also removes the need to use a pre-constrictor that may interfere with CGRP-induced vasorelaxation. This is the first study to investigate the effects of CGRP from myogenic tone, and thus the responses seen will hopefully more closely resemble those that one would expect to see *in vivo*.

Interestingly, the mesenteric arteries appear to be more sensitive to CGRP, with the vasorelaxation curve being left-shifted compared to the coronary arteries, despite relying on PE pre-constriction. This could be explained by differential CGRP receptor expression between these vascular beds, with the mesenteric arteries exhibiting a greater CGRP1 receptor density than the coronary arteries. It is known that the CGRP1 receptor components, CLR and RAMP1, are present on both the VSMCs and ECs in mesenteric

arteries (Boerman & Segal, 2016; Sheykhzade et al., 2017). These receptor components are also present in human coronary arteries (Hasbak et al., 2003a), but whether they are expressed on both VSMCs and ECs in coronary microvessels is yet to be conclusively determined. Furthermore, existing studies have employed immunohistochemical techniques rather than techniques that would allow expression quantification and thus comparison between vascular beds and cell types. Another possible explanation for the increased sensitivity of rat mesenteric arteries to CGRP compared to septal arteries could be that there is heterogeneity in the coupling to downstream signalling pathways. The mechanisms underlying CGRP-induced vasorelaxation in the coronary microvasculature are currently understudied and, as such, further investigation is necessary which will be the focus of the next chapters. Alternatively, CGRP may have an additional non-specific effect in the mesenteric vascular bed. Recent evidence has proposed that CGRP may also be able to bind to and exert effects via the amylin receptor, $AMY_{1(a)}$ (Hay et al., 2018). Amylin is co-secreted from the pancreas with insulin and is important in glycaemic regulation, but there are also studies that suggest amylin can have vasorelaxant effects in the pulmonary circulation and human skin (Golpon et al., 2001; Hasbak et al., 2006). While there is currently no evidence for the expression of $AMY_{1(a)}$ receptors in the rat mesenteric arteries, there may indeed be $AMY_{1(a)}$ receptors present which could explain the increased sensitivity of these vessels to CGRP.

Many studies have utilised CGRP1 receptor antagonists to characterise CGRP-induced vasorelaxation in different vascular beds. A wide range of pA_2 values have been reported for CGRP 8-37 in different vascular beds (Poyner et al., 2002). Foulkes et al. (1991) calculated that CGRP 8-37 had a pA_2 of 8.50 in the perfused rat mesenteric bed, which was similar to small diameter porcine coronary arteries where it had a pA_2 of 8.67. It is

important to note that CGRP-induced vasorelaxation in porcine coronary arteries is endothelium-independent, while it is endothelium-dependent in the mesenteric arteries, so this may not be a justified comparison. We demonstrated that 1 μM CGRP 8-37 significantly inhibited the response to CGRP in both mesenteric and coronary septal arteries. It is important to note that, while our results do not appear to show any significant differences in potencies between these vascular beds, these experiments would need to be conducted more systematically in the future to provide more rigorous analysis.

This study also confirmed the effectiveness of BIBN4096BS for use in rat coronary arteries, which is the first time that BIBN4096BS has been characterised in these vessels. Although it is more selective for human CGRP1 receptors than rat CGRP1 receptors (Doods et al., 2000; Hay et al., 2002), we observed a potent and significant inhibition of CGRP-induced vasorelaxation in the septal arteries with 0.1 μM BIBN4096BS. Edvinsson et al. (2002a) reported similar results in human coronary arteries, where BIBN4096BS had a pA_2 of 10.4. Comparatively to CGRP 8-37, our results indicate that BIBN4096BS has a similar potency in the mesenteric and coronary septal arteries. BIBN4096BS, or olcegepant, was originally investigated for use as an anti-migraine drug and had promising results in phase I/II clinical trials but later failed due to concerns with liver toxicity and drug administration. Although short-term use was not found to have adverse effects on haemodynamic properties (e.g.: blood pressure, coronary flow, and heart rate), concerns have been raised about the long-term use of CGRP1 receptor antagonists on the cardiovascular system (Favoni et al., 2019; MaassenVanDenBrink et al., 2016). Interestingly, BIBN4096BS had a pA_2 value of 10.1 in human cerebral arteries, similar to human coronary arteries (Edvinsson et al., 2002b). As such, this antagonist would likely have similar potencies in both vascular beds; therefore, it is relevant to

continue to study the effects of CGRP1 receptor antagonists on the cardiovascular system to reduce the risk of migraine therapies having adverse off-target effects in patients in the future.

3.5 Conclusions

The current study aimed to characterise the CGRP response in rat mesenteric and coronary arteries, and the effect that CGRP1 receptor antagonists had on this response. These findings confirm the hypothesis that CGRP is a potent vasodilator in both rat mesenteric and septal arteries and, in this way, is a clinically relevant endogenous agonist that requires further investigation, particularly in the coronary microvasculature.

The effects of CGRP in mesenteric arteries have been well-characterised and the need to use a pre-constricting agent in these vessels makes it difficult to study CGRP at low concentrations as it can be challenging to determine whether a small decrease in tension is the result of preconstrictor fade or a response to CGRP. In contrast, the mechanisms underlying CGRP-induced vasorelaxation are unknown in the septal arteries. Importantly, CGRP concentration-response curves can be conducted from myogenic tone to remove the possibility of pre-constricting agents obscuring the true response and to reflect the physiological state of the arteries *in vivo* more closely. We demonstrated CGRP-induced vasorelaxation using 2 *ex vivo* techniques: wire and pressure myography. While both techniques offer their own advantages, cannulating and pressurising coronary arteries is particularly technically challenging due to the large number of side branches in these vessels. As a result, further investigations will mainly utilise the wire myograph where septal arteries can be mounted and studied more readily.

We observed that the mesenteric arteries appear to be more sensitive to CGRP than the septal arteries. This is likely to reflect the heterogeneity between these vascular beds, but the precise explanation is yet to be determined. These data also confirm that both CGRP

8-37 and BIBN4096BS are effective inhibitors of CGRP-induced vasorelaxation in both mesenteric and coronary arteries, thus demonstrating that CGRP is indeed acting via the CGRP1 receptors. It is important to note that these experiments did not distinguish between EC- and VSMC-mediated effects, which will be the focus of the next chapter.

CHAPTER 4: CONTRIBUTION OF THE ENDOTHELIUM IN CGRP-INDUCED VASORELAXATION

4.1 Introduction

The importance of the endothelium in CGRP-induced vasorelaxation is inconsistent between vascular beds and species. Endothelium removal abolishes the CGRP response in rat aorta (Brain et al., 1985; Gray & Marshall, 1992a) and mesenteric arteries (Iwatani et al., 2008), but has no effect in cat cerebral (Edvinsson et al., 1985) or porcine coronary arteries (Yoshimoto et al., 1998). Interestingly, Prieto et al. (1991) found that removing the endothelium attenuated CGRP-induced vasorelaxation in rat proximal epicardial coronary arteries, but not in distal myocardial coronary arteries. The disparity between these studies emphasises the need for further investigation into the role of the endothelium in the CGRP response, particularly in the heart where its role appears to be heterogeneous throughout the coronary vascular bed.

The endothelium-dependent component of the CGRP response is often attributed to NO. Gray and Marshall (1992a) described how haemoglobin, which binds NO; methylene blue, which blocks cGMP production; and L-NOARG, which inhibits NOS, all attenuated CGRP-induced vasorelaxation in rat thoracic aortic rings, thus suggesting a role for NO synthesis and release in the CGRP response. Other studies have demonstrated that, despite observing an attenuated response to CGRP following endothelium removal, CGRP-induced vasorelaxation did not involve an increase in cGMP levels (Grace et al., 1987; Prieto et al., 1991). Iwatani et al. (2008), on the other hand, observed an augmentation of CGRP-induced vasorelaxation following endothelium removal or L-NAME treatment in the rat mesenteric vascular bed. This disparity in the literature is again likely to reflect differences between vascular beds and vessel sizes, especially as it is known that the influence of NO differs between coronary resistance and conduit vessels

(Jones et al., 1995; Nishikawa & Ogawa, 1997). It is necessary, therefore, to confirm whether NO is indeed the relaxing factor being released by the endothelium in response to CGRP, and whether this is contributing to the basal level of myogenic tone in the resistance vessels used in this study.

It is widely believed that CGRP activates the Gαs-mediated signalling pathway to cause cAMP accumulation and the subsequent activation of PKA (Russell et al., 2014; Sohn et al., 2020). While this pathway and its downstream targets has been studied extensively in VSMCs in response to CGRP, there are only a handful of studies that directly investigate the underlying signalling pathways in the ECs. CGRP has been shown to stimulate cAMP formation in HUVECs (Clark et al., 2021; Haegerstrand et al., 1990) but this has not yet been observed directly in the ECs of isolated arteries. Studies conducted in non-vascular cultured cells have also provided evidence that CGRP can activate the PLC-IP_3 pathway, potentially via a cAMP-independent mechanism mediated by the $G\alpha_{q/11}$ subunit (Drissi et al., 1998; Laufer & Changeux, 1989). While this might appear unlikely, there is evidence that PLC can be activated by the dissociated Gβγ subunit of some receptors (Camps et al., 1992), and as such may play a role. In ECs, we would expect activation of the PLC-IP_3 pathway to be coupled to an increase in intracellular Ca^{2+}, and this has been observed in response to CGRP in HEK-293 cells (Aiyar et al., 1999), OHS-4 cells (Drissi et al., 1998), and pulmonary EC tubes (Norton & Segal, 2018). Further exploration into the signalling pathways underlying CGRP-induced vasorelaxation is necessary to determine whether CGRP exerts its endothelium-dependent effects via the Gαs-mediated cAMP-PKA, or whether other signalling pathways are involved.

It would be useful to be able to detect and quantify NO synthesis and release in isolated vessels; however, measurement of NO is technically challenging due to its ability to readily react with other biological molecules and short half-life of sub-seconds *in vivo*, although this may be increased to minutes in the absence of oxyhaemoglobin in buffered solution *in vitro* (Liu et al., 1998). The current experimental approaches used to quantify NO have been extensively reviewed (Bryan & Grisham, 2007; Csonka et al., 2015; Moller et al., 2019), but several of these methods have technical limitations for use in pressurised arteries (Table 1.4.1). The development of NO-sensitive fluorescent dyes (NO-dyes) in recent years has offered a more promising solution for NO measurement. Diaminobenzene-based fluorophores were the first NO-dyes to be developed, such as diaminofluorosceins (DAFs) and diaminorhodamine (DARs); however, both have properties which limit their use is isolated arteries. DAF-2 fluorescence was shown to increase in the presence of Ca^{2+}, as well as NO, (Broillet et al., 2001) and DAR-4M fluorescence was affected by other oxidants in biological samples (Lacza et al., 2005), meaning that both NO-dyes would be challenging to use in living arteries. A potential solution is a transition-metal complex, CuFl, prepared by adding a fluorescein derivative to copper(II) chloride ($CuCl_2$). It was first developed by Lim (2007), who described its use for detecting NO in cultured cells. The advantages of this sensor are that it is cell permeable, non-toxic, and both highly specific and sensitive to NO. McQuade et al. (2010) advanced this NO-dye for use in biological systems by developing Cu_2FL2E: a cell-trappable probe that does not diffuse out of the cells, and can thus be utilised in experiments where intact tissue must be continually perfused. A study by Ghosh et al. (2013) demonstrated the use of Cu_2FL2E in isolated, pressurised mouse carotid artery and aorta with promising results; however, these protocols have required high concentrations of Cu^{2+} and DMSO which have been shown to cause arterial dysfunction

Table 4.1.1: Summary of methods to measure NO in biological samples

Technique	Method	Advantages	Disadvantages
Electron paramagnetic resonance (EPR) spectroscopy	NO spin trapping followed by spectrometry in magnetic field	Direct; specific	NO_2· production may interfere; requires specialised equipment; complex
Oxyhaemoglobin oxidation	Measure oxidation of oxyhaemoglobin by NO· using spectrophotometry	Sensitive; provides effective quantification *in vitro*	Nitrite and peroxynitrite also oxidise oxyhaemoglobin so may interfere
Electrochemical sensor	Amperometry or voltammetry using NO-specific electrode	Specific; direct; real-time; commercially available	Difficult to calibrate; influenced by temperature, ambient electrical noise, and electrode tip position
Griess assay	Diazotization assays measures nitrite by photometry	Cheap; fast; accessible	Indirect measurement
Chemiluminescence	NO· reacts with O_3 to produce NO_2*·, which produces light emission as it decays that can be measured	Sensitive; reproducible; can be used with any gas or liquid sample	Indirect measurement
Fluorogenic probes	Spectrometry or imaging of fluorophore-labelled NO	Membrane permeable; direct; sensitive; can be both 2D and 3D	Uncertain specificity; semiquantitative; pH and Ca^{2+} may interfere with signal
Measuring NOS activity	Biochemical enzyme activity assay that measures citrulline formation	Measures NO production; specific; sensitive	Indirect measurement; may not mimic *in vivo* NO synthesis
Bioassays	e.g.: cGMP levels; vessel relaxation; inhibition of platelet aggregation	Measures downstream signalling and effects of NO	Indirect measurement

(Wallis et al., 2023; Yi et al., 2017). Another major problem with the use of NO-dyes in intact arteries is that the binding of free NO to the dye is irreversible. This necessitates experimental design such that NO release is not stimulated to a large extent during dye loading. The Dora/Garland group has shown that 0.3% DMSO stimulates EC Ca^{2+} (unpublished), which would stimulate NO release; therefore, NO-dye loading itself might fully activate NO release and saturate the NO-dye. As a result, further optimisation of Cu_2FL2E NO-dye for use in *ex vivo* experiments would be useful in the present study for detecting NO synthesis and release in response to CGRP.

4.1.1 Aims and hypotheses

It was hypothesised in Chapter 3 that CGRP-induced vasorelaxation in rat septal arteries would have an endothelium-dependent component and, as such, the aims were as follows:

i. Determine the relative importance of the endothelium-dependent and -independent components in CGRP-induced vasorelaxation.
ii. Characterise the downstream signalling pathways of the CGRP response in the ECs.
iii. Optimise a NO-sensing dye for use in isolated, pressurised arteries.

4.2 Materials and Methods

4.2.1 Wire myography

Septal arteries were prepared for wire myography chambers, as described in Section 2.2. In all wire myography experiments, arteries were normalised to a resting tension equivalent to that generated at 90% of the diameter of the vessel at 80 mmHg. When necessary, ECs were removed with a hair and successful removal was confirmed by <10% relaxation to 1 μM ACh.

4.2.2 Pressure myography

Mesenteric and septal arteries were prepared for pressure myography experiments, as described in Section 2.3. In all pressure myography experiments, intraluminal pressure was set at 70 mmHg (mesenteric) or 80 mmHg (septal).

4.2.3 Calcium imaging

Septal arteries were prepared for pressure myography experiments (see Section 2.3). The ECs were selectively loaded with the Ca^{2+} indicator, Oregon Green 488 BAPTA-1 AM, until a clear signal was detected, as described in Section 2.5.

4.2.4 Cu_2FL2E

Cu_2FL2E was prepared for use at a 1 μM concentration with a working ratio 1:2, as described in Section 2.6.1. Cell-free experiments were performed in a 2 mL chamber secured to the stage of an inverted microscope, as described in Section 2.6.2. For Cu_2FL2E loading into intact arteries, mesenteric arteries were either prepared for pressure myography (See Section 2.3.1) or *en face* experiments (see Section 2.6.5) and the dye

was added to the chamber until a clear signal was detected, as described in Sections 2.6.4 and 2.6.5.

4.2.5 Inhibitors

The following drugs were used in this chapter to inhibit their respective targets, at concentrations which have previously been shown to be effective: 100 μM L-NAME to antagonise NOS (Garland & Dora, 2017).

4.3 Results

4.3.1 Removing the endothelium increases myogenic tone

Rat septal arteries will develop spontaneous myogenic tone, which provides a basal level of vasoconstriction. In arteries where the endothelium had been manually damaged (denuded), the level of myogenic tone significantly increased from a mean baseline of 1.30 ± 0.10 mN/mm to 3.87 ± 0.34 mN/mm (n = 12; Figure 4.3.1A). This observation suggests that the endothelium has an important influence over basal myogenic tone in these vessels.

4.3.2 Removing the endothelium attenuates CGRP-induced vasorelaxation

To assess whether there is an endothelium-dependent component in the vasorelaxation response to CGRP, cumulative CGRP concentration-response curves were repeated in denuded arteries. The CGRP-induced vasorelaxation was significantly attenuated in denuded arteries with a significant and approximate 30-fold rightward shift observed (EC_{50} 1.6 nM, log EC_{50} -8.9 ± 0.1; n = 14) compared to control (EC_{50} 51 pM, log EC_{50} -10.2 ± 0.2; n = 6–7; Figure 4.3.1B). However, unlike in the presence of the receptor antagonists, 10 nM CGRP was able to stimulate near maximal relaxation in denuded arteries (91.1 ± 3.9%, n = 14). This indicates that there is both an endothelium-dependent and -independent component contributing to CGRP-induced vasorelaxation, but the most potent component to CGRP-mediated relaxation is via the endothelium.

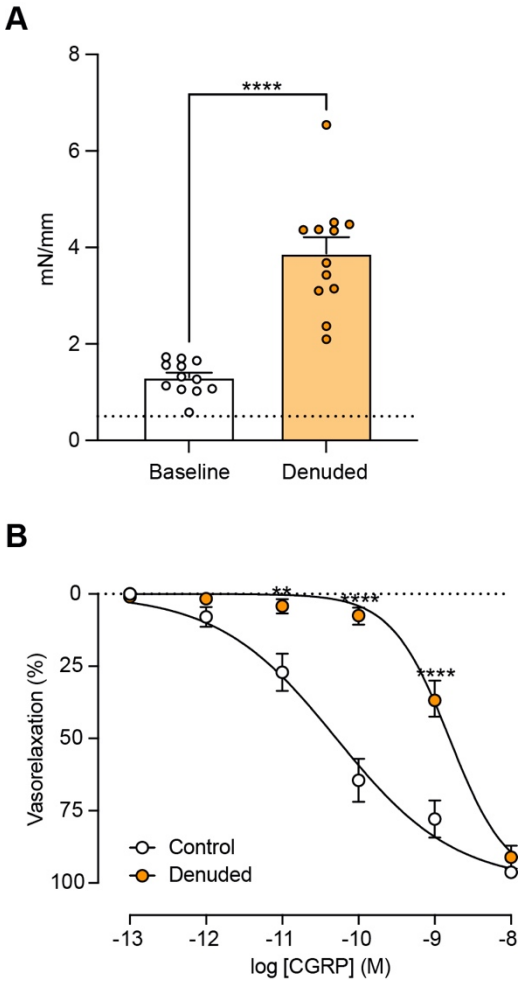

Figure 4.3.1 Effect of endothelium removal in septal arteries. (**A**) Bar graph summarising the level of myogenic tone before and after endothelium removal (denuding). Data represents paired experiments. The dotted line represents the minimum mN/mm required to consider an artery as being myogenically active. (**B**) Cumulative concentration-response curves summarising relaxation to CGRP in the absence and presence of the endothelium. Control data adapted from Figure 3.3.2. Data are means ± SEM; n = 6–14. $^{**}P < 0.005$, $^{****}P < 0.0001$ compared to control using paired t test (A) or mixed-effects analysis with Sidak's multiple comparisons test (B).

4.3.3 Nitric oxide synthase blockade increases myogenic tone

When the septal arteries were preincubated with the nitric oxide synthase (NOS) inhibitor, L-NAME (100 μM), the level of myogenic tone significantly increased from a baseline mean of 1.05 ± 0.09 mN/mm to 3.64 ± 0.33 mN/mm (n = 14; Figure 4.3.2A), like that observed in denuded vessels. This implies that NO is basally released from the endothelium and, in this way, influences the level of myogenic tone.

4.3.4 Nitric oxide synthase blockade attenuates CGRP-induced vasorelaxation

To investigate whether the endothelium-dependent component relies on NO synthesis and release, arteries were preincubated with the NOS inhibitor, L-NAME (100 μM). Blockade of NOS significantly attenuated CGRP-induced vasorelaxation (EC_{50} 1.4 nM, log EC_{50} -8.9 ± 0.1; n = 6) with an approximate 30-fold rightward shift being observed compared to control (EC_{50} 51 pM, log EC_{50} -10.2 ± 0.2; n = 6–7; Figure 4.3.2B). Again, 10 nM CGRP stimulated near maximal relaxation (97.3 ± 1.4%, n = 6). This suggests that the endothelium-dependent component is due to NO release and, at 10 nM CGRP, relaxation via signalling pathways in the smooth muscle are also involved.

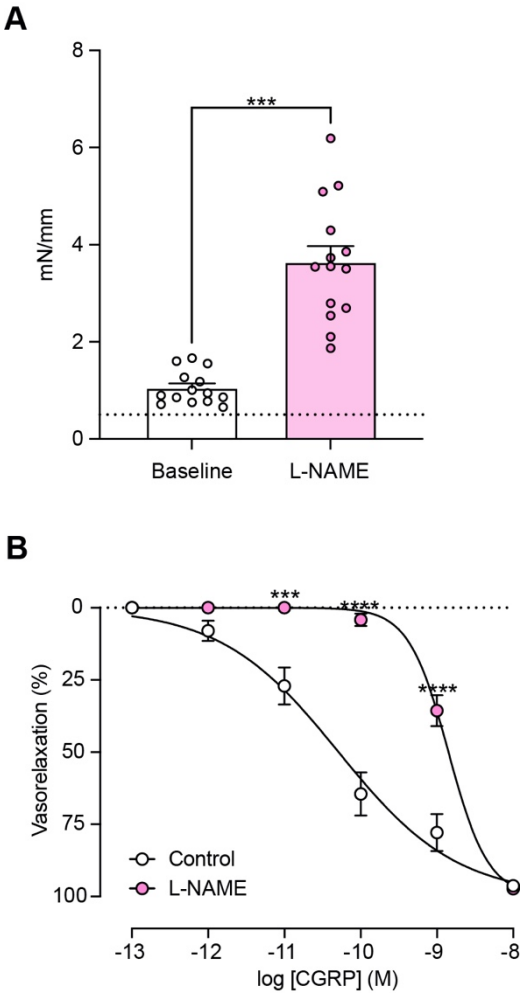

Figure 4.3.2 Effect of NOS inhibition on septal arteries. (**A**) Bar graph summarising the level of myogenic tone in the absence and presence of 100 μM L-NAME. Data represents paired experiments. The dotted line represents the minimum mN/mm required to consider an artery as being myogenically active. (**B**) Cumulative concentration-response curves summarising relaxation to CGRP in the absence and presence of 100 μM L-NAME. Control data adapted from Figure 3.3.2. Data are means ± SEM; n = 6–14. ***$P < 0.0005$, ****$P < 0.0001$ compared to control using Wilcoxon test (A) or mixed-effects analysis with Sidak's multiple comparisons test (B).

4.3.5 CGRP does not activate NOS via global intracellular Ca^{2+} release

NO synthesis and release can be activated by both Ca^{2+}-dependent and -independent pathways. If CGRP does indeed activate a Gαs-mediated signalling pathway, then it is unlikely that NO release in response to CGRP relies on intracellular Ca^{2+}-dependent mechanisms; however, some studies have suggested that CGRP can initiate the PLC-IP_3 pathway and Ca^{2+} mobilisation (Drissi et al., 1998; Laufer & Changeux, 1989). To determine whether CGRP causes an increase in intracellular Ca^{2+} release in the ECs of rat septal arteries, we selectively loaded the ECs with a Ca^{2+} indicator (Figure 4.3.3A-B) and measured EC intracellular Ca^{2+} activity before and after CGRP application. Whole cell, global EC Ca^{2+} activity did not increase in response to 10 nM CGRP ($F/F_0 = 0.98$, $n = 5$) but did in response to 0.1 μM ACh ($F/F_0 = 1.28$, $n = 5$, Figure 4.3.3C). This confirms that CGRP likely does not activate NO release via a mechanism involving intracellular Ca^{2+} release.

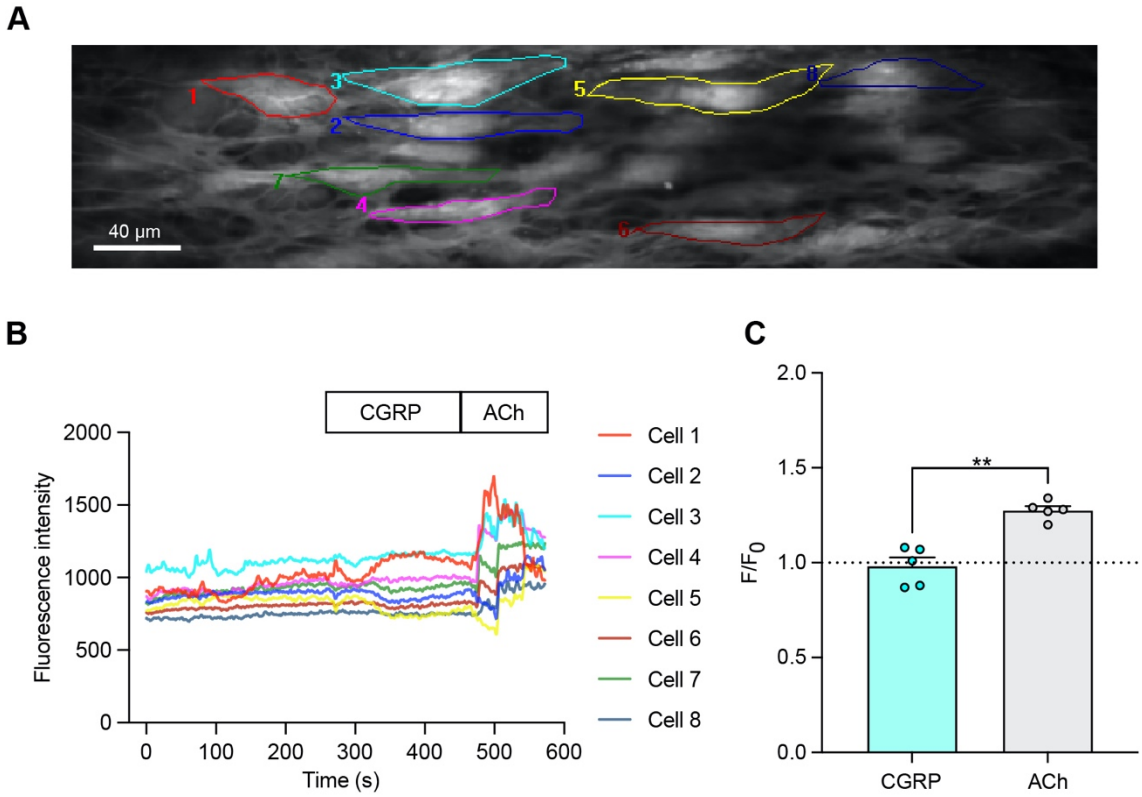

Figure 4.3.3 Effect of CGRP and ACh on EC global intracellular Ca^{2+} events. Oregon Green 488 BAPTA-1 AM fluorescence reporting EC Ca^{2+} in a pressurised septal artery (**A**) with the fluorescence time course of colour-coded ECs plotted below (**B**). 10 nM CGRP was added at 260s and 0.1 µM ACh was added at 460s. (**C**) Bar graph summarising Ca^{2+} activity expressed at F/F_0 in the presence of CGRP and ACh. Data represents paired experiments. The dotted line indicates no change in Ca^{2+} activity. Data are means ± SEM; $n = 5$. $^{**}P < 0.01$ using paired t test.

4.3.6 Response of Cu_2FL2E to SNAP in cell-free chambers

It was necessary to first test whether the NO-dye, Cu_2FL2E, responded to the NO donor, SNAP, in a cell-free environment. Cu_2FL2E (1 μM) was intrinsically fluorescent in cell-free chambers containing PBS, and the addition of SNAP (1-100 μM) caused an increase in the rate and magnitude of fluorescence (Figure 4.3.4A). 1 μM, 10 μM, and 100 μM SNAP caused a 3.7 ± 1.0-fold, 6.5 ± 1.0-fold, and 12.2 ± 1.7-fold (n = 3) increase in fluorescence compared to baseline (F_0), respectively (Figure 4.3.4B). 10 μM SNAP was used in further experiments because this concentration is sufficient to cause maximal vasorelaxation in mesenteric arteries (Wallis et al., 2023). Similar responses were observed in cell-free chambers containing gassed Krebs-buffered solution (Figure 4.3.5A), with 10 μM SNAP causing a 5.0 ± 1.0-fold increase in fluorescence (n = 5, Figure 4.3.5B) which was not statistically different to the response seen in PBS.

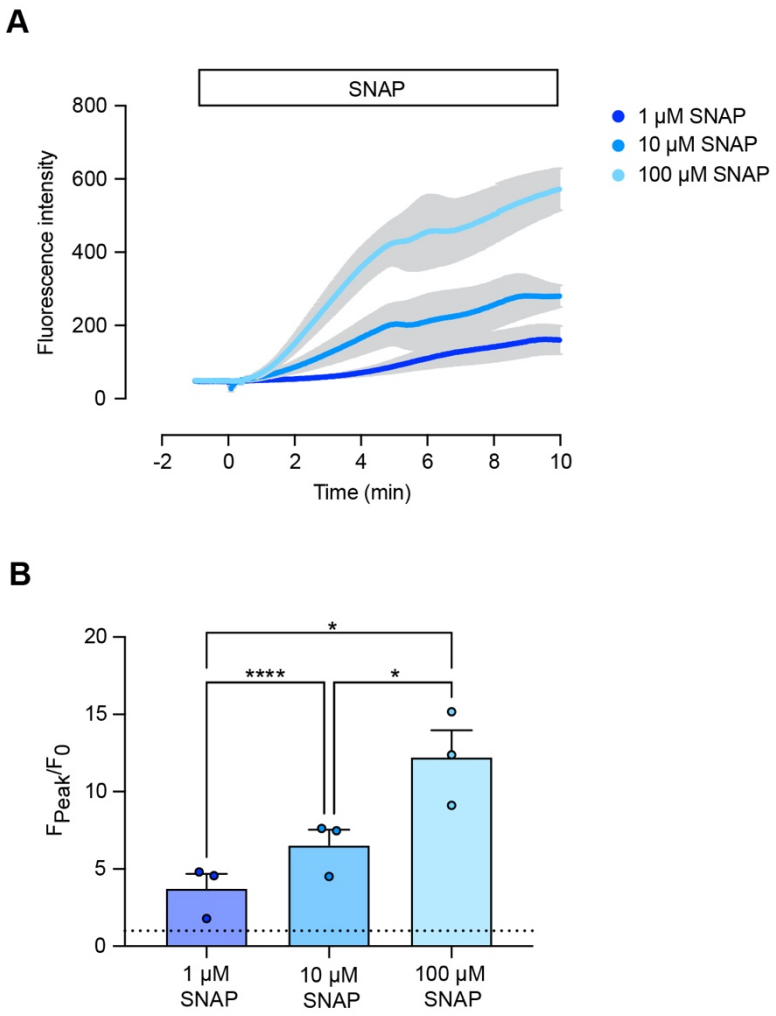

Figure 4.3.4 Cu_2FL2E response to SNAP in a cell-free environment. Time course (**A**) and summary (**B**) of concentration-dependent increases in Cu_2FL2E fluorescence in response to SNAP (1–100 µM). Cu_2FL2E was used at 1 µM, working ratio 1:2, in PBS at 25°C. SNAP was added to the chamber at 0 min. The dotted line indicates no change in fluorescence. Data are means ± SEM; n = 3–5. *$P < 0.05$, ****$P < 0.0001$ using 1-way ANOVA.

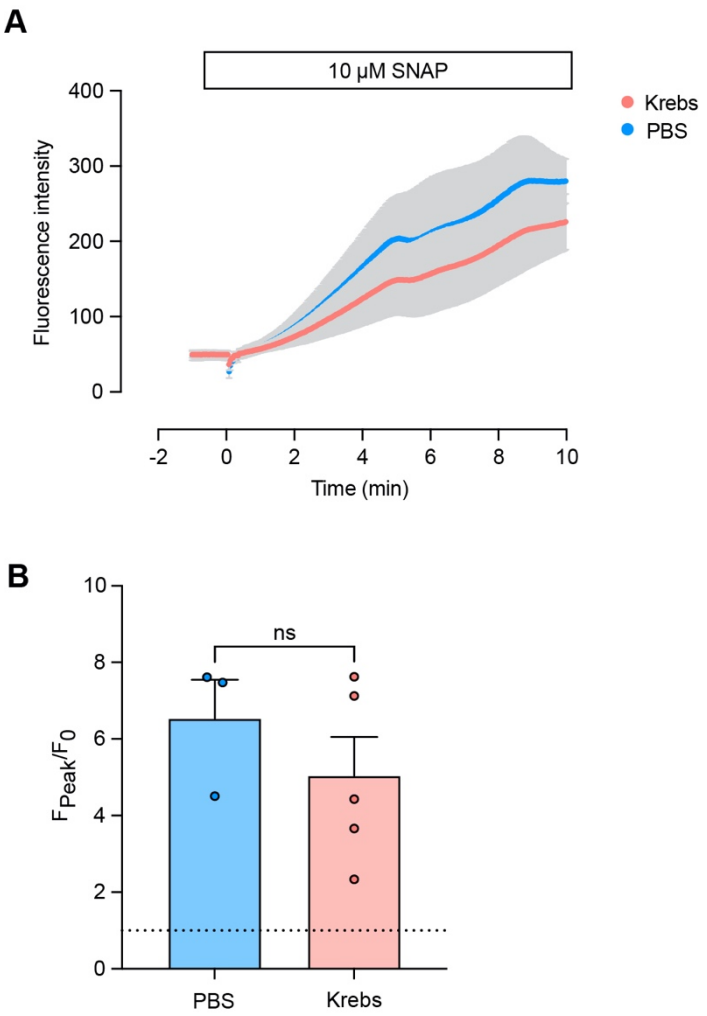

Figure 4.3.5 Effect of buffered-solution on Cu_2FL2E response to SNAP in a cell-free environment. Time course (**A**) and summary (**B**) of concentration-dependent increases in Cu_2FL2E in response to 10 µM SNAP in PBS (25°C) or Krebs-buffered solution (37°C). Cu_2FL2E was used at 1 µM, working ratio 1:2. SNAP was added at 0 min. The dotted line indicates no change in fluorescence. Data are means ± SEM; *n* = 5. Statistical analysis conducted using unpaired t test.

4.3.7 Response of Cu_2FL2E to SNAP in pressurised arteries

Having confirmed that Cu_2FL2E is able to respond to SNAP, we attempted to optimise a protocol for the use of the NO-dye in pressurised mesenteric arteries (Figure 4.3.6A). Before loading, the arteries displayed little autofluorescence but, following NO-dye loading, several ECs or VSMCs were able to be visualised (Figure 4.3.6B). The internal elastic lamina (IEL) also displayed strong labelling which indicated what the dye had passed through the VSMC layers of the vessel, but also meant that a large percentage of the fluorescence signal came from the elastin. Following the addition of the NO donor, SNAP (10 or 100 μM), the Cu_2FL2E fluorescence intensity remained unchanged, even after adjustments to the loading protocol (Figure 4.3.6C-D). This lack of response meant that it would be impossible to detect NO production in response to other agonists; therefore, Cu_2FL2E does not appear to be suitable for use in pressurised arteries.

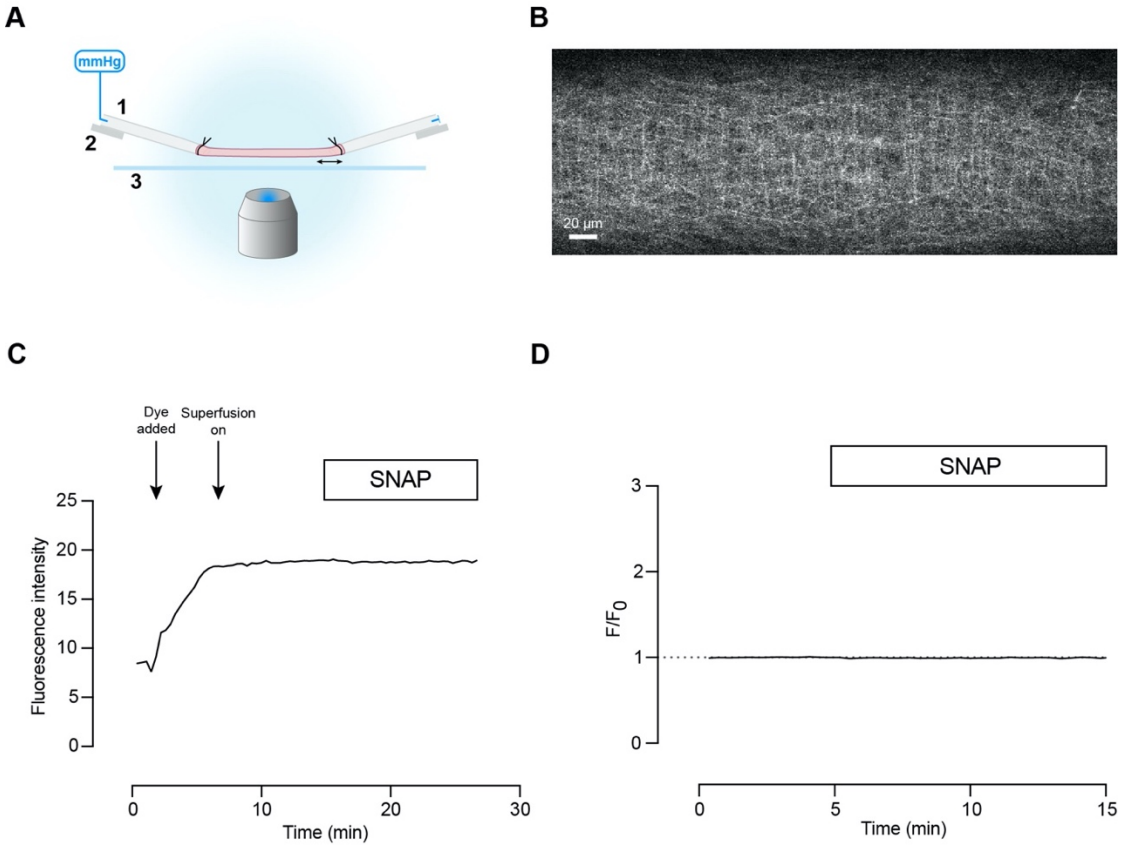

Figure 4.3.6 Cu_2FL2E in pressurised mesenteric arteries. (**A**) Schematic showing isolated, cannulated, and pressurised artery with VSMCs facing the coverslip. 1, pipette; 2, micromanipulator to secure pipette and adjust length of artery; 3, coverslip, images using an inverted confocal microscope (adapted from Wallis et al. (2023)). (**B**) Representative confocal myograph showing visible VSMCs, demonstrating the ability of Cu_2FL2E to load the arteries. (**C**) Time course of Cu_2FL2E fluorescence following addition of NO-dye and 10-100 µM SNAP to the chamber. (**D**) Cu_2FL2E fluorescence, expressed as $F/F_{0,}$ remains unchanged in the presence of 10-100 µM SNAP.

4.3.8 Response of Cu_2FL2E to ACh and SNAP in en-face arteries

To ensure that the insensitivity of Cu_2FL2E to NO was due to the dye being ineffective rather than insufficient cell-loading, we attempted to load and image intact arteries where the ECs had been exposed (Figure 4.3.7A). Although it appeared that the ECs had been effectively loaded with the dye (Figure 4.3.7B), there was no change in fluorescence intensity in response to either 1 μM ACh or SNAP (10 or 100 μM) (Figure 4.3.7C-D), further confirming that Cu_2FL2E was unable to respond to NO in intact arteries and thus unsuitable for use in further experiments.

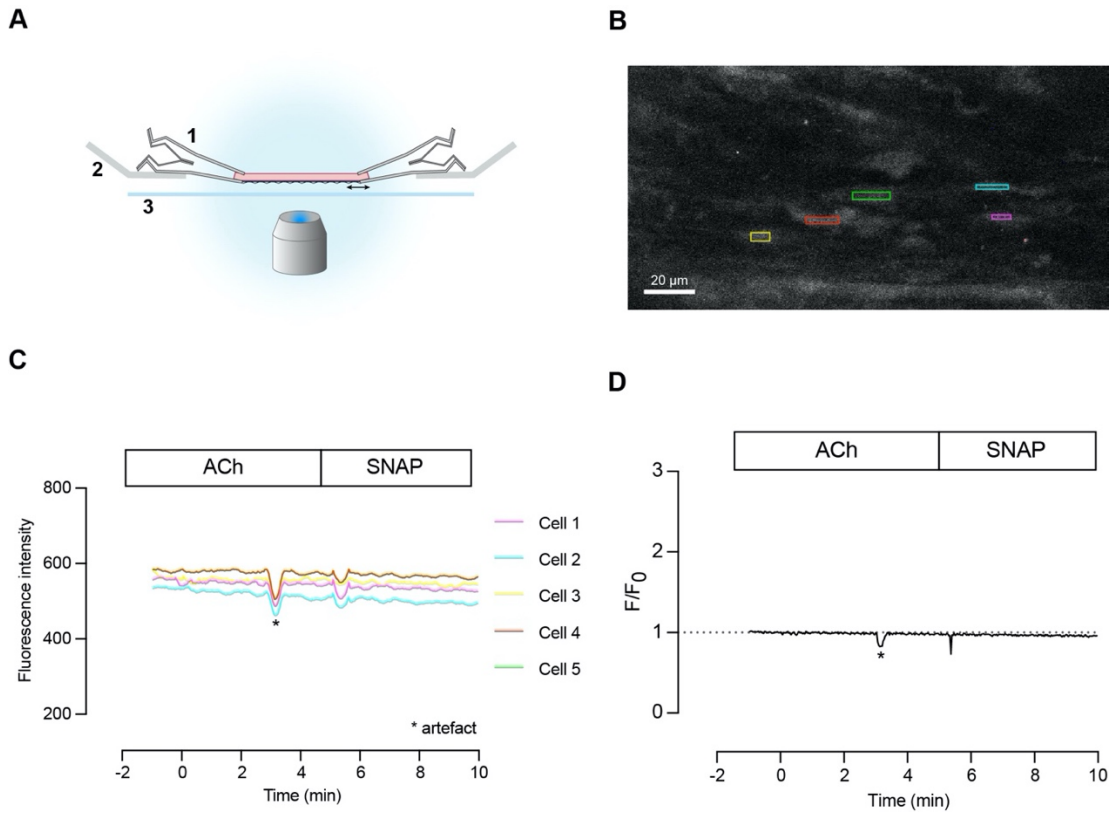

Figure 4.3.7 Cu_2FL2E in *en-face* mesenteric arteries. (**A**) Schematic showing isolated, opened, and stretched artery for *en face* imaging, with ECs facing the coverslip. 1, micro-clamp; 2, caliper to secure micro-clamp and adjust length of artery; 3, coverslip, imaged using an inverted microscope (adapted from Wallis et al. (2023)). (**B**) Representative confocal myograph showing visible ECs, demonstrating ability of Cu_2FL2E to load the arteries. (**C**) Cu_2FL2E fluorescence time course of colour-coded ECs from (**B**) in the presence of 1 µM ACh or 10-100 µM SNAP. (**D**) Cu_2FL2E fluorescence, expressed as F/F0 remains unchanged in the presence of both 1 µM ACh and 10-100 µM SNAP. Asterisk indicates imaging artefact.

4.4 Discussion

The current study aimed to investigate the role of the endothelium in CGRP-induced vasorelaxation in rat septal arteries. These data support the hypothesis that there is an important endothelium-dependent component in the CGRP response, which appears to rely on NO synthesis and release.

The present investigation clearly implicates a role for the endothelium in CGRP-induced vasorelaxation. We demonstrated that removing the endothelium of the rat septal arteries causes a significant attenuation of the vasorelaxation response to CGRP. While this finding is consistent with studies in rat aorta (Brain et al., 1985; Gray & Marshall, 1992b) and proximal epicardial arteries from rats (Prieto et al., 1991), the latter study also demonstrated that removal of the endothelium in distal intramyocardial arteries had no effect on the CGRP response (Prieto et al., 1991). Although we found that denudation attenuated CGRP-induced vasorelaxation, the vessels still maximally relaxed to 10 nM CGRP. This may explain the disparity seen, as it is likely that the contribution of the EC-dependent and -independent components varies within the heart, in this case the endocardial surface arteries being more endothelium-dependent.

It is widely reported that CGRP triggers NO release, and we also found this to be true in these vessels where the NOS inhibitor, L-NAME, caused significant attenuation of CGRP-induced vasorelaxation. The responses to CGRP in denuded arteries and those pre-incubated with L-NAME are strikingly similar, implying that NO release accounts for the EC-dependent component of the CGRP response. Interestingly, it appears that the inhibition seen in denuded vessels and in the presence of L-NAME is most pronounced

at the lowest concentrations of CGRP, suggesting that NO release is the primary mechanism of vasorelaxation at these concentrations. Basal CGRP plasma levels are normally in the low picomolar range (Russell et al., 2014; Wolfrum et al., 2005), so it is relevant to investigate the effects of CGRP at these concentrations. This finding could have been further confirmed using a NO-dye, which would have allowed NO production, basally or in response to CGRP, to be quantified in intact, myogenically active coronary arteries. Despite Cu_2FL2E responding to NO generated from SNAP extracellularly, we were unable to establish a protocol for its use in rat mesenteric arteries. In the study by Ghosh et al. (2013), Cu_2FL2E appeared to be successfully loaded into mouse carotid artery ECs and VSMCs, where an increase in fluorescence was observed in response to ACh and subsequently inhibited by L-NAME. While these data seem promising, this study used a high concentration of Cu_2FL2E (20 μM) and Cu^{2+} (40 μM) which would not be suitable for use in *ex vivo* arteries. Firstly, this would require high concentrations of both DMSO and pluronic which our group has shown can activate EC Ca^{2+}, and hence eNOS, during loading of the dye (unpublished). Our protocol aimed to limit the concentration of DMSO used to prevent this. Secondly, Cu^{2+} concentrations above 5 μM have been shown to cause arterial damage, although the precise mechanism is unclear (Wallis et al., 2023). In pressurised mesenteric vessels, we found that Cu_2FL2E intensely labelled the elastin, which may have interfered with the ability of Cu_2FL2E to bind NO or for a change in fluorescence to be detected. Furthermore, despite successfully loading ECs with Cu_2FL2E in the *en face* preparations, neither ACh nor SNAP produced a detectable response. The Cu_2FL2E NO-dye does not appear to be a reliable method for measuring and quantifying NO generation in intact vessels, and an attempt to optimise an alternate method was beyond the time constraints of the present study.

We also observed a significant increase in myogenic tone following denudation or incubation with L-NAME, as has been demonstrated by others in coronary arteries both *in vivo* and *ex vivo* (Graves et al., 2000; Nishikawa & Ogawa, 1997; Szekeres et al., 2004). This indicates that NO release from the endothelium is vital in the basal regulation of vascular resistance in these coronary arteries. Interestingly, NOS inhibition does not cause an increase in myogenic tone in other vascular beds, such as human subcutaneous arteries (Woolfson & Poston, 1990) and rat mesenteric arteries (Parsons et al., 1994), but does in rat middle cerebral arteries (McNeish et al., 2006). As such, the release of NO during myogenic tone appears to be specific to certain vascular beds. It has been reported by others that the contribution of NO, both stimulated and basal, decreases with vessel size. Shimokawa et al. (1996) found that the inhibitory effects of L-NAME on ACh-induced vasorelaxation were more pronounced in the rat abdominal aorta than in the proximal and distal mesenteric arteries. In the heart, one study observed that L-NAME dilated coronary arterioles (<100μm) but constricted small coronary arteries (>100μm) (Jones et al., 1995), while another found that L-NMMA infusion constricted both proximal and distal epicardial coronary arteries in healthy human patients (Nishikawa & Ogawa, 1997). These results, along with those published by Prieto et al. described previously, demonstrate the heterogeneity that exists within the heart with regards to the contribution of NO release from the endothelium, and thus the importance of studying the microcirculation alongside larger conduit vessels. Furthermore, a study in pressurised rat intramural coronary arteries by Szekeres et al. (2004) found that NOS inhibition attenuated the vasodilation to low intraluminal pressures and that increasing the intraluminal pressure did not reduce the vessel diameter as it did in control conditions. This observation suggests that NO contributes to pressure-induced changes in coronary vascular resistance, although the precise mechanism remains unclear. These findings,

together with those in the present study, clearly indicate that the NO release from the endothelium has a significant role in rat septal arteries, both in the CGRP-response and in the regulation of myogenic tone, and thus the regulation of coronary blood flow. This is clinically relevant for patients with endothelial dysfunction, which is present in a plethora of cardiovascular diseases, as they will have reduced NO bioavailability and thus likely to present with an impaired CGRP-induced vasorelaxation and increased vascular resistance. Fortunately, endothelial dysfunction is often reversible; therefore, therapeutic intervention may be able to rescue this phenotype. Future investigations are required to determine the purpose of basal NO release in the coronary vasculature and identify which signalling mechanisms are responsible.

CGRP-induced vasorelaxation is widely attributed to the activation of the Gαs-mediated signalling pathway, which causes cAMP accumulation and the subsequent activation of PKA (Russell et al., 2014; Sohn et al., 2020). Only a few studies have attempted to investigate the intracellular signalling pathways in ECs specifically, instead focusing on whole arteries or VSMCs alone. Gray and Marshall (1992a) observed a 2.5-fold rise in cAMP levels and a 12-fold rise in cGMP levels in response to CGRP; however, when the endothelium was removed, they observed no changes in either cGMP or cAMP levels. Furthermore, another study proposed that inhibition of PKA almost completely abolished CGRP-induced hyperpolarisation in both ECs and VSMCs. These findings indicate that CGRP does indeed activate the cAMP-PKA signalling pathway in ECs, but it is important to note that both studies used supraphysiological concentrations of CGRP (300 nM and 1 μM, respectively). Furthermore, a 2.5-fold increase in cAMP levels is a modest increase compared to the 12-fold rise in cGMP levels. More recently, evidence has emerged that supports the contrary: Stott et al. (2018) reported PKA inhibition having no effect on the

CGRP response in rat mesenteric vessels. We attempted to investigate the effects of inhibiting the Gαs-mediated signalling pathway in the rat septal arteries but found that the adenylate cyclase inhibitor, SQ 22536, and PKA inhibitors, H-89 and KT5720, failed to inhibit vasorelaxation to the β-adrenergic agonist, isoprenaline. Furthermore, they unexpectedly reversed myogenic tone when administered, rendering them unsuitable for further use. Similar inconclusive results using these agents were reported by Meens et al. (2012). We were able to rule out the possible activation of the PLC-IP_3 signalling pathway in septal arteries, as we did not observe any increase in global intracellular Ca^{2+} in ECs selectively loaded with a Ca^{2+} indicator following CGRP administration. These pathways are summarised in Figure 4.4.1. Further investigations are needed, however, to confirm the intracellular signalling pathway responsible for NO synthesis and release in the ECs in CGRP-induced vasorelaxation in septal arteries.

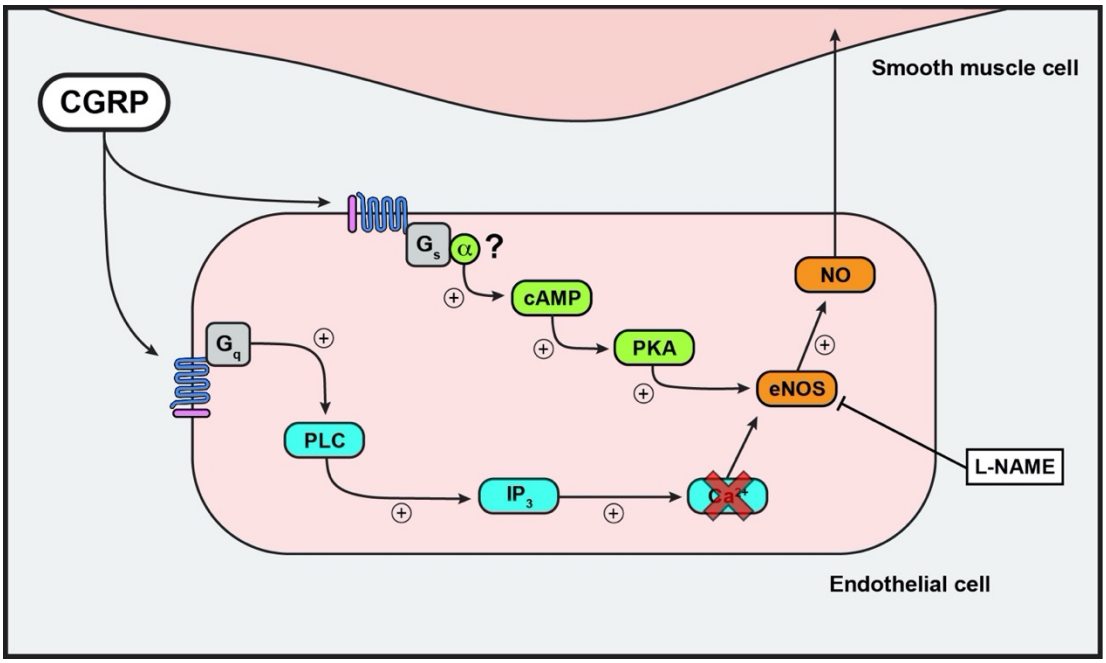

Figure 4.4.1 Summary of Chapter 4 findings. The endothelium-dependent component of CGRP-induced vasorelaxation relies predominantly on NO release. CGRP does not initiate NO production via the PLC-IP_3 pathway, but the role of the cAMP-PKA pathway is yet to be determined. Boxes with curved edges represent intracellular signalling components. Boxes with sharp edges represent inhibitors.

4.5 Conclusions

The findings in the present study confirmed the hypothesis that CGRP-induced vasorelaxation in the rat septal arteries would have an endothelium-dependent component. A significant role for the endothelium was confirmed, which seems to be particularly sensitive at the lower concentrations of CGRP, although an endothelium-independent component is also involved. NO synthesis and release appear to largely account for the EC contribution to CGRP-induced vasorelaxation, with a role for NO during the basal control of myogenic tone also being proposed; however, it was not possible to detect and quantify this contribution using a NO dye in intact arteries. In this study, it was also demonstrated that CGRP does not cause an increase in global EC Ca^{2+} levels, thus ruling out the involvement of a signalling pathway that initiates intracellular Ca^{2+} release, such as the PLC-IP_3 pathway, in the ECs. It was difficult to confirm precisely which intracellular signalling pathway is responsible for NO release during CGRP-induced vasorelaxation as inhibitors of the cAMP-PKA pathway were ineffective in these arteries.

The next chapter will continue to investigate and identify the downstream signalling pathways underlying the CGRP response, both in the ECs and VSMCs, with an additional focus on the mechanisms contributing to CGRP-induced hyperpolarization.

CHAPTER 5: A ROLE FOR A NOVEL SIGNALLING PATHWAY IN CGRP-INDUCED VASORELAXATION

5.1 Introduction

The endothelium-independent component of CGRP-induced vasorelaxation has been more widely studied than the endothelium-dependent component; however, the uncertainty in the precise signalling pathways involved is also seen in the studies investigating the NO-independent components of CGRP-induced vasorelaxation.

CGRP causes hyperpolarization of VSMCs, and there is evidence implicating K_{ATP} channels in this response in several vascular beds (Kitazono et al., 1993; Nelson et al., 1990a; Pinkney et al., 2017; Sakai & Saito, 1998), with the exception of porcine (Kageyama et al., 1993) and rat (Prieto et al., 1991) coronary arteries. Interestingly, a cardioprotective role for K_{ATP} channels has been proposed by which K_{ATP} channel activation induces ischaemic preconditioning (Broadhead et al., 2004; Duncker & Verdouw, 2000). If this is true, it may provide a possible mechanism for the cardioprotective effects of CGRP, and so further investigations in the coronary microcirculation are clinically important.

Meanwhile, more recent studies have demonstrated a role for K_V7 channels. There are 5 members of the K_V7 channel family ($K_V7.1$-5), encoded by the KCNQ genes. Functional K_V7 channels are assembled as a homo- or heterotetramer consisting of 4 subunits. Each K_V7 subunit has 6 transmembrane segments (S1-S6): the segments between S1 and S4 form the voltage-sensing domain and the S5 and S6 segments form the pore domain. The S4 segment contains positively charged arginines which makes it particularly crucial for voltage-sensing (Jepps et al., 2021). In addition to their voltage-dependent properties, these channels can also be activated by intracellular signalling molecules such as the Gβγ

subunit (Stott et al., 2015b), polyunsaturated fatty acids (PUFAs) (Larsson et al., 2020), PIP_2 (Zhang et al., 2003), and calmodulin (Alaimo & Villarroel, 2018). $K_V7.1$ expression is well-characterised in cardiac myocytes where it conducts the slow-delayed rectifier K^+ current (I_{Ks}) (Fosmo & Skraastad, 2017). Mutations in the KCNQ1 gene, encoding the α subunit of the $K_V7.1$ channel, cause type 1 long-QT syndrome (LQTS) (Wu et al., 2016). $K_V7.2$-$K_V7.5$ are instead expressed throughout the nervous system. $K_V7.2$ and $K_V7.3$ channels have been shown to form heterotetramers that generate the M-current (I_M), a subthreshold non-inactivating K^+ current which controls membrane excitability (Wang et al., 1998). On the other hand, while $K_V7.4$ and $K_V7.5$ indeed have a functional role in several neuronal cell types, they are also known to be present in the vasculature (Soldovieri et al., 2011). In fact, transcripts for $K_V7.1$, $K_V7.4$, and $K_V7.5$ have been identified in the ECs and VSMCs of rat mesenteric arteries (Baldwin et al., 2020; Soldovieri et al., 2011). K_V7 channel expression has also been demonstrated in rat aorta and proximal coronary arteries, but these studies did not discriminate between VSMC and EC localisation (Jepps et al., 2011; Khanamiri et al., 2013; Morales-Cano et al., 2015). It has been shown that inhibition of K_V7 channels attenuates CGRP-induced vasorelaxation in rat middle cerebral arteries, as does specific $K_V7.4$ knockdown in these vessels (Chadha et al., 2014; Stott et al., 2018), but this work has not yet been extended into the coronary microvasculature. It has been observed, however, that K_V7 channels are downregulated in the coronary vasculature in hypertension and diabetes, resulting in increased coronary vascular tone and a subsequent impairment of coronary flow (Jepps et al., 2011; Khanamiri et al., 2013; Morales-Cano et al., 2015). These findings emphasise the clinical relevance of studying the relationship between CGRP and K_V7 channels in small coronary arteries, as this may have important therapeutic implications for cardiovascular disease.

The literature widely attributes CGRP-induced vasorelaxation to a Gαs-mediated cAMP-PKA signalling pathway; however, recent studies have implicated alternative G-protein subunits, specifically Gβγ. Logothetis et al. (1987) was the first to propose that the Gβγ subunit could directly regulate intracellular signalling pathways by showing that Gβγ subunits alone activated ACh-regulated inwardly rectifying K^+ (IK_{ACh}) channels in isolated inside-out patches from atrial myocytes. It has since been demonstrated that the Gβγ subunit can regulate several downstream targets including adenylate cyclase, PLC, and G protein-gated inwardly rectifying K^+ (GIRK) channels (Clapham & Neer, 1993; Smrcka, 2008). IK_{ACh} channels are heterotetramers composed of two GIRK1 and two GIRK4 subunits, both of which have been shown to be directly activated by the Gβγ subunit (Krapivinsky et al., 1998; Reuveny et al., 1994). In this way, GIRK channels are crucial in determining heart rate *via* vagal nerve stimulation and dysfunctions in GIRK channel expression or regulation has been implicated in cardiac pathophysiology (Campos-Rios et al., 2022). The role of the Gβγ subunit in intracellular signalling, therefore, should not be underestimated. Meens et al. (2012) provided evidence for CGRP receptor activation being mediated by the Gβγ subunit in the VSMCs of rat mesenteric arteries and proposed that, while CGRP does indeed increase cAMP production, CGRP-induced vasorelaxation relies on the Gβγ subunit and not cAMP. A study by Stott et al. (2015b) demonstrated that Gβγ subunit inhibition using 3 distinct agents abolished K_V7 channel whole-cell currents in HEK293 cells expressing $K_V7.4$ channels. They also observed a colocalisation between the 2 proteins which was disrupted by the Gβγ subunit inhibitor, gallein, and thus their findings indicate that the Gβγ subunit was essential for K_V7 channel activation. This work was extended into the vasculature where it was observed that either K_V7 inhibition with linopirdine or Gβγ inhibition with gallein or

M119K attenuated the CGRP response in rat mesenteric arteries, but only K_V7 inhibition and not Gβγ inhibition attenuated this response in cerebral arteries (Stott et al., 2018). Together, these findings suggest a role for a novel signalling pathway in CGRP-induced vasorelaxation that involves a Gβγ-K_V7 relationship in certain vascular beds, although the precise mechanism is yet to be elucidated.

5.1.1 Aims and hypotheses

It was hypothesised that CGRP-induced vasorelaxation and hyperpolarization in the rat septal arteries rely on activation of K^+ channels; therefore, the aims of the present study were as follows:

i. Identify the K^+ channel(s) responsible for CGRP-induced relaxation and hyperpolarization.
ii. Determine whether the K^+ channel(s) involved is localised in both VSMCs and ECs.
iii. Investigate the downstream signalling mechanism responsible for K^+ channel activation.

5.2 Materials and Methods

5.2.1 Wire myography

Septal arteries were prepared for wire myography chambers, as described in Section 2.2. In all wire myography experiments, arteries were normalised to a resting tension equivalent to that generated at 90% of the diameter of the vessel at 80 mmHg. When necessary, ECs were removed with a hair and successful removal was confirmed by <10% relaxation to 1 μM ACh.

5.2.2 Immunohistochemistry

Mesenteric and septal arteries were prepared for immunohistochemistry, as described in Section 2.4. A polyclonal anti-rat/human KCNQ4 antibody raised in rabbit (0.8 mg/ml, 1:250; APC-164, Alomone labs) was used to stain $K_V7.4$ channels. The secondary antibody was a polyclonal anti-rabbit IgG antibody raised in goat and conjugated to Alexa Fluor 488 (2 mg/ml, 1:1000, A11034, Invitrogen). A polyclonal anti-rat/human KCNQ5 antibody raised in rabbit (0.8 mg/ml, 1:250; APC-155, Alomone labs) was used to stain $K_V7.5$ channels. The secondary antibody was the Alexa Fluor 488 anti-rabbit IgG antibody described above. Arteries were imaged as described in Section 2.4.4.

5.2.3 Inhibitors

The following drugs were used in this chapter to inhibit their respective targets, at concentrations which have been previously shown to be effective but were further optimised and confirmed for use in the present study: 100 μM L-NAME to antagonise NOS (Garland & Dora, 2017), 5 μM glibenclamide to block K_{ATP} channels (Garland et

al., 2011), 1–10 μM linopirdine to block K_V7 channels (Stott et al., 2016), 100 μM gallein to inhibit the Gβγ subunit (Stott et al., 2015b).

5.3 Results

5.3.1 45 mM K^+ inhibits CGRP-induced vasorelaxation

While there is an important NO-component in CGRP-induced vasorelaxation, there are clearly other mechanisms contributing to CGRP-induced vasorelaxation, particularly in the VSMCs. It is known that CGRP causes VSMC hyperpolarization, which is likely to be mediated by K^+ channels (Nelson et al., 1990b; Norton et al., 2021). To investigate the involvement of K^+ channels in CGRP-induced vasorelaxation, septal arteries were incubated in isotonic 45 mM K^+ Krebs-buffered solution to prevent hyperpolarization. This significantly inhibited the response to CGRP, reducing vasorelaxation at 10 nM CGRP from 96.3 ± 1.3% to 11.3 ± 5.2% (n = 3-7; Figure 5.3.1A). A significant inhibition was also observed in isoprenaline-induced vasorelaxation, with vasorelaxation at 10 μM isoprenaline being reduced from 94.2 ± 3.0% to 43.9 ± 5.5% (n = 5–6; Figure 5.3.1B). These data confirm that both CGRP and isoprenaline rely on K^+ channels to cause vasorelaxation; however, 45 mM K^+ caused a more pronounced inhibition of CGRP-induced vasorelaxation, indicating that K^+ channels play a greater role compared to isoprenaline-induced vasorelaxation.

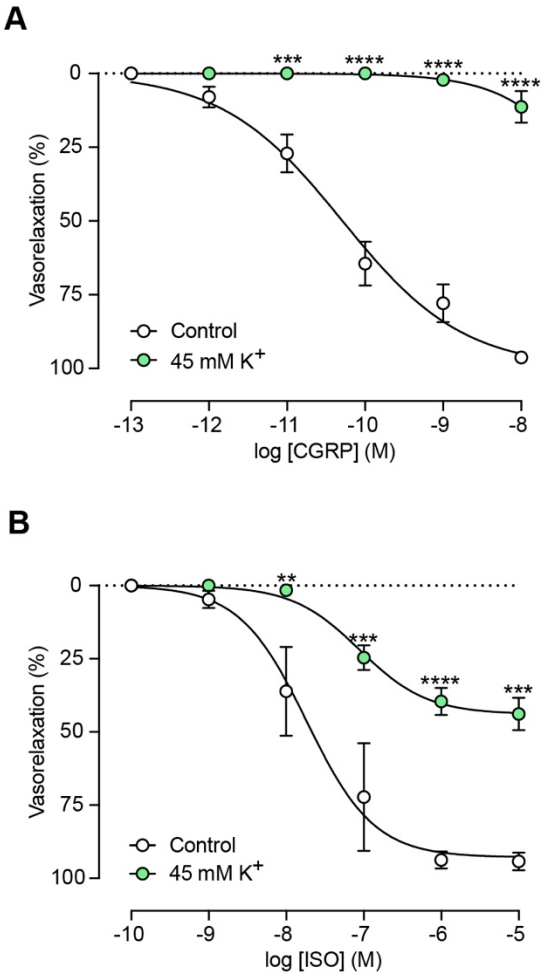

Figure 5.3.1 Effect of 45 mM K+ in septal arteries. Cumulative concentration-response curves summarising relaxation to CGRP (**A**) and isoprenaline (**B**) in isotonic 3.6 mM K^+ (control) and 45 mM K^+ Krebs-buffered solution. CGRP control data adapted from Figure 3.3.2. Data are means ± SEM; n = 3–6. $^{**}P < 0.01$, $^{***}P < 0.0005$, $^{****}P < 0.0001$ compared to control using mixed-effects analysis with Sidak's multiple comparisons test.

5.3.2 K_{ATP} channel inhibition does not attenuate CGRP-induced vasorelaxation

Several papers have implicated K_{ATP} channels in CGRP-mediated vasorelaxation and hyperpolarization (Kitazono et al., 1993; Nelson et al., 1990a; Sakai & Saito, 1998). To investigate whether these channels were important in CGRP-induced vasorelaxation in the septal arteries, vessels were preincubated with the K_{ATP} inhibitor, 5 μM glibenclamide. Arteries were also preincubated with 100 μM L-NAME to remove the NO-dependent component of the CGRP response. Glibenclamide did not inhibit CGRP-induced vasorelaxation (EC_{50} 2.7 nM, log EC_{50} -8.6 ± 0.1; n = 5) compared to L-NAME alone (EC_{50} 4.2 nM, log EC_{50} -8.4 ± 0.2; n = 10, Figure 5.3.2A) in these arteries. Successful inhibition of K_{ATP} channels was confirmed using the K_{ATP} channel activator levcromakalin (1–3 μM, n = 5–7, Figure 5.3.2B-C). These findings indicate that, while K_{ATP} channels are indeed present in the rat septal arteries, they do not contribute to CGRP-induced vasorelaxation in the presence of L-NAME.

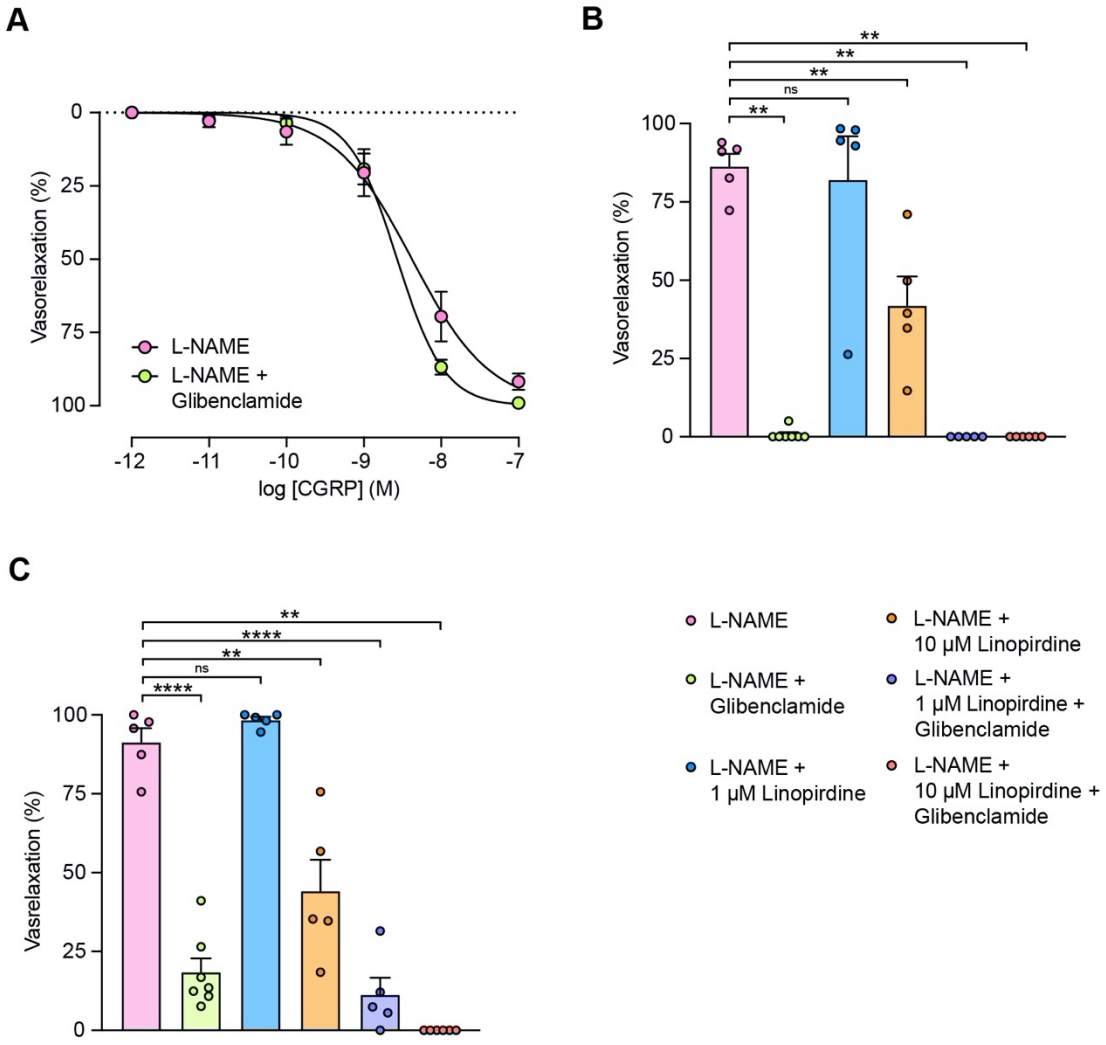

Figure 5.3.2 Effect of K_{ATP} channel inhibition in septal arteries. (**A**) Cumulative concentration-response curves summarising relaxation to CGRP in the presence of 100 µM L-NAME alone and in combination with 5 µM glibenclamide. Bar graphs summarising relaxation to 1 µM (**B**) and 3 µM (**C**) levcromakalin in the presence of 100 µM L-NAME alone or in combination with 1 µM linopirdine, 10 µM linopirdine, or 5 µM glibenclamide. Data are means ± SEM; n = 5–10. $^{**}P < 0.01$, $^{****}P < 0.0001$ compared to L-NAME using mixed-effects analysis with Sidak's multiple comparisons test (A), unpaired t test (B), or Mann-Whitney (B-C).

5.3.3 K_V7 channel inhibition attenuates CGRP-induced vasorelaxation

K_V7 channels contribute to CGRP-mediated vasorelaxation in other vascular beds (Chadha et al., 2014; Stott et al., 2018). To investigate whether K_V7 channel activation was responsible for the NO-independent component of CGRP-induced vasorelaxation in these vessels, arteries were incubated with the K_V7 channel blocker, 1 μM linopirdine, in the presence of 100 μM L-NAME. K_V7 channel inhibition significantly attenuated CGRP-induced vasorelaxation, reducing the vasorelaxation at 10 nM CGRP from 69.6 ± 8.4%, in the presence of L-NAME alone to 47.4 ± 9.8% (n = 8–10; Figure 5.3.3A). When glibenclamide was applied in combination with linopirdine and L-NAME, it tended to block a small component of the relaxation at 10 nM CGRP (29.0 ± 8.2%, n = 7; Figure 5.3.3A), although this difference was not significant to L-NAME and linopirdine in the absence of glibenclamide. Successful inhibition of K_V7 channels was confirmed using the $K_V7.2$-7.5 channel activator, retigabine (10 μM; n = 5; Figure 5.3.3B). Notably, 10 μM, but not 1 μM, linopirdine appeared to have off-target effects at K_{ATP} channels as it significantly attenuated vasorelaxation to levcromakalin (n = 5; Figure 5.3.2B-C). Furthermore, preincubation with linopirdine and L-NAME significantly increased the myogenic tone of the vessels (5.4 ± 0.9 mN/mm) compared to preincubation with L-NAME alone (4.7 ± 0.8 mN/mm; n = 5; Figure 5.3.3C). These results indicate that K_V7 channels play an important role in CGRP-induced vasorelaxation and basal myogenic tone.

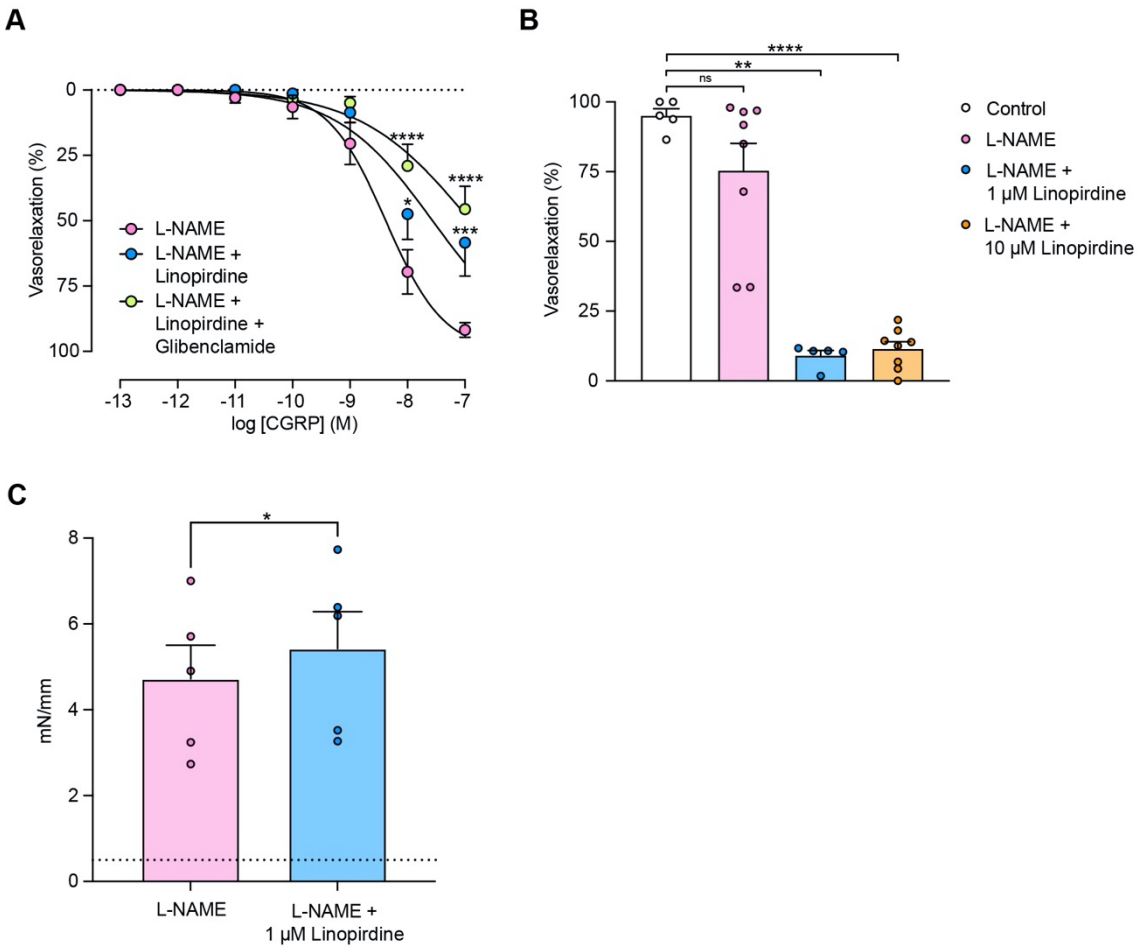

Figure 5.3.3 Effect of K_V7 channel inhibition in septal arteries. (**A**) Cumulative concentration-response curves summarising relaxation to CGRP in the presence of 100 µM L-NAME alone or in combination with 1 µM linopirdine and 5 µM glibenclamide. L-NAME data adapted from Figure 5.3.2. (**B**) Bar graph summarising relaxation to retigabine in the presence of 100 µM L-NAME alone or in combination with 1 µM or 10 µM linopirdine. (**C**) Bar graph summarising the level of myogenic tone in the presence of 100 µM L-NAME alone or in combination with 1 µM linopirdine. Data represents paired experiments. The dotted line represents the minimum mN/mm required to consider an artery as being myogenically active. Data are means ± SEM; n = 5–10. *P < 0.05, **P < 0.01, ***P < 0.0005, ****P < 0.0001 compared to L-NAME or control using mixed-effects analysis with Sidak's multiple comparisons test (A), Mann-Whitney or unpaired t test (B), or paired t test (C).

5.3.4 K_V7 channels are expressed on the VSMCs and ECs of rat septal arteries

The expression of K_V7 channels in the VSMCs has been well-characterised, but a study by Baldwin et al. (2020) indicated that these channels are also expressed in the ECs of rat mesenteric arteries. Immunohistochemistry confirmed the expression of K_V7.4 (Figure 5.3.4A-B), and K_V7.5 (Figure 5.3.5A-B) in the ECs and VSMCs of rat septal arteries, as well as rat mesenteric arteries (Figure 5.3.4C and Figure 5.3.5C) which were used as a positive control (n = 3). This suggests that K_V7 channels contribute to both the EC-dependent and -independent components of CGRP-induced vasorelaxation.

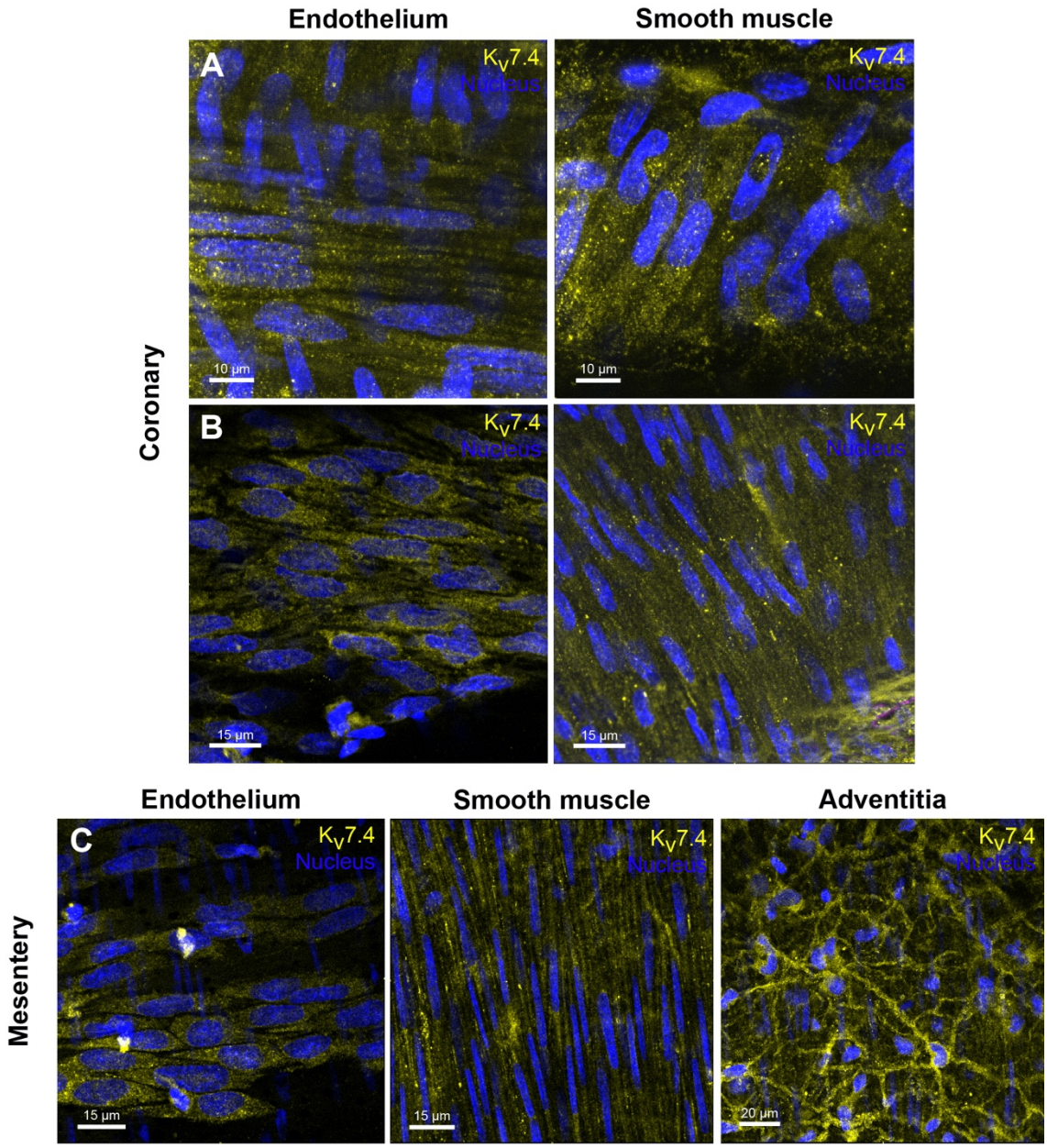

Figure 5.3.4 K_V7.4 channel expression in isolated arteries. K_V7.4 labelling in the ECs and VSMCs of pressurised (**A**) and wire mounted (**B**) coronary septal arteries. (**C**) K_V7.4 labelling in the ECs, VSMCs, and perivascular nerves of wire mounted mesenteric arteries (positive control). K_V7.4, yellow; nuclei, blue. Images are representative of 3 experiments.

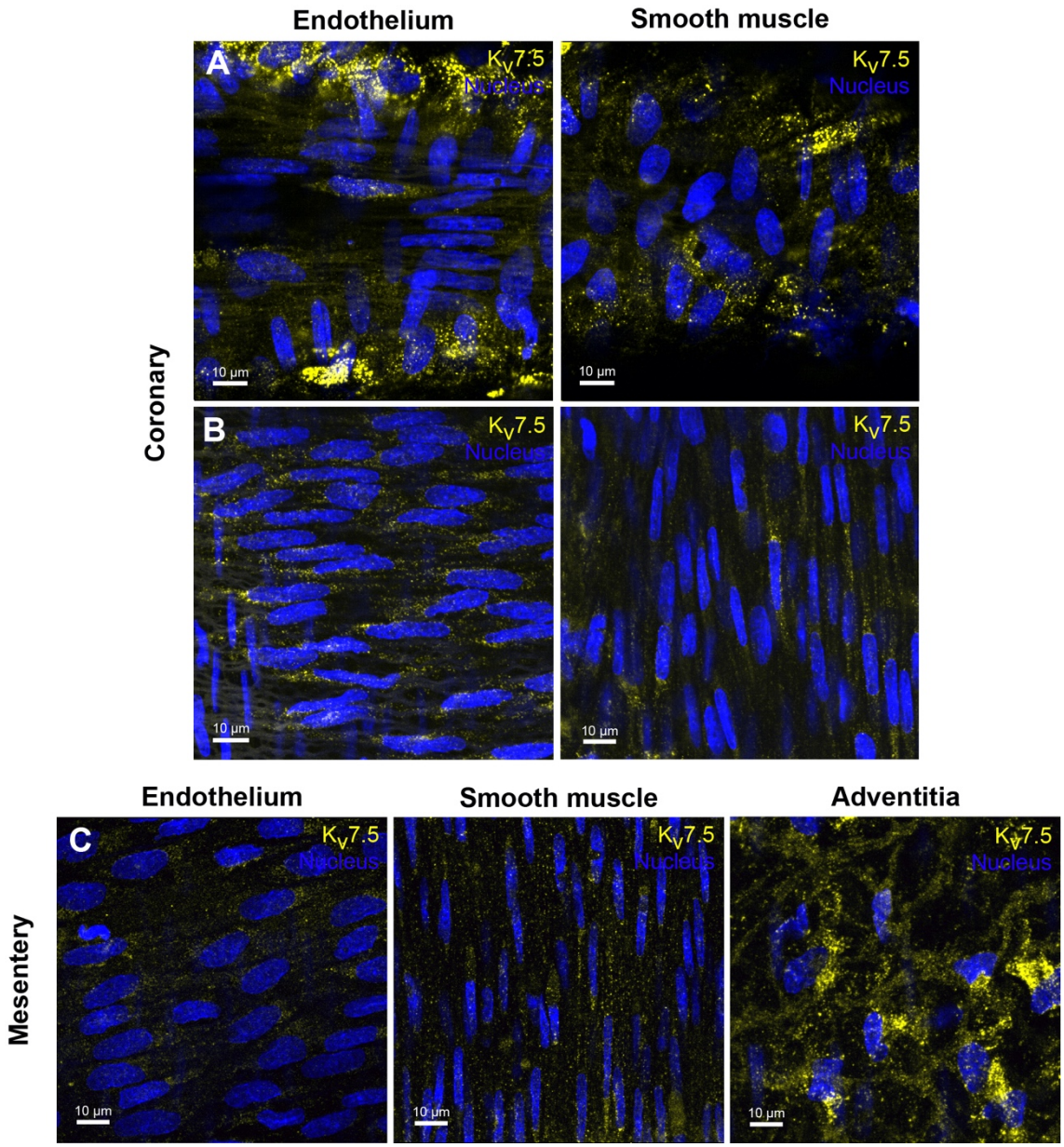

Figure 5.3.5 K_V7.5 channel expression in isolated arteries. K_V7.5 staining in the ECs and VSMCs of pressurised (**A**) and wire mounted (**B**) coronary septal arteries. (**C**) K_V7.5 staining in the ECs, VSMCs, and perivascular nerves of wire mounted mesenteric arteries (positive control). K_V7.5, yellow; nuclei, blue. Images are representative of 3 experiments.

5.3.5 K_V7 channel inhibition blocks CGRP-induced hyperpolarization

While the involvement of K_V7 channels in CGRP-induced vasorelaxation has been investigated (Chadha et al., 2014; Stott et al., 2018), there are currently no studies exploring their involvement in CGRP-induced hyperpolarization. To investigate this, VSMCs of isolated septal arteries were impaled with a sharp microelectrode to allow the membrane potential (E_m) to be recorded. When arteries were preincubated with 100 μM L-NAME and 1 μM linopirdine, hyperpolarization to CGRP was almost fully inhibited compared to when the arteries were incubated with L-NAME alone (*n* = 3–5; Figure 5.3.6A). The change in E_m in response to 10 μM retigabine was also attenuated in the presence of L-NAME and linopirdine, compared to L-NAME alone (*n* = 2; Figure 5.3.6B). Preincubating the vessels with L-NAME and 10 μM linopirdine abolished the hyperpolarization response, and the same was seen when these inhibitors were applied in combination with 5 μM glibenclamide (*n* = 4–5; Figure 5.3.6A). These data suggest that, in the presence of L-NAME, K_V7 channels are primarily responsible for the hyperpolarization response to CGRP with K_{ATP} channel activation conferring a minor role at most, similarly to CGRP-induced vasorelaxation. It was also observed that while 1 μM linopirdine had no effect on levcromakalin-induced hyperpolarization, 10 μM linopirdine attenuated the response to CGRP, both in the presence and absence of glibenclamide (*n* = 2–4; Figure 5.3.6C). This further indicates that 10 μM linopirdine has off-target effects on K_{ATP} channels. Interestingly, L-NAME alone appeared to attenuate CGRP-induced hyperpolarization (*n* = 5–7; Figure 5.3.6A). It was also observed that L-NAME caused ~5 mV depolarisation of the E_m at baseline (Figure 5.3.6A), further supporting a basal activation of NO and K^+ channels in these myogenic arteries. Together with the finding that vasorelaxation to retigabine was also attenuated in the presence of L-NAME (Figure 5.3.3B), these results may indicate an interaction between K_V7

channels and NO signalling pathways, and that NO may be contributing to CGRP-induced hyperpolarization. Studies have implicated HNO as an endothelium-derived hyperpolarizing factor (Andrews et al., 2009), as well as being a K_V channel activator (Irvine et al., 2003); therefore, we hypothesised that these findings might be explained by a contribution from HNO in CGRP-induced vasorelaxation. We found in the rat septal arteries that the HNO donor, IPA-NO (10 nM-10 μM), only caused a modest hyperpolarization (~10 mV) in the presence of L-NAME, and this was not markedly attenuated by linopirdine (1 μM; n = 2–4; Figure 5.3.6D). This indicates that HNO is not likely to be the form of NO linked to CGRP-induced hyperpolarization but requires further study.

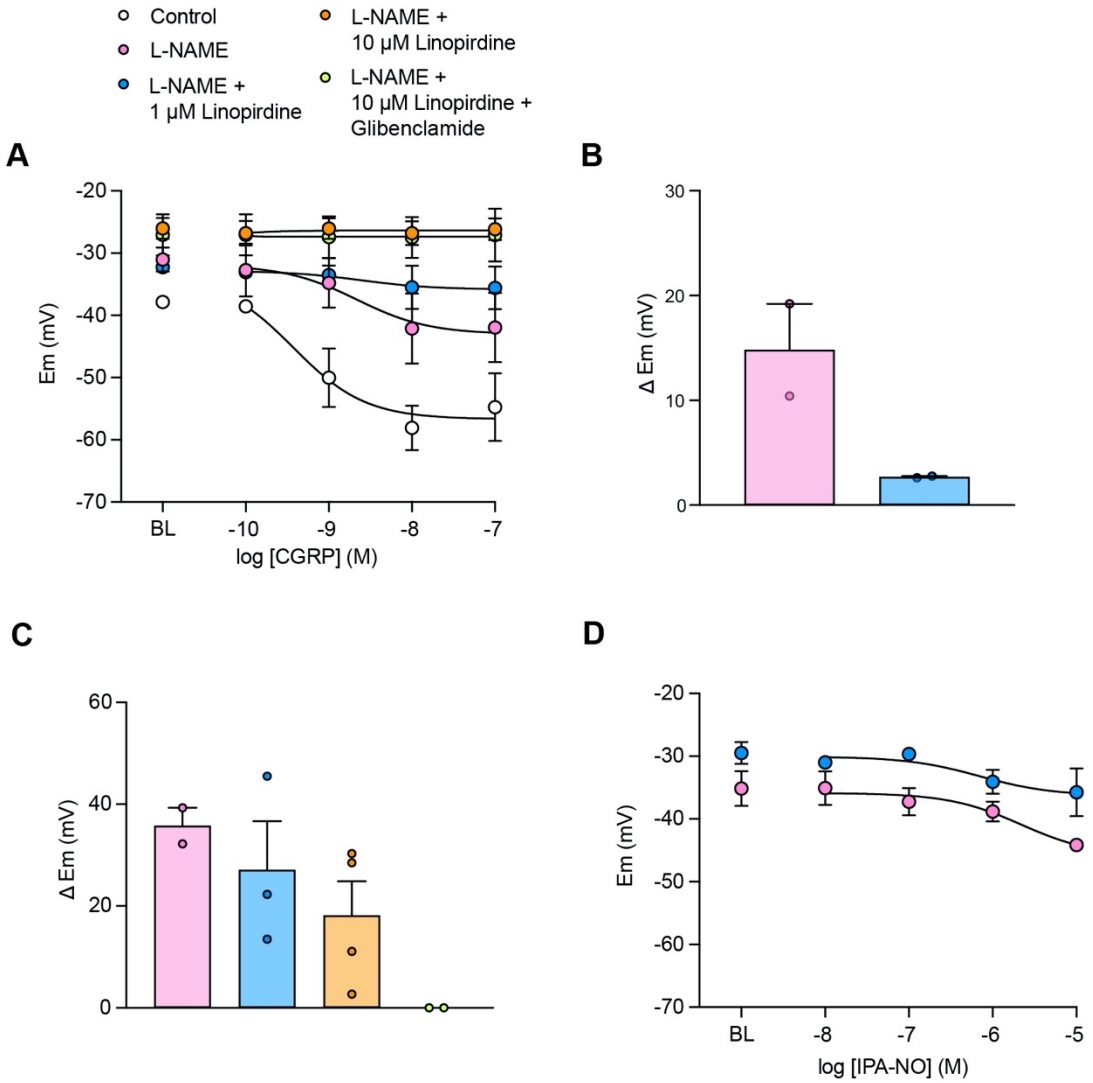

Figure 5.3.6 Effect of K_{ATP} and K_V7 channel inhibition on membrane potential in septal arteries. (**A**) Cumulative concentration-response curves summarising hyperpolarization to CGRP in the absence and presence of 100 µM L-NAME alone or in combination with 1 µM/10 µM linopirdine and 5 µM glibenclamide. Resting membrane potential is indicated by baseline (BL). (**B**) Bar graph summarising hyperpolarization to 10 µM retigabine in the presence of 100 µM L-NAME alone or in combination with 1 µM linopirdine. (**C**) Bar graph summarising hyperpolarization to 1 µM levcromakalin in the presence of 100 µM L-NAME alone or in combination with 1 µM/10 µM linopirdine and 5 µM glibenclamide. (**D**) Cumulative concentration-response curves summarising hyperpolarisation to IPA-NO in the presence of 100 µM L-NAME alone or in

combination with 1 μM linopirdine. Resting membrane potential is indicated by baseline (BL). Data are means ± SEM; n = 2–7. These data are preliminary, so statistics have not been performed. These experiments were conducted by Professor Chris Garland.

5.3.6 Gβγ-subunit inhibition reduces CGRP-induced vasorelaxation

Recent studies have implicated the Gβγ subunit in CGRP-mediated vasorelaxation in other vascular beds (Meens et al., 2012; Stott et al., 2018) and a previous study by Stott et al. (2015b) demonstrated that the Gβγ subunit can modulate K_V7 channel activity. These studies did not differentiate between its role in the VSMCs and the ECs; therefore, we wanted to investigate the contribution of the Gβγ subunit in both the VSMCs and ECs of the coronary microvasculature. Arteries were preincubated with the Gβγ subunit inhibitor, gallein (100 μM). This resulted in a significant inhibition of CGRP-induced vasorelaxation with relaxation at 10 nM CGRP reduced from 96.3 ± 1.3% to 5.7 ± 3.6% in the presence of gallein (n = 5-7; Figure 5.3.7A). The same inhibition was also observed in denuded vessels, where maximal relaxation was reduced to 9.0 ± 4.9% (n = 17, Figure 5.3.7B). Preincubation with gallein did not cause any increase in myogenic tone (n = 11; Figure 5.3.7C). This indicates that the Gβγ subunit has an important role in both the endothelium-dependent and -independent components of CGRP-induced vasorelaxation but does not influence basal myogenic tone. It has been reported that the Gβγ subunit can inhibit or activate isoforms of adenylate cyclase (Bayewitch et al., 1998a, 1998b) so, to confirm that gallein was not having an off-target effect on the Gαs-mediated signalling pathway, the effects of gallein on the β-adrenergic agonist, isoprenaline (0.1 nM–10 μM) were also assessed. No change in the isoprenaline-induced vasorelaxation was observed in the presence of gallein (EC_{50} 15 nM, $logEC_{50}$ -7.8 ± 0.2; n = 5) compared to control (EC_{50} 25 nM, $logEC_{50}$ -7.6 ± 0.3; n = 5; Figure 5.3.7D), suggesting that CGRP is activating a Gβγ-mediated signalling pathway that is effectively independent from the Gαs-mediated pathway usually associated with isoprenaline signalling.

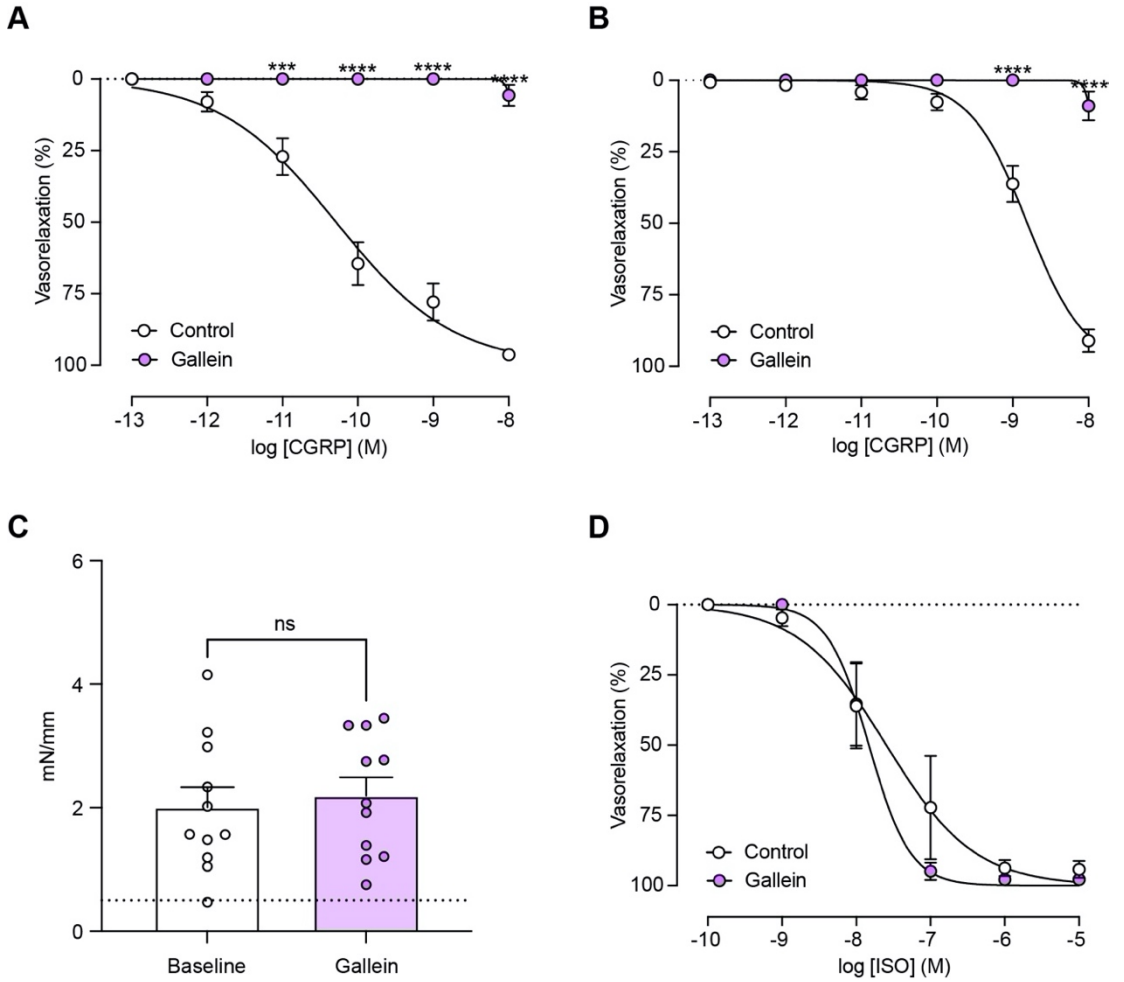

Figure 5.3.7 Effects of Gβγ subunit inhibition in septal arteries. Cumulative concentration-response curves summarising relaxation to CGRP in the absence and presence of 100 μM gallein in arteries with (**A**) and without (**B**) an intact endothelium. Control data adapted from Figure 3.3.2 and Figure 4.3.1. (**C**) Bar graph summarising the level of myogenic tone in the absence and presence of 100 μM gallein. Data represents paired experiments. The dotted line represents the minimum mN/mm required to consider an artery as being myogenically active. (**D**) Concentration-response curves summarising relaxation to isoprenaline in the absence and presence of 100 μM gallein in arteries with an intact endothelium. Control data adapted from Figure 5.3.1. Data are means ± SEM; *n* = 5–17. ***$P < 0.0005$, ****$P < 0.0001$ compared to control using mixed-effects analysis with Sidak's multiple comparisons test (A, B, and D) or paired t test (C).

5.4 Discussion

The present investigation aimed to explore the role of K^+ channels in CGRP-induced vasorelaxation and hyperpolarization, and the signalling pathways leading to their activation. These results confirm the hypothesis that K^+ channels contribute significantly to both the relaxation and hyperpolarization response to CGRP and support a role for K_V7 channels and a Gβγ subunit-mediated signalling pathway, as well as a novel role for NO in hyperpolarization.

Several studies have shown that CGRP hyperpolarizes VSMCs, including in rabbit (Nelson et al., 1990a), rat (Pinkney et al., 2017), and mouse (Norton et al., 2021) mesenteric arteries. K_{ATP} channels have often been implicated in CGRP-induced vasorelaxation (Kitazono et al., 1993; Nelson et al., 1990a; Pinkney et al., 2017; Sakai & Saito, 1998), but the present findings in rat septal arteries support those from porcine (Kageyama et al., 1993) and rat (Prieto et al., 1991) coronary arteries which demonstrate that the K_{ATP} channel inhibitor, glibenclamide, has no effect on relaxation to CGRP. Interestingly, the K_{ATP} channels do appear to be present in the septal arteries, as a pronounced vasorelaxation and hyperpolarization to the K_{ATP} channel activator, levcromakalin, was observed; however, they have only a minor, if any, contribution to CGRP-induced vasorelaxation and hyperpolarization in the coronary microcirculation, at least in the presence of L-NAME.

Instead, we turned our attention to K_V7 channels. A study in mouse cerebral arteries illustrated that the K_V7 channel inhibitor, linopirdine (10 μM), significantly attenuated CGRP-induced vasorelaxation and abolished vasorelaxation when in combination with

glibenclamide (Chadha et al., 2014). We found in the rat septal arteries that linopirdine significantly attenuated CGRP-induced vasorelaxation in the presence of L-NAME; however, glibenclamide did not cause a significant further attenuation when applied in combination, confirming that K_V7 channels confer the dominant effect. These data are supported by electrophysiological experiments where linopirdine significantly inhibited CGRP-evoked hyperpolarization in VSMCs in the presence of L-NAME. Furthermore, CGRP vasorelaxation was transient in the presence of L-NAME and linopirdine, suggesting that the signalling pathway involved is desensitised. We have shown that $K_V7.4$ and $K_V7.5$ channels are indeed present on the ECs as well as the VSMCs of the rat septal arteries, supporting studies in porcine coronary (Chen et al., 2016) and rat mesenteric (Baldwin et al., 2020) arteries. A study using siRNA knockdown of specific K_V7 subtypes in isolated arteries proposed that only $K_V7.4$, and not $K_V7.5$ channels, are involved in the CGRP signalling pathway in rat cerebral arteries (Chadha et al., 2014), but it is yet to be confirmed if this is also the case in rat coronary arteries. Together, our findings indicate that K_V7 channels have a significant role in CGRP-induced vasorelaxation in these vessels, via hyperpolarization of the VSMCs, parallel to a possible contribution from K_V7 channel activation in the ECs.

It is widely reported that CGRP activates the Gαs-mediated cAMP-PKA signalling pathway to elicit vasorelaxation, as many studies have observed an increase in intracellular cAMP levels in response to CGRP (Edvinsson et al., 1985; Gray & Marshall, 1992a; Kubota et al., 1985; Meens et al., 2012). As discussed in Chapter 4, we attempted to investigate the effects of inhibiting the Gαs-mediated signalling pathway in the rat septal arteries but found that both the adenylate cyclase and PKA inhibitors failed to inhibit vasorelaxation to isoprenaline and reversed myogenic tone when administered;

therefore, we were unable to determine the role of the Gαs-mediated cAMP-PKA signalling pathway in CGRP-induced vasorelaxation in these vessels directly. A study by Meens et al. (2012), however, proposed a novel role for a Gβγ subunit-mediated signalling pathway by demonstrating that Gβγ subunit inhibition with gallein (30 or 100 μM) or M119K (100 μM) significantly inhibited CGRP-induced vasorelaxation from either 40 mM K^+ or endothelin-1 pre-constriction in rat mesenteric arteries. They argued that, while CGRP does indeed cause cAMP production, cAMP is not responsible for the vasodilatory effects of CGRP. The attenuation of CGRP-induced vasorelaxation by gallein (50 μM) or M119K (10 μM) was reproduced more recently by Stott et al. (2018). Our findings corroborate these data by demonstrating that gallein (100 μM) significantly inhibited the vasorelaxant response to CGRP in both intact and denuded rat septal arteries, indicating that both the EC-dependent and -independent components of CGRP-induced vasorelaxation rely on a Gβγ-mediated pathway. In the ECs, the Gβγ subunit may trigger NO release in response to CGRP via the PLC-IP_3 pathway (Camps et al., 1992), but this was ruled out by our EC Ca^{2+} imaging experiments in Chapter 4 which showed no global increase in intracellular Ca^{2+} in response to CGRP. The mechanism by which CGRP may activate NO release from the ECs via a Gβγ-mediated pathway thus remains unclear.

An interaction between $K_V7.4$ and Gβγ subunits, whereby inhibiting the Gβγ subunit prevents K_V7 activity, has been identified (Stott et al., 2015b). The results published by Stott et al (2018) corroborate our own as they show that both linopirdine and gallein attenuate CGRP-induced vasorelaxation in rat mesenteric arteries, similarly to the rat septal arteries in the present study. Stott et al. (2018) also observed that gallein attenuates relaxation to the β-adrenoceptor agonist, isoprenaline, in rat renal but not mesenteric arteries. We demonstrated that gallein did not alter isoprenaline-induced vasorelaxation

in the septal arteries either, indicating that the Gβγ-mediated signalling pathways in the rat mesenteric and coronary vascular beds may be similar. Having said this, both linopirdine and gallein caused an increase in the basal tone of renal arteries, but this was not seen in mesenteric vessels. In the septal arteries, gallein did not cause an increase in myogenic tone, but an increase in myogenic tone was observed in the presence of linopirdine. This implies that K_V7 channels are basally active and influence vascular resistance; these channels are likely to be involved in the maintenance of the resting membrane potential and may also be slightly activated by the basal release of CGRP, as seen by slight contraction to receptor antagonists in Chapter 3. Furthermore, the inhibition of CGRP-induced vasorelaxation observed in the presence of gallein was more pronounced than that observed in the presence of L-NAME and linopirdine; therefore, this suggests that the residual vasorelaxation seen during K_V7 channel inhibition is Gβγ-mediated, but further investigation is required to identify this pathway.

Stott et al. (2018) saw no effect of PKA inhibition on the CGRP response in rat mesenteric vessels but, interestingly, there is evidence suggesting that K_V7 channels may be regulated by cAMP (van der Horst et al., 2020). Mani et al. (2016) described that isoprenaline-induced cAMP-PKA activation enhanced $K_V7.5$ currents and modestly enhanced heteromeric $K_V7.4/K_V7.5$ channels in A7r5 rat aortic SMCs but had no effect on $K_V7.4$ channel currents. More specifically, EPAC, the exchange protein activated by cAMP, has been linked to K_V7 channel activation. Stott et al. (2016) demonstrated that EPAC-induced vasorelaxation with an EPAC activator, 8-pCPT-2Me-cAMP-AM, was sensitive to linopirdine in the rat mesenteric and renal arteries, and that isoprenaline-induced vasorelaxation in the mesenteric artery was attenuated by both K_V7 and EPAC inhibition, but not PKA inhibition. This may provide an explanation as to why the PKA

inhibitors that we attempted to use in our investigations were unsuccessful in inhibiting isoprenaline-induced vasorelaxation in the septal arteries. It is important to note that 10 μM linopirdine was used in the published study, which we have shown to have off-target effects on K_{ATP} channels.

Baldwin et al. (2020) demonstrated in rat mesenteric arteries that linopirdine failed to attenuate carbachol-induced vasorelaxation in the presence of L-NAME and suggested that linopirdine was involved in the eNOS-sensitive component of this relaxation response. They also observed that L-NAME caused significant attenuation of the vasorelaxation response to the K_V7.2-7.5 channel activator, S-1. While we showed that the CGRP response was still attenuated by linopirdine in the presence of L-NAME, we did observe attenuation of the response to retigabine in the presence of L-NAME. Further evidence demonstrated that linopirdine attenuated vasorelaxation to the NO donor, sodium nitroprusside (SNP), in rat aorta but not in the renal artery (Stott et al., 2015a). This study also showed, using whole cell electrophysiology recordings of HEK cells, that K^+ currents were significantly enhanced by cGMP, and that this was abolished by 10 μM linopirdine. It is interesting that L-NAME causes significant increases in myogenic tone in these vessels, and that this is associated with a depolarization of the VSMCs, indicating that NO and perhaps K_V7 channels are both basally active. Our finding that 45 mM K^+ effectively abolishes the response to CGRP further implies that NO is contributing to CGRP-induced hyperpolarization. It is known that HNO serves as an endothelium-derived relaxing and hyperpolarizing factor in resistance vessels (Andrews et al., 2009), and a study by Favaloro and Kemp-Harper (2007) also demonstrated the vasodilatory effects of HNO in rat coronary vessels which was attenuated with CGRP 8-37, thus providing a possible link to CGRP release. Furthermore, Irvine et al. (2003) proposed that

HNO activates K_V channels having shown that the voltage-dependent K^+ channel inhibitor, 4-aminopyridine (4-AP), reduced relaxation to the HNO donor, Angeli's salt, in rat mesenteric arteries. Our electrophysiological experiments, however, demonstrated that IPA-NO causes an unremarkable hyperpolarization in rat septal arteries that was not noticeably attenuated by linopirdine. This observation supports the study by Favaloro and Kemp-Harper (2007) who found that 4-AP had no effect on the relaxation to Angeli's salt in rat coronary arteries. This may reflect K_V channel heterogeneity between the mesenteric and coronary vascular beds, but it is also worth noting that it has been suggested that low concentrations of 4-AP can, in fact, augment $K_V7.4$ channel activity (Khammy et al., 2018). Either way, it appears unlikely that the involvement of HNO explains the effects seen with L-NAME on K_V7 channel activation and with increased $[K^+]$ on the CGRP response. An alternative explanation could be that, rather than NO causing hyperpolarization, increased $[K^+]$ or K^+ channel inhibition prevents the release of NO or its hyperpolarization-independent actions. Together, these results indicate a possible link between CGRP, NO, and K_V7 channels, as summarised in Figure 5.4.1, although further investigation is required to identify the exact mechanism.

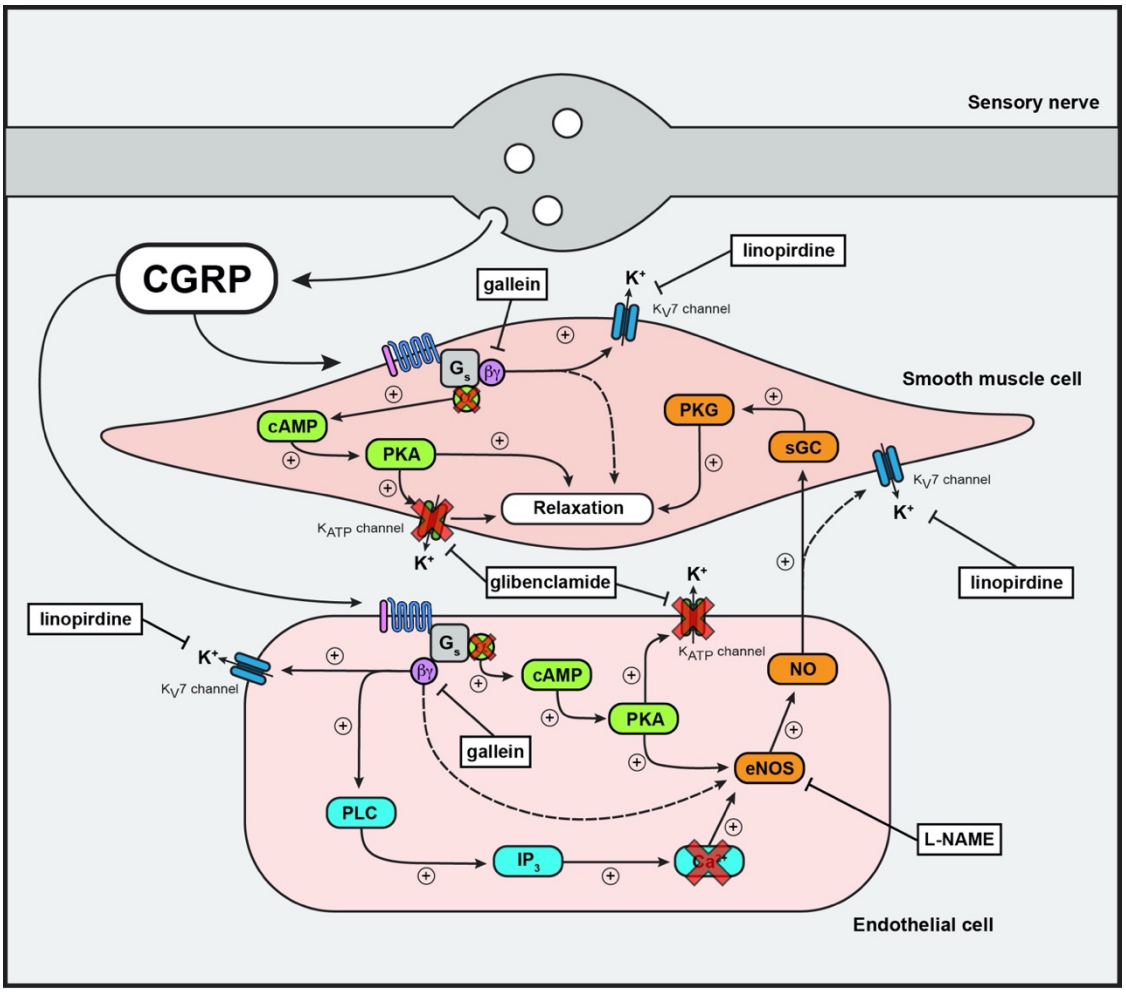

Figure 5.4.1 Summary of Chapter 5 findings. K_V7 channels, and not K_{ATP}, channels are predominantly responsible for CGRP-induced hyperpolarization and vasorelaxation in the absence of NO. NO itself appears to play a role in hyperpolarization, potentially via K_V7 channel activation. CGRP-induced vasorelaxation appears to be mediated via the Gβγ subunit in both VSMCs and ECs. Boxes with curved edges represent intracellular signalling components. Boxes with sharp edges represent inhibitors. Dashed arrows represent signalling pathways that are yet to be consolidated.

5.5 Conclusions

The data in the current investigation confirmed the hypothesis that K^+ channels contribute significantly to the CGRP response in the rat septal arteries. Unlike in other vascular beds, it appears that K_{ATP} channels confer a minor role, at most, to both CGRP-induced vasorelaxation and hyperpolarization in the coronary microvasculature. Instead, our findings indicate that K_V7 channel activation is an important component of the relaxation response to CGRP and is entirely responsible for the observed hyperpolarization of the VSMCs in the presence of L-NAME. We demonstrated the localisation of $K_V7.4$ and $K_V7.5$ channels in both the ECs and VSMCs of the septal arteries, indicating that these channels may also contribute to the endothelium-dependent component of CGRP-induced vasorelaxation.

The present study also established a significant role for a Gβγ subunit-mediated signalling pathway in both the ECs and VSMCs during the CGRP response. It is likely that this pathway leads to K_V7 channel activation. The Gβγ-mediated pathway may also be responsible for initiating NO release in the ECs following CGRP application; however, this cannot be explained by the PLC-IP_3 pathway and thus further investigation is required. Our findings, in combination with other evidence, also implicate a novel relationship between NO and K^+ channel activation, whereby NO release from ECs may cause hyperpolarization of ECs and/or VSMCs in the septal arteries, but the exact mechanism is yet to be elucidated.

While we cannot rule out a role for cAMP and its downstream signalling molecules, and it is likely that the precise intracellular signalling pathways differ between vascular beds,

our findings undoubtedly support a key, novel role for a Gβγ-mediated pathway and K_V7 channel activation in rat small coronary arteries.

CHAPTER 6: CGRP RELEASE FROM ENDOTHELIAL CELLS

6.1 Introduction

Perivascular nerves, predominantly sympathetic and sensory-motor, innervate blood vessels and influence vascular function. It is understood that CGRP is localised in sensory C fibres (Lundberg et al., 1985; Rosenfeld et al., 1983), from where it can be released to exert its vasodilatory effects. Gulbenkian et al. (1993) demonstrated the presence of CGRP-containing perivascular nerves innervating human epicardial coronary arteries and observed that the density of these nerve fibres was greater in the distal artery segments compared to the proximal segments. It has been reported that there is also heterogeneity in the sensitivity to CGRP within the coronary vascular bed, with some studies demonstrating that CGRP has a greater effect on epicardial coronary arteries (Ludman et al., 1991; Sekiguchi et al., 2019) while others argue that the CGRP response is more pronounced in intramyocardial arteries (Gulbenkian et al., 1990; Sheykhzade & Berg Nyborg, 1998). Despite this, immunohistochemical studies of CGRP-positive sensory nerves innervating intramyocardial arteries have not been performed; therefore, we are not able to determine whether the heterogeneity in sensitivity to CGRP is reflected by the sensory nerve innervation of these vessels.

An alternate source of CGRP was proposed by Cai et al. (1993), who observed CGRP expression in the ECs of human umbilical vessels, both in culture and in intact tissue. These vessels are unique in that they lack innervation; therefore, it is likely that the ECs contribute to the regulation of vascular tone. This finding was later extended to the arterial vasculature, where CGRP immunoreactivity was demonstrated in the ECs of the rat carotid body artery using both light and immunoelectron microscopy (Ozaka et al., 1997). CGRP was localised to the rough endoplasmic reticulum (rER) and Weibel-Palade

bodies, indicating that the peptide is both synthesised and stored in the ECs. Using the same techniques, Doi et al. (2001) also reported CGRP expression in the ECs of the rat thoracic aorta and femoral artery, where it was again localised to the rER and Weibel-Palade bodies. Furthermore, they detected prepro-CGRP mRNA in the ECs of both arteries with *in situ* hybridisation. The expression of both CGRP protein and mRNA has been further confirmed in the intima and adventitia layers of rat mesenteric arteries and aorta (Ye et al., 2007). Together, these findings indicate that ECs in several vascular beds are a novel source of CGRP and are responsible for both synthesising and storing the peptide. Interestingly, it has been shown that chronic electrical stimulation of perivascular nerves of the rabbit central ear artery resulted in CGRP and NPY expression in the vascular ECs, despite these cells not expressing CGRP and NPY when unstimulated (Loesch et al., 1992). Further investigations are necessary to reveal the functional role of CGRP in the vascular ECs and determine the relationship between the ECs and perivascular nerves.

TRPV1 channels have been implicated in CGRP release from sensory nerves following the observation that the TRPV1 activator, capsaicin, can induce CGRP release (Lundberg et al., 1985; Szabados et al., 2020). TRPV1 is also extensively expressed in the VSMCs of the arterial circulation, including in coronary arterioles where it is predominantly localised to small vessels (<150 μm diameter) (Phan et al., 2020). Luo et al. (2008) demonstrated in HUVECs that capsaicin increased the concentration of CGRP in the culture medium, thus inferring that TRPV1 is also at least partly responsible for CGRP release from ECs. While TRPV1 channels were expressed in cultured ECs from human brain microvessels (Golech et al., 2004), Phan et al. (2020) did not detect endothelial

TRPV1 expression in skeletal, cardiac, and adipose resistance arteries, indicating that the involvement of TRPV1 in CGRP release from ECs may be not be universal.

Alongside its vasodilatory effects in the vasculature, CGRP has also been shown to have positive inotropic and chronotropic effects in the heart (Franco-Cereceda et al., 1987a; Kumar et al., 2019; Sigrist et al., 1986). Sigrist et al. (1986) demonstrated that the inotropic and chronotropic effects of CGRP could be mimicked by capsaicin, suggesting that these effects are also dependent on TRPV1-induced CGRP release. Although it is possible that these effects are the result of CGRP release from sensory nerves in the myocardium, the endocardial endothelial cells (EECs) are often overlooked as a source of signalling peptides. The EECs are specialised ECs that line the chambers of the heart and are known to contribute to cardiac contractility, metabolism, and development through the synthesis and release of mediators (Smiljic, 2017). The expression of CGRP in the EECs is yet to be explored but may offer an alternate source of CGRP in the heart similarly to the vascular ECs.

CGRP is known to be cardioprotective and has been implicated in several cardiovascular diseases including hypertension, myocardial I/R injury, and myocardial infarction (Kumar et al., 2019; Russell et al., 2014); however, the precise mechanisms underlying this phenomenon are still unclear. TRPV1 channels can be activated by various stimuli, including those produced during hypoxia, heat, and tissue injury (Szabados et al., 2020) and, in this way, may contribute to the cardioprotective role of CGRP. Notably, Ye et al. (2007) reported that CGRP protein and mRNA expression increased in mesenteric and aortic ECs following heat stress, which protects the myocardium from I/R injury. An increase in CGRP plasma levels was also observed, which could be abolished with the

TRPV1 antagonist, capsazepine. Moreover, EC injury induced by lysophosphatidylcholine (LPC) in HUVECs could be attenuated with capsaicin pre-treatment (Luo et al., 2008). Together, these findings indicate a protective role for TRPV1-induced CGRP release and, as such, emphasise the clinical importance of advancing our understanding of CGRP release both in physiological and pathophysiological conditions.

6.1.1 Aims and hypotheses

We hypothesised that CGRP and TRPV1 expression would be detected in the rat septal arteries and ventricular EECs; therefore, the aims of the present study were as follows:

i. Determine the localisation of CGRP and TRPV1 expression
ii. Determine the CGRP mRNA expression levels
iii. Investigate CGRP release from the perivascular nerves and/or ECs

6.2 Materials and Methods

6.2.1 Immunohistochemistry

Mesenteric and septal arteries, and cardiac strips from the left ventricle, were prepared for immunohistochemistry, as described in Section 2.4. A polyclonal anti-rat/mouse CGRP IgG antibody raised in goat (5 mg/mL; 1:1000; ab36001, abcam) was used to stain CGRP. The secondary antibody was a polyclonal anti-goat IgG antibody raised in donkey and conjugated to Alexa Fluor 633 (2 mg/mL; 1:1000; A21082, Invitrogen). A polyclonal anti-rat TRPV1 IgG antibody raised in guinea-pig (1:1000; ab10295, abcam) was used to stain TRPV1. The secondary antibody was a polyclonal anti-guinea-pig IgG antibody raised in goat and conjugated to Alexa Fluor 488 (2 mg/mL; 1:1000; A11073, Invitrogen). A polyclonal anti-human vWF antibody raised in sheep was used to stain vWF as an EC marker (10 mg/mL; 1:1000; ab8822, abcam). This antibody was FITC-conjugated. A monoclonal anti-human/dog ZO-1antibody raised in mouse (0.5 mg/mL; 1:250; 339188, Invitrogen) was used to stain ZO-1 fusion protein as an EC marker. The secondary antibody was a polyclonal anti-mouse IgG antibody raised in donkey and conjugated to Alexa Fluor 546 (2 mg/mL; 1:1000; A10036, Invitrogen). Arteries were imaged as described in Section 2.4.4.

6.2.2 RNAscope™

Septal arteries were prepared and used for RNAscope™, as described in Section 2.8. Following this, a monoclonal anti-human/dog ZO-1antibody raised in mouse (0.5 mg/ml; 1:250; 339188, Invitrogen) was used to stain ZO-1 fusion protein as an EC marker (see Section 2.4). The secondary antibody was a polyclonal anti-mouse IgG antibody raised in goat and conjugated to Alexa Fluor 633 (2 mg/ml; 1:500; A21126, Invitrogen). Arteries

were also co-stained with Hoechst 33342 (10μg/mL) to stain the nuclei. Arteries were imaged as described in Section 2.4.4.

6.3 Results

6.3.1 Rat septal arteries are weakly innervated by sensory nerves

Immunohistochemistry confirmed the expression and colocalisation of CGRP and TRPV1 in the sensory nerves of the rat mesenteric arteries (Figure 6.3.1A-B), demonstrating that these vessels are densely innervated by CGRP- and TRPV1-positive perivascular nerves. This also provides a positive control, as it is widely known that CGRP and TRPV1 are localised in these nerves (Aalkjaer et al., 2021; Scotland et al., 2004; Uddman et al., 1986). In comparison, CGRP- and TRPV1-positive sensory nerves were rarely seen in the rat septal arteries (Figure 6.3.1C-D), suggesting that these vessels do not receive widespread innervation from these perivascular nerves.

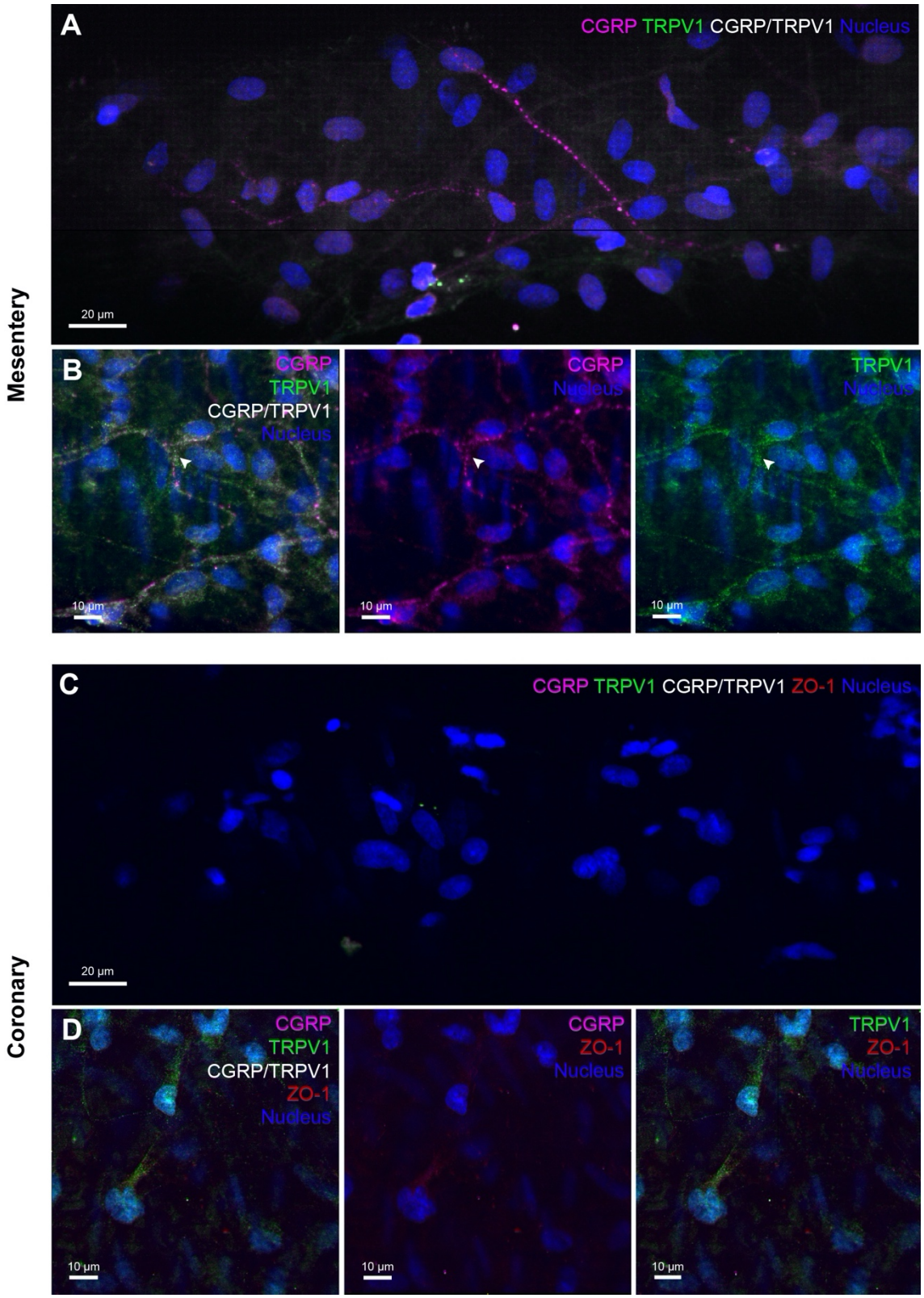

Figure 6.3.1 Expression of CGRP- and TRPV1-positive sensory nerves in isolated arteries. CGRP and TRPV1 labelling is clear in the perivascular nerves of mesenteric arteries (**A**-**B**) but is not visible in coronary septal arteries (**C**-**D**). (**A** and **C**) Confocal

fluorescence images of pressurised arteries. (**B** and **D**) Confocal fluorescence images of wire mounted arteries. CGRP, pink; TRPV1, green; CGRP/TRPV1 colocalisation, white; ZO-1, red; nuclei, blue. Images are representative of 3 experiments.

6.3.2 CGRP is expressed in septal and mesenteric artery endothelial cells

Rat septal arteries were co-stained for CGRP and von Willebrand factor (vWF). vWF mediates platelet adherence at sites of vascular injury and is stored in the Weibel-Palade bodies in ECs (Nightingale & Cutler, 2013), and thus serves as a positive control by which to identify ECs. We observed CGRP expression in the ECs of both septal (Figure 6.3.2A) and mesenteric (Figure 6.3.2B) arteries, where it was effectively always colocalised with vWF. CGRP expression was not seen in the VSMCs of either septal or mesenteric arteries. This indicates that CGRP is stored within the Weibel-Palade bodies of the ECs and, in this way, may be released from the ECs.

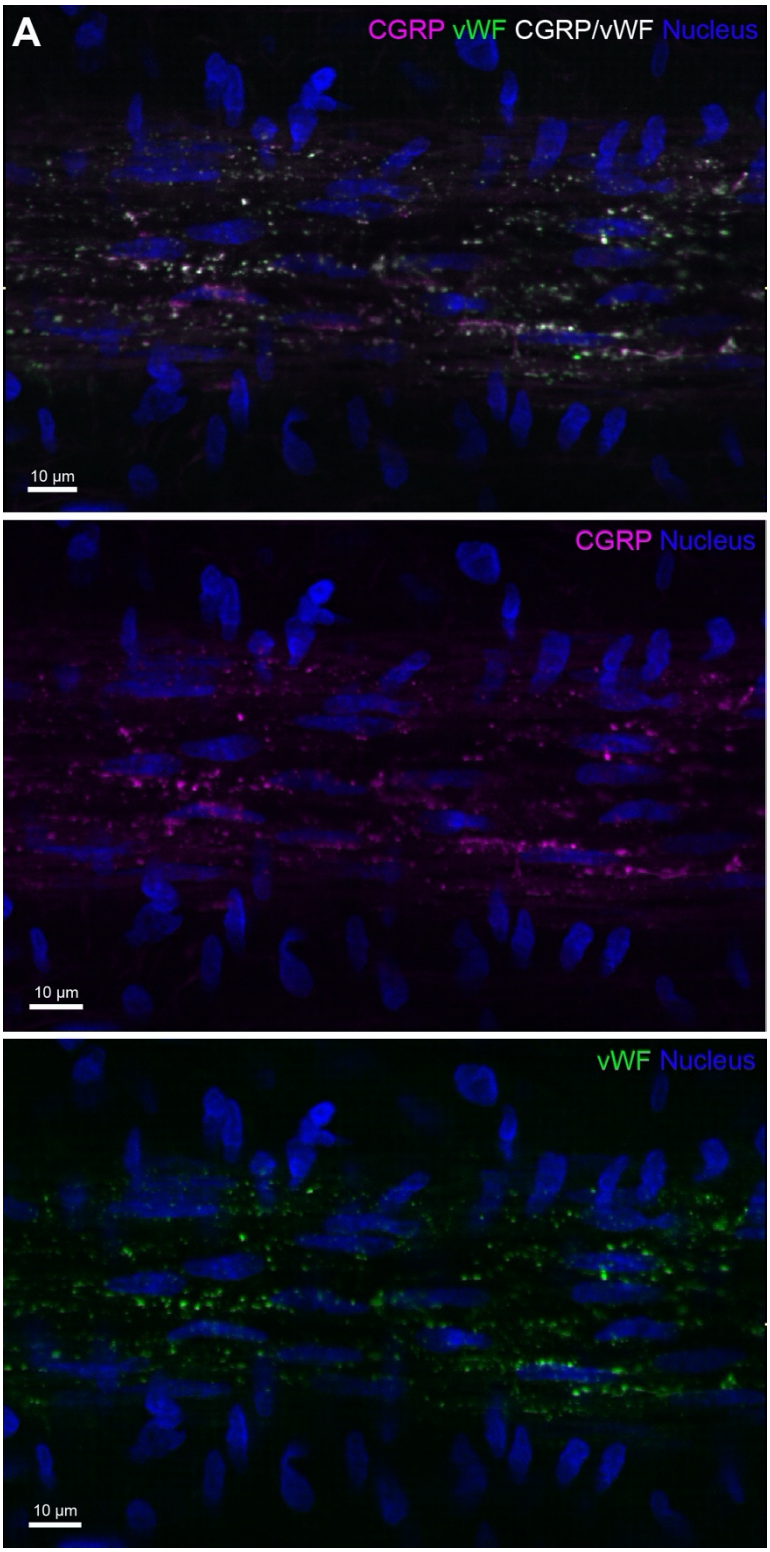
A
CGRP vWF CGRP/vWF Nucleus
10 µm
CGRP Nucleus
10 µm
vWF Nucleus
10 µm

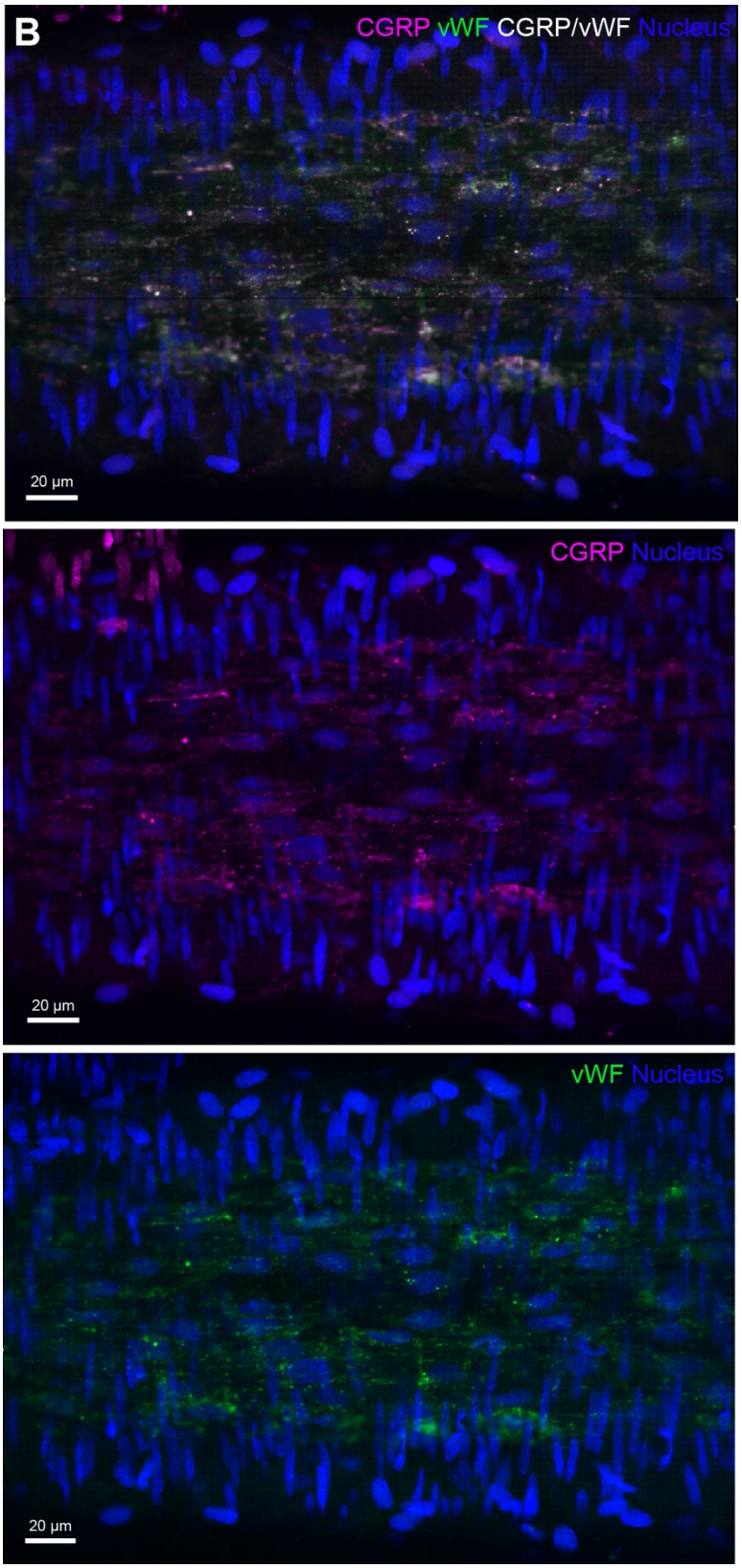

Figure 6.3.2 CGRP expression in the ECs of isolated arteries. CGRP and vWF are colocalised in the ECs of pressurised septal (**A**) and mesenteric (**B**) arteries. CGRP, pink;

vWF, green; CGRP/vWF colocalisation, white; nuclei, blue. Images are representative of 3 experiments.

6.3.3 CGRP is expressed in endocardial endothelial cells

Cardiac strips from the left ventricles of rat hearts were isolated to allow for immunohistochemical analysis of the EECs, as previously described (Borysova et al., 2021). Similarly to the vascular ECs, the EECs expressed CGRP colocalised with vWF. This suggests that CGRP may be released from EECs and thus contribute to the regulation of myocardial function.

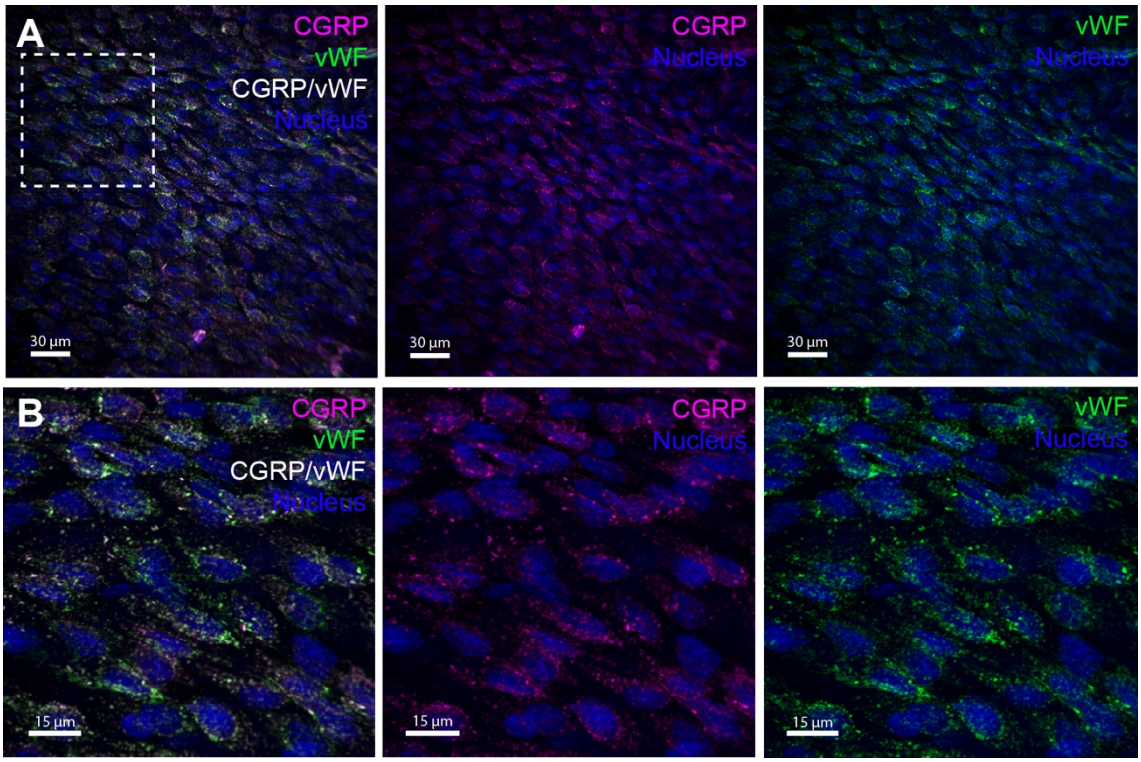

Figure 6.3.3 CGRP expression in the endocardial endothelium. (**A** and **B**) CGRP and vWF are colocalised in left ventricular EECs. The dashed box (**A**) represents the region of magnification (**B**). CGRP, pink; vWF, green; CGRP/vWF colocalisation, white; nuclei, blue. Images are representative of 3 experiments.

6.3.4 CGRP mRNA is not present in septal artery endothelial or smooth muscle cells

To investigate whether CGRP mRNA was present in the ECs of rat septal arteries, RNAscope™ *in situ* hybridisation was utilised with isolated vessels to allow for the visualisation of single RNA molecules. There was effectively no CGRP mRNA detected in the ECs of the septal arteries using a *Calca* probe (Figure 6.3.4A). Interestingly, there appeared to be some CGRP mRNA present in the VSMCs (Figure 6.3.4B). This finding implies that either the CGRP mRNA is very rapidly translated to prepro-CGRP and stored as such, or the promoter is not activated under basal conditions in *ex vivo* arteries.

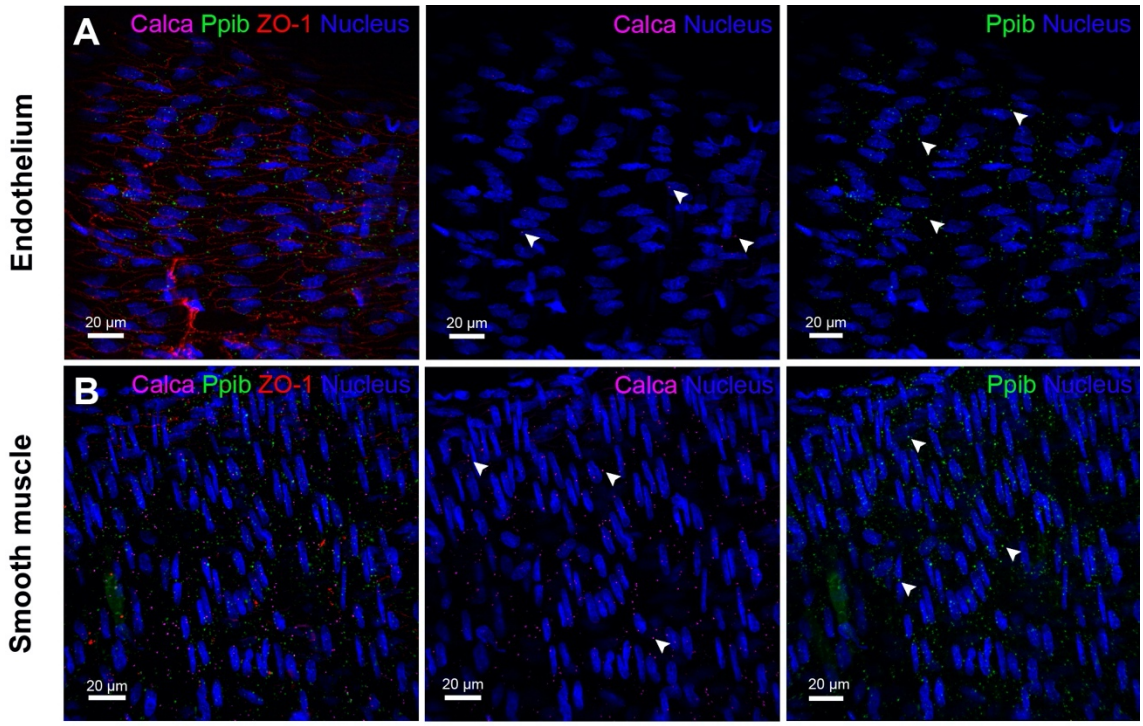

Figure 6.3.4 Expression of *Calca* mRNA in isolated septal arteries. Few *Calca* mRNA molecules were detected in the ECs (**A**), indicated by white arrowheads. A greater number of *Calca* mRNA molecules were detected in the VSMCs (**B**). *Ppib* serves as a positive control. *Calca*, pink; *Ppib*, green; ZO-1, red; nuclei, blue.

6.3.5 TRPV1 channels are expressed in mesenteric and septal arteries

TRPV1 activation causes CGRP release from sensory nerves (Assas et al., 2014; Szabados et al., 2020; Szallasi et al., 2006). To investigate the localisation of TRPV1 channels in the rat mesenteric and septal arteries, arteries were stained for TRPV1. TRPV1 expression was detected in the VSMCs and ECs of both the mesenteric and septal arteries (Figure 6.3.5A-B), but TRPV1-positive perivascular nerves were only visualised in the mesenteric arteries (Figure 6.3.5A). This indicates that the lack of sensory nerve innervation is specific to the coronary microvasculature. Septal arteries co-stained for CGRP and TRPV1 demonstrated colocalisation of the 2 proteins in the ECs (Figure 6.3.6); therefore, the ECs may offer the primary mechanism by which CGRP is released from septal arteries.

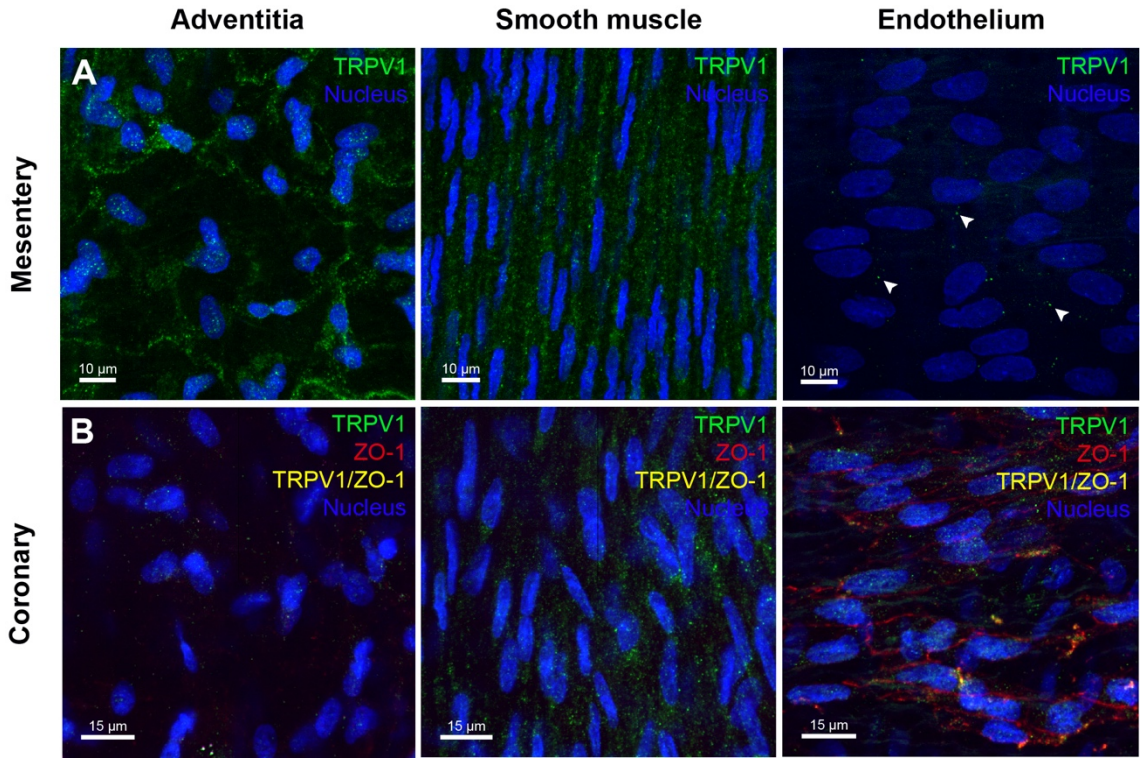

Figure 6.3.5 TRPV1 expression in isolated arteries. (**A**) TRPV1 labelling is clear in the sensory nerves and VSMCs of the mesenteric arteries and is detectable in the ECs, indicated by white arrowheads. (**B**) TRPV1 labelling is present in the VSMCs and ECs of the septal arteries but not in the adventitia. TRPV1, green; ZO-1, red; TRPV1/ZO-1 colocalisation, yellow; nuclei, blue. Images are representative of 3 experiments.

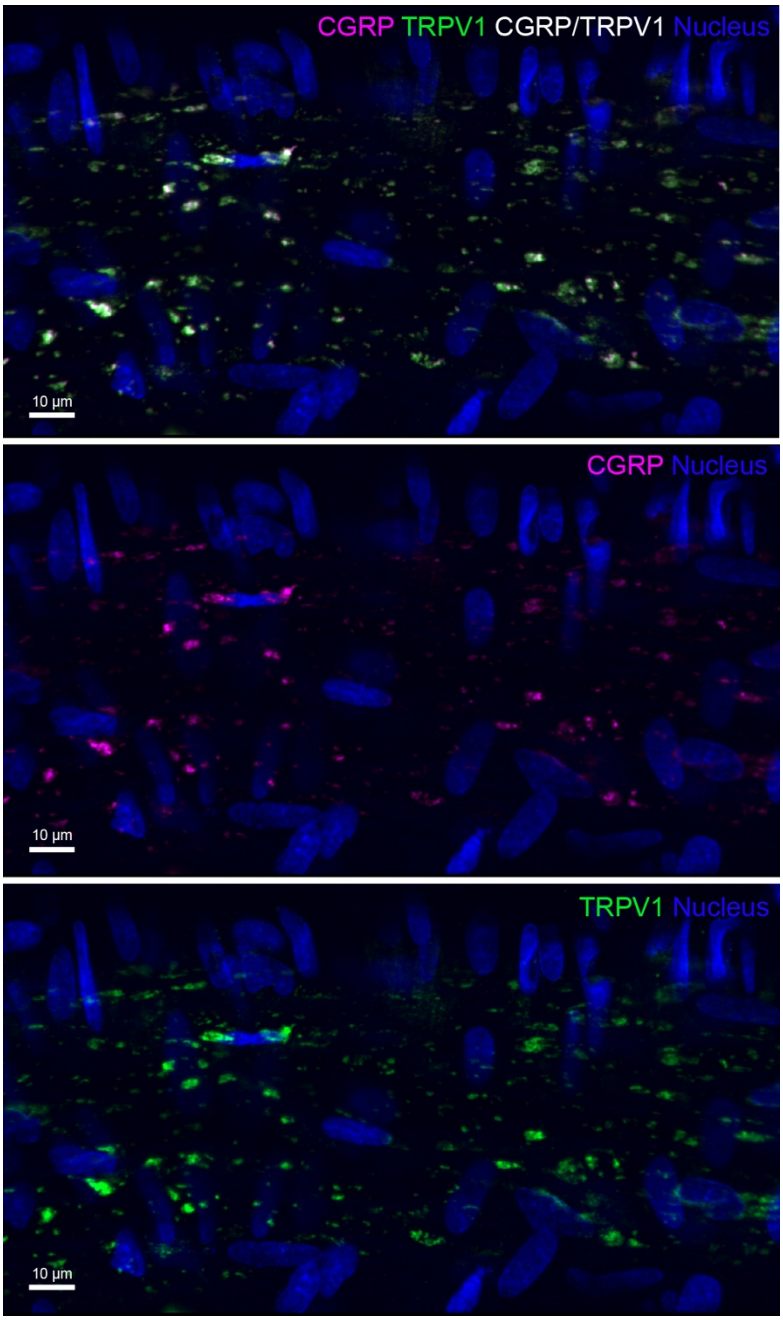

Figure 6.3.6 CGRP and TRPV1 expression in isolated septal arteries. CGRP and TRPV1 are colocalised in the ECs of pressurised septal arteries. CGRP, pink; TRPV1, green; CGRP/TRPV1 colocalisation, white; nuclei, blue. Images are representative of 3 experiments.

6.4 Discussion

The present study aimed to investigate the expression of CGRP in the ECs of the rat septal arteries and endocardium. These results demonstrate the expression of CGRP in the rat coronary artery ECs and EECs for the first time. Furthermore, we also confirmed the expression of TRPV1 channels in the ECs of septal arteries, indicating a possible mechanism for CGRP release.

While immunohistochemical studies have shown that the coronary arteries are indeed innervated, these studies often do not discriminate between autonomic and sensory innervation or solely focus on larger, epicardial coronary arteries (Bulwada et al., 1997; Gulbenkian et al., 1990; Gulbenkian et al., 1993). A dense network of NPY-immunoreactive nerves has been visualised in the myocardium, endocardium, and blood vessels of the human right atrial appendage (RAA) (Wharton et al., 1988), as well as human and pig epicardial arteries (Gulbenkian et al., 1990; Gulbenkian et al., 1993), indicating sympathetic innervation. In contrast, Wharton et al. (1988) reported very few CGRP-positive nerves associated with the coronary arteries in the RAA, suggesting that these vessels do not receive extensive sensory innervation. The current investigation demonstrated that small intramuscular coronary arteries receive little to no sensory innervation as we failed to detect either CGRP or TRPV1 expression in the perivascular nerves. Both CGRP and TRPV1 were abundantly expressed in the perivascular nerves of rat mesenteric arteries, as expected, indicating that this lack of sensory innervation is specific to the coronary microvasculature. Although both CGRP- and TRPV1-positive nerves have been visualised in coronary epicardial arteries (Gulbenkian et al., 1990; Gulbenkian et al., 1993), they are significantly less abundant than the sympathetic nerves.

Gulbenkian et al. (1993) observed an increase in CGRP-positive nerve fibres in the distal region of the epicardial arteries compared with the proximal regions; therefore, it is unsurprising that further heterogeneity exists when comparing to the small intramuscular coronary vessels. Interestingly, Zygmunt et al. (1999) discovered that the vasodilator response to the endogenous cannabinoid receptor agonist, anandamide, was inhibited by CGRP 8-37 and capsazepine in rat hepatic and small mesenteric arteries. The relaxation response to anandamide was also abolished by depletion of the sensory nerves with capsaicin pre-treatment, and they measured a significant release of CGRP following anandamide application. These findings indicate that anandamide can cause CGRP release by activating TRPV1 on sensory nerves. In contrast, neither capsaicin pre-treatment nor capsazepine attenuated vasorelaxation to anandamide in rat LAD coronary arteries (White et al., 2001). This observation could be due to the lack of sensory nerve innervation in rat coronary arteries. Notwithstanding, capsaicin was able to cause vasorelaxation in these vessels, suggesting that a functional sensory nerve system may be present; therefore, one explanation could be that the coronary microcirculation does indeed have sensory nerve innervation, but these nerves do not express CGRP or TRPV1. Alternatively, the observed vasorelaxation in response to capsaicin could reflect TRPV1-mediated CGRP release from the ECs, thus corroborating our hypothesis that this is the primary source of CGRP in coronary arteries.

The presence and role of TRPV1 in the VSMCs and ECs of the vasculature is disputed. In the present investigation, while TRPV1 did not appear to be localised in the perivascular nerves of the rat septal arteries, TRPV1 expression in both the VSMCs and ECs of these vessels was observed, although it appeared to be more abundant in the VSMCs. It is important to note that non-specific labelling has been reported for several

TRPV1 antibodies (Sand et al., 2015; Toth et al., 2014), hence several studies have chosen to investigate functional TRPV1 expression by observing the effects of capsaicin on intracellular Ca^{2+} dynamics. While we are confident that the TRPV1 antibody used in the present study is specific due to the punctate staining observed in the perivascular nerves, VSMCs, and ECs of the rat mesenteric arteries, further experiments utilising our Ca^{2+} imaging techniques in intact septal arteries would provide further evidence for the role of TRPV1 in these vessels. There is evidence for TRPV1 localisation in the VSMCs of resistance arterioles from several vascular beds (Czikora et al., 2012; Kark et al., 2008; Phan et al., 2020; Toth et al., 2014). Phan et al. (2020) utilised validated mouse reporter lines to demonstrate abundant TRPV1 expression in the smooth muscle of small arterioles (<150 μm) of the heart, skeletal muscle, and adipose tissue. Notably, TRPV1 did not appear to be present in the larger, epicardial arteries of the heart but expression was only detected in the VSMCs once these arteries penetrated the myocardium. More recently, Phan et al. (2022) proposed a role for TRPV1 in the myogenic response of coronary arteries after reporting that infusion of the TRPV1 antagonist, BCTC, into isolated rat hearts significantly increased coronary blood flow that partially recovered after 15 minutes. Controversially, other studies failed to see Ca^{2+} influx in response to capsaicin in primary rat aortic VSMCs (Blazevic et al., 2023) and freshly isolated murine aortic VSMCs (Sand et al., 2015), although these results may not be representative of VSMCs in intact vessels.

The disagreement over the expression and role of TRPV1 also extends to the ECs. The study by Phan et al. (2020) observed no TRPV1 expression in the vascular ECs of several vascular beds, but others have reported TRPV1 mRNA in vascular ECs from several sources (Golech et al., 2004; Luo et al., 2008; Poblete et al., 2005; Yao & Garland, 2005).

In fact, TRPV1 activation in the vascular ECs has been linked to NO release. Poblete et al. (2005) found that either nanomolar concentrations of anandamide, which do not cause vasorelaxation, or capsaicin elicited NO release in the rat mesenteric bed, assessed by measuring NO levels in the perfusate with chemiluminescence. This could be inhibited by 3 separate TRPV1 antagonists, CB_1 receptor antagonism, endothelium removal, or NOS inhibition. Similar findings were exhibited by Ching et al. (2011) in BAECs and mouse aortas where TRPV1 ligands caused NO production, quantified indirectly using the Griess assay, and eNOS phosphorylation, determined with Western blot, which could be abolished with capsazepine or removal of extracellular Ca^{2+}. This study also reported that TRPV1 activation resulted in Akt and calmodulin-dependent protein kinase II (CaMKII) phosphorylation, suggesting that TRPV1 induces NO production via the Ca^{2+}-dependent PI3K-Akt-CaMKII signalling pathway, thus implicating a role for TRPV1 in vascular ECs. Both publications conducted control experiments to negate the possibility that the observed TRPV1-induced NO synthesis was instead due to CGRP release from sensory nerves by using chronically denervated mesenteric vessels or the CGRP antagonist, SB268262, respectively. There is a possibility that TRPV1 activation causes CGRP release from the ECs which may act in an autocrine manner to elicit NO production.

A small number of studies have proposed the vascular endothelium as an alternative source of CGRP (Cai et al., 1993; Doi et al., 2001; Ozaka et al., 1997). These findings concur with the present data which demonstrate CGRP expression in the ECs of rat septal arteries. Notably, we have also shown that CGRP is expressed in the EECs lining the ventricles. CLR and CGRP-positive nerve fibers have been identified in the endocardium previously (Hagner et al., 2001; Wharton et al., 1988), but this is the first time that CGRP

has been visualised within the EECs. It is known that CGRP has both inotropic and chronotropic effects on the heart (Franco-Cereceda et al., 1987a; Kumar et al., 2019; Sigrist et al., 1986) and, in this way, CGRP release from the EECs would be able to regulate the contractility of the heart. In both the vascular ECs and EECs, CGRP was co-localised with vWF, indicating that CGRP is stored within the Weibel-Palade bodies. This finding is consistent with previous studies in intact arteries (Doi et al., 2001; Ozaka et al., 1997). These studies also observed CGRP localisation in the rER which they proposed as evidence for the synthesis of CGRP in the ECs. Doi et al. (2001) successfully detected prepro-CGRP mRNA in the endothelium of rat thoracic aorta and femoral arteries using *in situ* hybridisation, and Luo et al. (2008) demonstrated the presence of CGRP mRNA in HUVECs using RT-PCR. Despite consistently visualising CGRP protein expression, we were unable to detect any CGRP mRNA in the septal artery ECs using RNAscope™. Intriguingly, there appeared to be a modest amount of CGRP mRNA in the VSMCs, even though CGRP protein expression was never observed in these cells. The regulation of CGRP synthesis is poorly understood, with few studies in existence that explore CGRP production in the ECs. Treatment with capsaicin or hyperthermia was reported to upregulate CGRP mRNA expression in HUVECs after 12 and 8 hours, respectively (Luo et al., 2008). These effects could be blocked with capsazepine, indicating that TRPV1 can regulate the synthesis of CGRP as well as its release. The upregulation of CGRP mRNA expression by heat stress has also been demonstrated in rat dorsal root ganglia (Peng et al., 2001). A possible explanation for the absence of CGRP mRNA in the present study, therefore, is that it may only be produced in the ECs of these vessels upon stimulation. Further investigations are thus necessary to determine the mechanism of CGRP synthesis in the ECs of intact arteries and the EECs of the heart.

6.5 Conclusions

The current study proposes a role for the ECs in CGRP storage and release in the septal arteries. These vessels appear to receive modest, if any, innervation from CGRP-containing sensory nerves; therefore, CGRP may instead be released from ECs to act in an autocrine and paracrine manner on the endothelium and smooth muscle. Despite CGRP being clearly detected, we were unsuccessful in demonstrating CGRP mRNA expression in the ECs. This may indicate that the ECs do not synthesise CGRP. Another possible explanation is that CGRP synthesis only occurs upon stimulation, or that CGRP mRNA is immediately translated and stored in its peptide form. Furthermore, TRPV1 expression was observed in both the VSMCs and ECs, although the protein was more abundantly expressed in the VSMCs. It is possible, therefore, that TRPV1 activation may provide an important mechanism for CGRP release from the ECs, analogous to CGRP's well-characterised release from sensory nerves.

While these data are preliminary, they suggest an exciting and novel function of the ECs in these arteries whereby they are responsible for CGRP release. Further investigations will hopefully elucidate whether the ECs are also a site of CGRP synthesis in response to physiological and pathological stimuli, as well as functionally demonstrate and characterise the mechanisms for CGRP release from the endothelium in intact arteries.

CHAPTER 7: SUMMARY AND FUTURE DIRECTIONS

This thesis investigated the effects of the vasoactive peptide, CGRP, on the coronary microcirculation. Specifically, it aimed to elucidate the intracellular signalling pathways responsible for CGRP-induced vasorelaxation and explore CGRP synthesis and release in rat intramuscular coronary septal arteries. This is the first time that a functional study has used myogenically-contracted isolated coronary arteries to conduct concentration-response curves and electrophysiology. This has avoided the influence of agonist-induced pre-constriction and, arguably, may better reflect the basic underlying mechanisms which should be considered in future studies, including *in vivo*.

We have shown that CGRP is a potent vasodilator when applied exogenously to isolated rat septal arteries. CGRP induces a gradual vasorelaxation, particularly at lower concentrations. We were thus forced to implement a protocol where increasing concentrations of CGRP were administered cumulatively at 2-minute intervals, as described in Chapter 3, due to timing limitations that could impact artery viability. Future investigations may consider administering individual CGRP concentrations separately, to confirm the maximal response to each concentration. While the exogenous CGRP concentrations used are physiologically relevant, the present study could be extended to investigate the response to endogenous CGRP in the septal arteries by initiating the release of stored CGRP, as others have done using capsaicin (Geppetti et al., 1991; Luo et al., 2008; Szabados et al., 2020).

The data in Chapter 4 indicate that the endothelium has a significant contribution to CGRP-induced vasodilation. It appears that this endothelium-dependent component can be predominantly attributed to NO synthesis and release (Figure 6.5.1). While we were

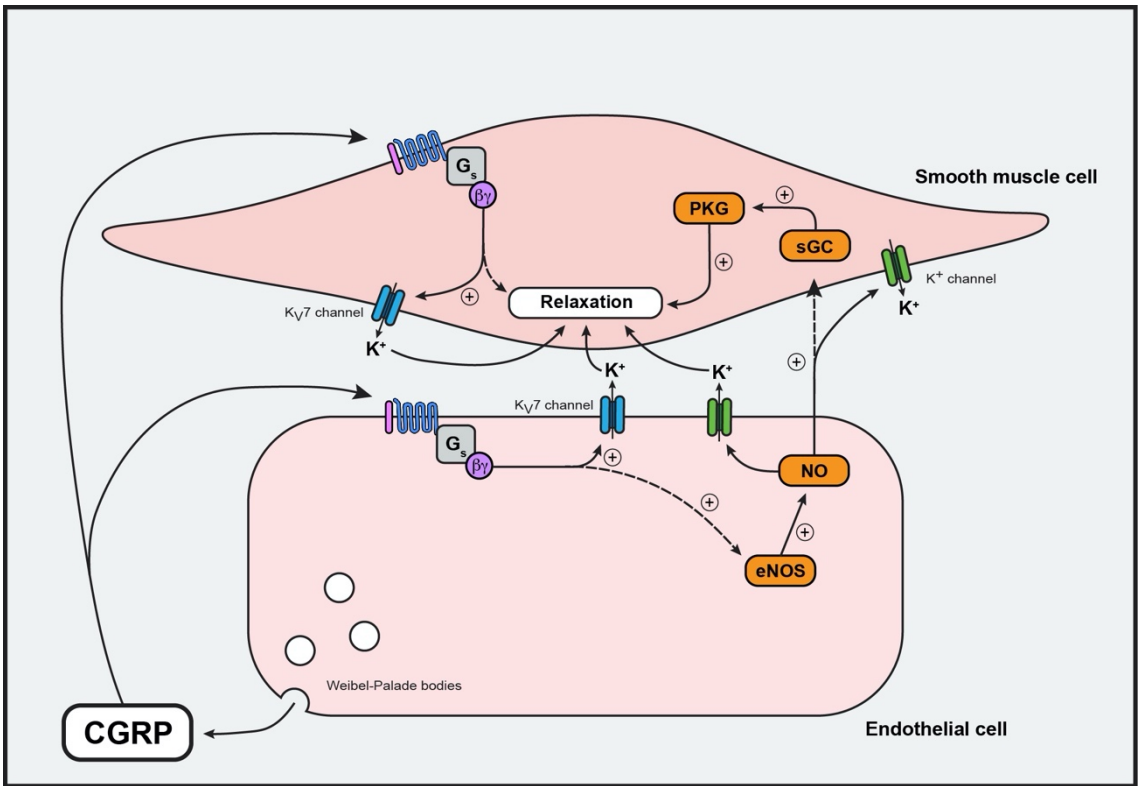

Figure 6.5.1 Summary of thesis findings. CGRP is primarily released from ECs in the coronary arteries since these vessels lack sensory innervation. CGRP activates a Gβγ subunit-mediated pathway in both the ECs and VSMCs. NO release is largely responsible for the EC-dependent component of CGRP-induced vasorelaxation and appears to cause hyperpolarization via K^+ channel activation. CGRP also activates K_V7 channels, present on the VSMCs and ECs, to cause vasorelaxation and hyperpolarization. Boxes with curved edges represent intracellular signalling components. Dashed arrows represent signalling pathways that are yet to be consolidated.

unsuccessful in quantifying NO release directly using the Cu_2FL2E dye, our research group has since optimised another NO-sensitive fluorescent dye, DAR-4M AM, with more promising results (Wallis et al., 2023). This may enable us to measure NO release in response to CGRP as well as establishing whether NO is released from the ECs under basal conditions, which would explain the increased level of myogenic tone observed in the presence of NOS inhibition. We attempted to use Western blotting to determine whether CGRP stimulates NOS phosphorylation, as would be expected if CGRP does induce NO synthesis and release, to support our functional data. Unfortunately, it proved challenging to extract sufficient protein from the rat septal arteries to conduct these experiments. Instead, we have turned our attention to developing an immunohistochemistry protocol to detect phosphorylated eNOS expression relative to total eNOS expression in arteries mounted in the wire myograph. This will allow us to link functional data with spatial protein expression and phosphorylation. If the endothelium does indeed have an important role in the CGRP response as the present investigation suggests, this would have substantial clinical implications *in vivo*. Endothelial dysfunction is present in many cardiovascular diseases resulting in a reduced NO bioavailability; therefore, these patients would have an impaired response to CGRP. Further research into how CGRP-induced vasodilation is impacted in disease states may result in novel therapeutic strategies that could reduce coronary vascular resistance and relieve symptoms.

It is fundamental to investigate the effects of CGRP on smooth muscle membrane potential alongside its vasodilatory effects to fully understand the intracellular signalling pathways involved. Voltage changes are particularly important in resistance arteries where it has been observed, both by our research group and others, that the L-type Ca^{2+}

channel blocker, nifedipine, prevents spontaneous myogenic tone from developing (Potocnik et al., 2000). This indicates that depolarization and hyperpolarization underlie vasoconstriction and vasorelaxation, respectively, in these vessels; however, studies rarely explore how these processes are integrated. In Chapter 5, electrophysiological techniques were employed to measure the changes in tension and membrane potential simultaneously in isolated septal arteries in response to CGRP for the first time. Despite K_{ATP} channels being widely implicated in CGRP-induced hyperpolarization (Norton & Segal, 2018; Norton et al., 2021; Wellman et al., 1998), these data corroborate findings indicating that K_{ATP} channels do not, in fact, underpin CGRP-mediated hyperpolarization in the coronary vascular bed (Prieto et al., 1991; Sheykhzade & Berg Nyborg, 2001). Instead, the present study revealed that K_V7 channels are responsible for CGRP-induced hyperpolarization in the septal arteries (Figure 6.5.1). A role for K_V7 channels in CGRP-induced vasorelaxation has already been demonstrated in other vascular beds (Chadha et al., 2014; Stott et al., 2018), but this is the first time that their role in the CGRP response has been assessed in the coronary vasculature. K_V7 channels are downregulated in several cardiovascular diseases; therefore, this would likely result in severe dysfunctions in CGRP signalling and increased vascular resistance. Our data also implies that the NO and K_V7 signalling pathways may be linked and that NO may contribute to hyperpolarization, either via K_V7 channel activation or activation of other K^+ channels (Figure 6.5.1). Further investigations are necessary to establish the relationship between NO and hyperpolarization as this may be important in understanding not only the CGRP signalling pathways, but also myogenic tone regulation. If NO does indeed cause hyperpolarization of the ECs and/or VSMCs, this would provide a novel mechanism that may be specific to the coronary microcirculation.

While it does appear the K_V7 channels are the predominant K^+ channel involved, with linopirdine effectively abolishing CGRP-induced hyperpolarization, there have been studies also proposing a role for K_{Ca} channels (Norton et al., 2021; Sheykhzade & Berg Nyborg, 2001). Similar experimental studies to those described in Chapter 5, using antagonists such as apamin (SK_{Ca} inhibitor), TRAM-34 (IK_{Ca} inhibitor), and iberiotoxin (BK_{Ca} inhibitor), could be conducted to clarify whether these channels have a minor contribution to the CGRP response in the septal arteries. Furthermore, agonists that initiate a local vascular hyperpolarization may cause conducted vasodilation, whereby the hyperpolarizing current spreads along the endothelium and into adjacent VSMCs via MEGJs. This was first demonstrated in skeletal muscle (Segal & Duling, 1986), but has since been demonstrated by our research group in human and porcine small intramyocardial coronary arteries (Dora et al., 2022b). It is likely, therefore, that CGRP causes a robust conducted vasodilation and, in this way, may be an important regulator of coronary microvascular blood flow. Further investigation into the mechanisms underlying CGRP-induced hyperpolarization and the potential subsequent conducted vasodilation is highly warranted.

There has been recent evidence proposing a Gβγ subunit-mediated signalling pathway in CGRP-induced vasorelaxation, rather than the CGRP response relying on a Gαs subunit-mediated cAMP-PKA pathway as previously described (Meens et al., 2012; Stott et al., 2018). The results in Chapter 5 support this, implicating a significant role for the Gβγ subunit in both the ECs and VSMCs (Figure 6.5.1). The present study was not able to rule out a role for the cAMP-PKA pathway due to current antagonists of this pathway being ineffective in our experiments, and thus future work utilising effective cAMP-PKA antagonists could support our conclusions. Furthermore, the precise signalling pathway,

downstream from Gβγ subunit activation, that results in vasorelaxation has yet to be established. Our Ca^{2+} imaging data in the ECs indicates that the Gβγ subunit does not initiate NO release via the PLC-IP_3 pathway, or any other Ca^{2+}-dependent pathway. One possibility is that the Gβγ subunit activates the PI3K-Akt, which has been shown to stimulate NO synthesis (Ching et al., 2011; Dimmeler et al., 1999; Michell et al., 1999). We attempted to use the Akt inhibitor, Akti-1/2, to investigate the effects this would have on CGRP-induced vasorelaxation but found that the inhibitor prevented contraction to both PE and ANG II. We concluded that the inhibitor must also be inhibiting the PI3K-Akt pathway in the VSMCs, thus making it difficult to study the ECs directly. Further experiments are thus required to explore whether the PI3K-Akt pathway contributes to the CGRP response, either by using effective antagonists of this pathway in functional experiments and/or by using our developed whole-mount immunolabelling protocol to determine whether CGRP causes Akt phosphorylation.

One of the most surprising findings in this thesis is that the rat septal arteries do not receive dense innervation from CGRP-positive sensory nerves. Furthermore, CGRP appears to be expressed in the ECs where it is colocalised with von-Willebrand factor. This indicates that the source of CGRP in these arteries may, in fact, be the endothelium rather than the perivascular nerves, which illustrates another facet contributing to the severity of endothelial dysfunction in coronary arteries. Despite other studies demonstrating CGRP mRNA expression in ECs (Doi et al., 2001; Luo et al., 2008), we were unable to detect its presence in the ECs of isolated septal arteries using RNAscope. We also attempted to use both RT-PCR and qPCR to determine CGRP mRNA expression, but it was not possible to collect sufficient cDNA from these arteries without using an inappropriate number of animals. As discussed in Chapter 6, the absence of CGRP mRNA

may not necessarily indicate that the ECs do not synthesis CGRP but could instead be due to the CGRP mRNA not being produced and stored following stimulation of the promoter. A preliminary experiment was conducted where HAECs were exposed to hypoxia for 30 min, 6 hours, and 12 hours to investigate whether this stimulated CGRP synthesis and/or release. Although we confirmed CGRP expression in untreated HAECs using immunohistochemistry, CGRP mRNA was undetected by both human and rat CGRP probes in both normoxic and hypoxic HAEC pellets; we are yet to determine whether this is due to the probes being ineffective or CGRP mRNA not being present. In future experiments, we hope to employ immunohistochemistry and ELISA to establish whether the CGRP protein level changes in the HAECs and media to ascertain whether hypoxia induces CGRP release from ECs. If this is the case, it would explain why CGRP levels in plasma have been reported to increase during ischaemia (Kumar et al., 2019). If a region of the heart becomes ischaemic and initiates local CGRP release, this would result in an improvement in blood flow to that area; in this way, the endothelium itself may act as the sensor. It is also necessary to optimise a technique that will enable us to detect CGRP mRNA if it is present. *In situ* hybridisation, using the rat probes designed by Doi et al. (2001), may be the logical next approach as this publication provides a positive control. Another novel finding of the present study is that CGRP is also expressed in the EECs of the heart. Our knowledge of the endocardial endothelium and the role of peptides stored in the EECs is limited, but the presence of CGRP in these cells suggests that it may contribute to cardiac function and development. Further research to advance our understanding into the function of CGRP in the EECs is crucial and is likely to yield clinically significant results.

TRPV1 channel activation has been widely attributed as the mechanism responsible for CGRP release from perivascular nerves (Scotland et al., 2004; Szabados et al., 2020). While the present study identified that TRPV1 channels are expressed in the VSMCs and ECs of the septal arteries, further functional experiments are required to determine whether TRPV1 activation causes CGRP release from the ECs of these vessels. These experiments could employ TRPV1 activators such as capsaicin, hypoxia, or hyperthermia. Surprisingly, TRPV1 expression was significantly more abundant in the VSMCs than the ECs, which may indicate that these channels do not contribute to CGRP release from the ECs. TRPA1 channels have also been implicated in CGRP release (Eberhardt et al., 2014; Quallo et al., 2015). Although our group did not observe any TRPA1 expression in the VSMCs and ECs of mesenteric arteries (Pinkney et al., 2017), it has been reported to be expressed in these cell types within dural and pial arteries (Hansted et al., 2020); therefore, further exploration into TRP channels in the septal arteries may help identify the mechanism of CGRP release from vascular ECs.

It is worth noting that the experiments in the present investigation were conducted in male Wistar rats as inclusion of female rats would have doubled the number of animals, costs, and time needed to account for potential sex differences. Both pregnancy and female sex steroid hormones have been shown to enhance the vasodilation response to CGRP (Gangula et al., 1999; Gangula et al., 2001; Gangula et al., 2002), with evidence reporting an increase in CGRP receptor density (Yallampalli et al., 2004) and CGRP mRNA levels in the dorsal root ganglia in response to pregnancy or estradiol and progesterone treatment (Gangula et al., 2000). Gangula et al. (2001) demonstrated that the coronary vasculature was more sensitive to CGRP during pregnancy and in ovariectomised rats treated with estrodiol and progesterone. Interestingly, both migraine and CMVD are more prevalent

in women; therefore, this may reflect sex differences in CGRP signalling. The research in this thesis could thus be repeated in female rats and, if the results indicate that sex-dependent variation does exist, this may provide novel insights into migraine and CMVD pathophysiology, particularly for female patients.

This thesis demonstrates that CGRP is a potent vasodilator in rat septal arteries, and thus a clinically relevant endogenous agonist. The findings in this study indicate that, at the lowest concentrations, CGRP-induced vasorelaxation relies on the release of NO from the endothelium. Interestingly, the response to NO appears to involve hyperpolarization; however, the K^+ channel involved has not been identified and requires further investigation. When the NO-dependent pathway is blocked, the vasorelaxation to CGRP is driven by hyperpolarization that is mediated predominantly by K_V7 channels. The present study confirms the importance of hyperpolarization in CGRP-induced vasorelaxation and, as such, it should be considered as a significant mechanism in the coordination of blood flow in the coronary microcirculation. This investigation also provides evidence supporting a role for the Gβγ subunit in both endothelium-dependent and -independent vasorelaxation to CGRP, but further research is necessary to identify the precise downstream signalling pathway involved. Finally, this thesis reports a novel finding of CGRP expression in the coronary vascular ECs and EECs which may have promising clinical relevance, particularly in ischaemia. We hope that the present study, along with the future work described, will translate into the human coronary microvasculature to further our clinical understanding of these vessels, and develop new therapeutic strategies that target their pathophysiology.

CHAPTER 8: REFERENCES

Aalkjaer, C., Nilsson, H., & De Mey, J. G. R. (2021). Sympathetic and Sensory-Motor Nerves in Peripheral Small Arteries. *Physiol Rev*, *101*(2), 495-544.

Aiyar, N., Disa, J., Stadel, J. M., & Lysko, P. G. (1999). Calcitonin gene-related peptide receptor independently stimulates 3',5'-cyclic adenosine monophosphate and Ca2+ signaling pathways. *Molecular and Cellular Biochemistry*, *197*(1-2), 179-185.

Alaimo, A., & Villarroel, A. (2018). Calmodulin: A Multitasking Protein in Kv7.2 Potassium Channel Functions. *Biomolecules*, *8*(3).

Amara, S., Jonas, V., & Rosenfeld, M. (1982). Alternative RNA processing in calcitonin gene expression generates mRNAs encoding different polypeptide products. *Nature*, *298*, 240-244.

Amara, S. G., Arriza, J. L., Leff, S. E., Swanson, L. W., Evans, R. M., & Rosenfeld, M. G. (1985). Expression in Brain of a Messenger RNA Encoding a Novel Neuropeptide Homologous to Calcitonin Gene-Related Peptide. *Science*, *229*(4718), 1094-1097.

Andrews, K. L., Irvine, J. C., Tare, M., Apostolopoulos, J., Favaloro, J. L., Triggle, C. R., & Kemp-Harper, B. K. (2009). A role for nitroxyl (HNO) as an endothelium-derived relaxing and hyperpolarizing factor in resistance arteries. *Br J Pharmacol*, *157*(4), 540-550.

Argunhan, F., & Brain, S. D. (2022). The Vascular-Dependent and -Independent Actions of Calcitonin Gene-Related Peptide in Cardiovascular Disease. *Front Physiol*, *13*, 833645.

Arnold, W. P., Mittal, C. K., Katsuki, S., & Murad, F. (1977). Nitric oxide activates guanylate cyclase and increases guanosine 3':5'-cyclic monophosphate levels in various tissue preparations. *Proc Natl Acad Sci U S A*, *74*(8), 3203-3207.

Assas, B. M., Pennock, J. I., & Miyan, J. A. (2014). Calcitonin gene-related peptide is a key neurotransmitter in the neuro-immune axis. *Front Neurosci*, *8*, 23.

Bagher, P., Beleznai, T., Kansui, Y., Mitchell, R., Garland, C. J., & Dora, K. A. (2012). Low intravascular pressure activates endothelial cell TRPV4 channels, local Ca2+ events, and IKCa channels, reducing arteriolar tone. *Proceedings of the National Academy of Sciences of the United States of America*, *109*(44), 18174-18179.

Baldwin, S. N., Sandow, S. L., Mondejar-Parreno, G., Stott, J. B., & Greenwood, I. A. (2020). K(V)7 Channel Expression and Function Within Rat Mesenteric Endothelial Cells. *Front Physiol*, *11*, 598779.

Barja, F., Mathison, R., & Huggel, H. (1983). Substance P-containing nerve fibres in large peripheral blood vessels of the rat. *Cell and Tissue Research*, *229*, 411-422.

Bayewitch, M. L., Avidor-Reiss, T., Levy, R., Pfeuffer, T., Nevo, I., Simonds, W. F., & Vogel, Z. (1998a). Differential modulation of adenylyl cyclases I and II by various G beta subunits. *J Biol Chem*, *273*(4), 2273-2276.

Bayewitch, M. L., Avidor-Reiss, T., Levy, R., Pfeuffer, T., Nevo, I., Simonds, W. F., & Vogel, Z. (1998b). Inhibition of adenylyl cyclase isoforms V and VI by various Gbetagamma subunits. *FASEB J*, *12*(11), 1019-1025.

Bayliss, W. M. (1902). On the local reactions of the arterial wall to changes of internal pressure. *J Physiol*, *28*(3), 220-231.

Bevan, J. A., & Osher, J. V. (1972). A direct method for recording tension changes in the wall of small blood vessels in vitro. *Agents and Actions*, *2*, 257-260.

Blazevic, T., Ciotu, C. I., Gold-Binder, M., Heiss, E. H., Fischer, M. J. M., & Dirsch, V. M. (2023). Cultured rat aortic vascular smooth muscle cells do not express a functional TRPV1. *PLoS One*, *18*(2), e0281191.

Boerman, E. M., & Segal, S. S. (2016). Depressed perivascular sensory innervation of mouse mesenteric arteries with advanced age. *Journal of Physiology*, *594*(8), 2323-2338.

Bohr, D. F., & Goulet, P. L. (1961). Role of electrolytes in the contractile machinery of vascular smooth muscle. *The American Journal of Cardiology*, *8*(4), 549-556.

Bolton, T. B., Lang, R. J., & Takewaki, T. (1984). Mechanisms of action of noradrenaline and carbachol on smooth muscle of guinea-pig anterior mesenteric artery. *J Physiol*, *351*, 549-572.

Borysova, L., Ng, Y. Y. H., Wragg, E. S., Wallis, L. E., Fay, E., Ascione, R., & Dora, K. A. (2021). High spatial and temporal resolution Ca(2+) imaging of myocardial strips from human, pig and rat. *Nat Protoc*, *16*(10), 4650-4675.

Brain, S. D., Williams, T. J., Tippins, J. R., Morris, H. R., & MacIntyre, I. (1985). Calcitonin gene-related peptide is a potent vasodilator. *Nature*, *313*(5997), 54-56.

Brayden, J. E., Li, Y., & Tavares, M. J. (2012). Purinergic Receptors Regulate Myogenic Tone in Cerebral Parenchymal Arterioles. *Journal of Cerebral Blood Flow & Metabolism*, *33*(2), 293-299.

Broadhead, M. W., Kharbanda, R. K., Peters, M. J., & MacAllister, R. J. (2004). KATP channel activation induces ischemic preconditioning of the endothelium in humans in vivo. *Circulation*, *110*(15), 2077-2082.

Broillet, M., Randin, O., & Chatton, J. (2001). Photoactivation and calcium sensitivity of the fluorescent NO indicator 4,5-diaminofluorescein (DAF-2): implications for cellular NO imaging. *FEBS Lett*, *491*(3), 227-232.

Brozovich, F. V., Nicholson, C. J., Degen, C. V., Gao, Y. Z., Aggarwal, M., & Morgan, K. G. (2016). Mechanisms of Vascular Smooth Muscle Contraction and the Basis

for Pharmacologic Treatment of Smooth Muscle Disorders. *Pharmacol Rev*, *68*(2), 476-532.

Bryan, N. S., & Grisham, M. B. (2007). Methods to detect nitric oxide and its metabolites in biological samples. *Free Radical Biology Medicine*, *43*(5), 645-657.

Bulwada, J., Colnot, D. R., Bleys, R. L. A. W., Groen, G. J., Thrasivoulou, C., & Cowen, T. (1997). Imaging and analysis of perivascular nerves in human mesenteric and coronary arteries: a comparison between epi-fluorescence and confocal microscopy. *Journal of Neuroscience Methods*, *73*, 129-134.

Cai, W. Q., Dikranian, K., Bodin, P., Turmaine, M., & Burnstock, G. (1993). Colocalization of vasoactive substances in the endothelial cells of human umbilical vessels. *Cell Tissue Res*, *274*, 533-538.

Campos-Rios, A., Rueda-Ruzafa, L., & Lamas, J. A. (2022). The Relevance of GIRK Channels in Heart Function. *Membranes (Basel)*, *12*(11).

Camps, M., Carozzi, A., Schnabel, P., Scheer, A., Parker, P., & Giershick, P. (1992). Isozyme-selective stimulation of phospholipase C-beta2 by G protein betagamma subunits. *Nature*, *360*, 684-686.

Chadha, P. S., Jepps, T. A., Carr, G., Stott, J. B., Zhu, H. L., Cole, W. C., & Greenwood, I. A. (2014). Contribution of kv7.4/kv7.5 heteromers to intrinsic and calcitonin gene-related peptide-induced cerebral reactivity. *Arterioscler Thromb Vasc Biol*, *34*(4), 887-893.

Chan, K. Y., Edvinsson, L., Eftekhari, S., Kimblad, P. O., Kane, S. A., Lynch, J., Hargreaves, R. J., de Vries, R., Garrelds, I. M., van den Bogaerdt, A. J., Danser, A. H., & Maassenvandenbrink, A. (2010). Characterization of the calcitonin gene-related peptide receptor antagonist telcagepant (MK-0974) in human isolated coronary arteries. *J Pharmacol Exp Ther*, *334*(3), 746-752.

Chen, G., Suzuki, H., & Weston, A. H. (1988). Acetylcholine releases endothelium-derived hyperpolarizing factor and EDRF from rat blood vessels. *Br J Pharmacol*, *95*(4), 1165-1174.

Chen, X., Li, W., Hiett, S. C., & Obukhov, A. G. (2016). Novel Roles for Kv7 Channels in Shaping Histamine-Induced Contractions and Bradykinin-Dependent Relaxations in Pig Coronary Arteries. *PLoS One*, *11*(2), e0148569.

Chiba, T., Yamaguchi, A., Yamatani, T., Nakamura, A., Morishita, T., Inui, T., Fukase, M., Noda, T., & Fujita, T. (1989). Calcitonin gene-related peptide antagonist human CGRP-(8-37). *American Journal of Physiology Endocrine and Metabolism*, *256*(2), 331-335.

Ching, L. C., Kou, Y. R., Shyue, S. K., Su, K. H., Wei, J., Cheng, L. C., Yu, Y. B., Pan, C. C., & Lee, T. S. (2011). Molecular mechanisms of activation of endothelial nitric oxide synthase mediated by transient receptor potential vanilloid type 1. *Cardiovasc Res*, *91*(3), 492-501.

Clapham, D. E., & Neer, E. J. (1993). New roles for G-protein betagamma-dimers in transmembrane signalling. *Nature Progress*, *365*, 403-406.

Clark, A. J., Mullooly, N., Safitri, D., Harris, M., de Vries, T., MaassenVanDenBrink, A., Poyner, D. R., Gianni, D., Wigglesworth, M., & Ladds, G. (2021). CGRP, adrenomedullin and adrenomedullin 2 display endogenous GPCR agonist bias in primary human cardiovascular cells. *Commun Biol*, *4*(1), 776.

Cohen, F., Yuan, H., & Silberstein, S. D. (2022). Calcitonin Gene-Related Peptide (CGRP)-Targeted Monoclonal Antibodies and Antagonists in Migraine: Current Evidence and Rationale. *BioDrugs*, *36*(3), 341-358.

Croop, R., Madonia, J., Stock, D. A., Thiry, A., Forshaw, M., Murphy, A., Coric, V., & Lipton, R. B. (2022). Zavegepant nasal spray for the acute treatment of migraine:

A Phase 2/3 double-blind, randomized, placebo-controlled, dose-ranging trial. *Headache*, *62*(9), 1153-1163.

Crossman, D. C., Dashwood, M. R., Brain, S. D., McEwan, J., & Pearson, J. D. (1990). Action of calcitonin gene-related peptide upon bovine vascular endothelial and smooth muscle cells grown in isolation and co-culture. *Br J Pharmacol*, *99*, 71-76.

Csonka, C., Pali, T., Bencsik, P., Gorbe, A., Ferdinandy, P., & Csont, T. (2015). Measurement of NO in biological samples. *Br J Pharmacol*, *172*(6), 1620-1632.

Czikora, A., Lizanecz, E., Bako, P., Rutkai, I., Ruzsnavszky, F., Magyar, J., Porszasz, R., Kark, T., Facsko, A., Papp, Z., Edes, I., & Toth, A. (2012). Structure-activity relationships of vanilloid receptor agonists for arteriolar TRPV1. *Br J Pharmacol*, *165*(6), 1801-1812.

Davis, M. J., & Hill, M. A. (1999). Signaling mechanisms underlying the vascular myogenic response. *Physiological Reviews*, *79*(2), 387-423.

De Mey, J. G. R., Megens, R., & Fazzi, G. E. (2008a). Functional antagonism between endogenous neuropeptide Y and calcitonin gene-related peptide in mesenteric resistance arteries. *J Pharmacol Exp Ther*, *324*(3), 930-937.

De Mey, J. G. R., Megens, R., & Fazzi, G. E. (2008b). Functional antagonism between endogenous neuropeptide Y and calcitonin gene-related peptide in mesenteric resistance arteries. *Journal of Pharmacology and Experimental Therapeutics*, *324*(3), 930-937.

Deng, P. Y., Ye, F., Zhu, H. Q., Cai, W. J., Deng, H. W., & Li, Y. J. (2003). An increase in the synthesis and release of calcitonin gene-related peptide in two-kidney, one-clip hypertensive rats. *Regul Pept*, *114*(2-3), 175-182.

Dennis, T., Fournier, A., St. Pierre, S., & Quirion, R. (1989). Structure-Activity Profile of Calcitonin Gene-Related Peptide in Peripheral and Brain Tissues. Evidence for Receptor Multiplicity. *The Journal of Pharmacology and Experimental Therapeutics*, *251*(2), 718-725.

Dimmeler, S., Fleming, I., Fisslthaler, B., Hermann, C., Busse, R., & Zeiher, A. M. (1999). Activation of nitric oxide synthase in endothelial cells by Akt-dependent phosphorylation. *Letters to Nature*, *399*, 601-605.

Doi, Y., Kudo, H., Nishino, T., Kayashima, K., Kiyonaga, H., Nagata, T., Nara, S., Morita, M., & Fujimoto, S. (2001). Synthesis of calcitonin gene-related peptide (CGRP) by rat arterial endothelial cells. *Histol Histopathol*, *16*, 1073-1079.

Donnerer, J., & Stein, C. (1992). Evidence for an increase in the release of CGRP from sensory nerves during inflammation. *Ann N Y Acad Sci*, *657*, 505-506.

Doods, H., Hallermayer, G., Wu, D., Entzeroth, M., Rudolf, K., Engel, W., & Eberlein, W. (2000). Pharmacological profile of BIBN4096BS, the first selective small molecule CGRP antagonist. *British Journal of Pharmacology*, *129*(3), 420-423.

Dora, K. A., Borysova, L., Ye, X., Powell, C., Beleznai, T. Z., Stanley, C. P., Bruno, V. D., Starborg, T., Johnson, E., Pielach, A., Taggart, M., Smart, N., & Ascione, R. (2022a). Human coronary microvascular contractile dysfunction associates with viable synthetic smooth muscle cells. *Cardiovasc Res*, *118*(8), 1978-1992.

Dora, K. A., Doyle, M. P., & Duling, B. R. (1997). Elevation of intracellular calcium in smooth muscle causes endothelial cell generation of NO in arterioles. *Proceedings of the National Academy of Sciences of the United States of America*, *94*(12), 6529-6534.

Dora, K. A., Lin, J., Borysova, L., Beleznai, T., Taggart, M., Ascione, R., & Garland, C. (2022b). Signaling and structures underpinning conducted vasodilation in human and porcine intramyocardial coronary arteries. *Front Cardiovasc Med*, *9*, 980628.

Drissi, H., Lasmoles, F., Le Mellay, V., Marie, P. J., & Lieberherr, M. (1998). Activation of phospholipase C-beta1 via Galphaq/11 during calcium mobilization by calcitonin gene-related peptideG. *The Journal of Biological Chemistry*, *273*(32), 20168-20174.

Duling, B. R., Gore, R. W., Dacey, J. R. G., & Damon, D. N. (1981). Methods for isolation, cannulation, and in vitro study of single microvessels. *The American Journal of Physiology*, *241*(1), 108-116.

Duncker, D. J., & Verdouw, P. D. (2000). Role of K+(ATP) channels in ischemic preconditioning and cardioprotection. *Cardiovascular Drugs and Therapy*, *14*(1), 7-16.

Eberhardt, M., Dux, M., Namer, B., Miljkovic, J., Cordasic, N., Will, C., Kichko, T. I., de la Roche, J., Fischer, M., Suarez, S. A., Bikiel, D., Dorsch, K., Leffler, A., Babes, A., Lampert, A., Lennerz, J. K., Jacobi, J., Marti, M. A., Doctorovich, F., . . . Filipovic, M. R. (2014). H2S and NO cooperatively regulate vascular tone by activating a neuroendocrine HNO-TRPA1-CGRP signalling pathway. *Nat Commun*, *5*, 4381.

Edvinsson, L., Alm, R., Shaw, D., Rutledge, R., Koblan, K., Longmore, J., & Kane, S. (2002a). Effect of the CGRP receptor antagonist BIBN4096BS in human cerebral, coronary and omental arteries and in SK-N-MC cells. *European Journal of Pharmacology*, *434*, 49-53.

Edvinsson, L., Alm, R., Shaw, D., Rutledge, R. Z., Koblan, K. S., Longmore, J., & Kane, S. A. (2002b). Effect of the CGRP receptor antagonist BIBN4096BS in human

cerebral, coronary and omental arteries and in SK-N-MC cells. *European Journal of Pharmacology*, *434*(1-2), 49-53.

Edvinsson, L., Fredholm, B. B., Hamel, E., Jansen, I., & Verrecchia, C. (1985). Perivascular peptides relax cerebral arteries concomitant with stimulation of cyclic adenosine monophosphate accumulation or release of an endothelium-derived relaxing factor in the cat. *Neuroscience Letters*, *58*, 213-217.

Edvinsson, L., Nilsson, E., & Jansen-Olesen, I. (2007). Inhibitory effect of BIBN4096BS, CGRP(8-37), a CGRP antibody and an RNA-Spiegelmer on CGRP induced vasodilatation in the perfused and non-perfused rat middle cerebral artery. *Br J Pharmacol*, *150*(5), 633-640.

Edwards, G., Dora, K. A., Gardener, M. J., Garland, C. J., & Weston, A. H. (1998). K^+ is an endothelium-derived hyperpolarizing factor in rat arteries. *Letters to Nature*, *396*, 269-272.

Emerson, G. G., & Segal, S. S. (2000). Electrical coupling between endothelial cells and smooth muscle cells in hamster feed arteries. *Circ Res*, *87*, 474-479.

Erdling, A., Sheykhzade, M., & Edvinsson, L. (2017). Differential inhibitory response to telcagepant on alphaCGRP induced vasorelaxation and intracellular Ca(2+) levels in the perfused and non-perfused isolated rat middle cerebral artery. *J Headache Pain*, *18*(1), 61.

Evans, B. N., Rosenblatt, M. I., Mnayer, L. O., Oliver, K. R., & Dickerson, I. M. (2000). CGRP-RCP, a novel protein required for signal transduction at calcitonin gene-related peptide and adrenomedullin receptors. *J Biol Chem*, *275*(40), 31438-31443.

Favaloro, J. L., & Kemp-Harper, B. K. (2007). The nitroxyl anion (HNO) is a potent dilator of rat coronary vasculature. *Cardiovasc Res*, *73*(3), 587-596.

Favoni, V., Giani, L., Al-Hassany, L., Asioli, G. M., Butera, C., de Boer, I., Guglielmetti, M., Koniari, C., Mavridis, T., Vaikjarv, M., Verhagen, I., Verzina, A., Zick, B., Martelletti, P., Sacco, S., & European Headache Federation School of Advanced, S. (2019). CGRP and migraine from a cardiovascular point of view: what do we expect from blocking CGRP? *J Headache Pain*, *20*(1), 27.

Fisher, L. A., Kikkawa, D. O., Rivier, J., Amara, S., Evans, R. M., Rosenfeld, M., Vale, W. W., & Brown, M. R. (1983). Stimulation of noradrenergic sympathetic outflow by calcitonin gene-related peptide. *Letters to Nature*, *305*, 534-536.

Fleming, I., Bauersachs, J., & Busse, R. (1997). Calcium-dependent and calcium-independent activation of endothelial NO synthase. *J Vasc Res*, *34*, 165-174.

Fosmo, A. L., & Skraastad, O. B. (2017). The Kv7 Channel and Cardiovascular Risk Factors. *Front Cardiovasc Med*, *4*, 75.

Foulkes, R., Shaw, N., Bose, C., & Hughes, B. (1991). Differential vasodilator profile of calcitonin-gene related peptide in porcine large and small diameter coronary artery rings. *European Journal of Pharmacology*, *201*, 143-149.

Franco-Cereceda, A., Gennari, C., Nami, R., Agnusdei, D., Pernow, J., Lundberg, J., & Fischer, J. (1987a). Cardiovascular Effects of Calcitonin Gene-Related Peptides I and II in Man. *Circulation Research*, *60*(3), 393-397.

Franco-Cereceda, A., Rudehill, A., & Lundberg, J. (1987b). Calcitonin gene-relatedpeptide but not substanceP mimics capsaicin-induced coronary vasodilation in the pig. *European Journal of Pharmacology*, *142*, 235-243.

Franco-Cereceda, A., Saria, A., & Lundberg, J. M. (1989). Differential release of calcitonin gene-related peptide and neuropeptide Y from the isolated heart by capsaicin, ischaemia, nicotine, bradykinin and ouabain. *Acta Physiologica Scandinavica*, *135*(2), 173-187.

Fujioka, S., Sasakawa, O., Kishimoto, H., Tsumara, K., & Morii, H. (1991). The antihypertensive effect of calcitonin gene-related peptide in rats with norepinephrine- and angiotensin II-induced hypertension. *Journal of Hypertension*, *9*(2), 175-179.

Fulton, D., Gratton, J. P., McCabe, T. J., Fontana, J., Fujio, Y., Walsh, K., Franke, T. F., Papapetropoulos, A., & Sessa, W. C. (1999). Regulation of endothelium-derived nitric oxide production by the protein kinase Akt. *Nature*, *399*(6736), 597-601.

Furchgott, R. F., & Zawadski, J. V. (1980). The obligatory role of endothelial cells in the relaxation or arteriolar smooth muscle by acetylcholine. *Nature*, *288*, 373-376.

Gangula, P. R., Lanlua, P., Wimalawansa, S. J., Supowit, S. C., Dipette, D. J., & Yallampalli, C. (2000). Regulation of Calcitonin Gene-Related Peptide Expression in Dorsal Root Ganglia of Rats by Female Sex Steroid Hormones. *Biology of Reproduction*, *62*, 1033-1039.

Gangula, P. R., Zhao, H., Wimalawansa, S., Supowit, S., DiPette, D., & Yallampalli, C. (2001). Pregnancy and Steroid Hormones Enhance the Systemic and Regional

Hemodynamic Effects of Calcitonin Gene-Related Peptide in Rats. *Biology of Reproduction*, *64*, 1776-1783.

Gangula, P. R. R., Wimalawansa, S. J., & Yallampalli, C. (2002). Sex Steroid Hormones Enhance Hypotensive Effects of Calcitonin Gene-Related Peptide in Aged Female Rats1. *Biology of Reproduction*, *67*(6), 1881-1887.

Gangula, P. R. R., Zhao, H., Supowit, S., Wimalawansa, S., DiPette, D., & Yallampalli, C. (1999). Pregnancy and steroid hormones enhance the vasodilation responses to CGRP in rats. *American Journal of Physiology - Heart and Circulatory Physiology*, *276*(1 45-1).

Garcia, S. R., Izzard, A. S., Heagerty, A. M., & Bund, S. J. (1997). Myogenic tone in coronary arteries from spontaneously hypertensive rats. *Journal of Vascular Research*, *34*(2), 109-116.

Garland, C. J., & Dora, K. A. (2017). EDH: endothelium-dependent hyperpolarization and microvascular signalling. *Acta Physiol (Oxf)*, *219*(1), 152-161.

Garland, C. J., & McPherson, G., A. (1992). Evidence that nitric oxide does not mediate the hyperpolarization and relaxation to acetylcholine in the rat small mesenteric artery. *British Journal of Pharmacology*, *105*, 429-435.

Garland, C. J., Plane, F., Kemp, B. K., & Cocks, T. M. (1995). Endothelium-dependent hyperpolarization: a role in the control of vascular tone. *Trends in Pharmacological Sciences*, *16*, 23-30.

Garland, C. J., Yarova, P. L., Jiménez-Altayó, F., & Dora, K. A. (2011). Vascular hyperpolarization to β-adrenoceptor agonists evokes spreading dilatation in rat isolated mesenteric arteries. *British Journal of Pharmacology*, *164*(3), 913-921.

Gennari, C., Nami, R., Agnusdei, D., & Fischer, J. A. (1990). Improved cardiac performance with human calcitonin gene related peptide in patients with congestive heart failure. *Cardiovascular Research*, *24*(3), 239-241.

Geppetti, P., Del Bianco, E., Patacchini, R., Santicioli, P., Maggi, C. A., & Tramontana, M. (1991). Low pH-induced release of calcitonin gene-related peptide from capsaicin-sensitive sensory nerves: mechanism of action and biological response. *Neuroscience*, *41*(1), 295-301.

Ghosh, M., van den Akker, N. M. S., Wijnands, K. A. P., Poeze, M., Weber, C., McQuade, L. E., Pluth, M. D., Lippard, S. J., Post, M. J., Molin, D. G. M., van Zandvoort, M. A., & ? (2013). Specific visualisation of nitric oxide in the

vasculature with two-photon microscopy using a copper based fluorescent probe. *PLoS One*, *8*(9), 1-14.

Gibbins, I. L., Furness, J. B., Costa, M., MacIntyre, I., Hillyard, C. J., & Girgis, S. (1985). Co-localisation of calcitonin gene-related peptide-like immunoreactivity with substance P in cutaneous, vascular and visceral sensory neurons of guinea pigs. *Neurosci Lett*, *57*, 125-130.

Girgis, S. I., MacDonald, D. W. R., Stevenson, J. C., Bevis, P. J. R., Lynch, C., Wimalawansa, S. J., Self, C. H., Morris, H. R., & MacIntyre, I. (1985). Calcitonin-gene related peptide: potent vasodilator and major product of calcitonin gene. *The Lancet*, *2*, 14-16.

Goadsby, P. J., Charbit, A. R., Andreou, A. P., Akerman, S., & Holland, P. R. (2009). Neurobiology of migraine. *Neuroscience*, *161*(2), 327-341.

Goadsby, P. J., & Edvinsson, L. (1993). The trigeminovascular system and migraine: studies characterizing cerebrovascular and neuropeptide changes seen in humans and cats. *Ann Neurol*, *33*(1), 48-56.

Goadsby, P. J., Edvinsson, L., & Ekman, R. (1990). Vasoactive peptide release in the extracerebral circulation of humans during migraine headache. *Ann Neurol*, *28*(2), 183-187.

Godo, S., Suda, A., Takahashi, J., Yasuda, S., & Shimokawa, H. (2021). Coronary Microvascular Dysfunction. *Arterioscler Thromb Vasc Biol*, *41*(5), 1625-1637.

Golech, S. A., McCarron, R. M., Chen, Y., Bembry, J., Lenz, F., Mechoulam, R., Shohami, E., & Spatz, M. (2004). Human brain endothelium: coexpression and function of vanilloid and endocannabinoid receptors. *Brain Res Mol Brain Res*, *132*(1), 87-92.

Golpon, H. A., Puechner, A., Welte, T., Wichert, P. V., & Feddersen, C. O. (2001). Vasorelaxant effect of glucagon-like peptide-(7-36) amide and amylin on the pulmonary circulation of the rat. *Regul Pept*, *102*, 81-86.

Grace, G. C., Dusting, G. J., Kemp, B. E., & Martin, T. J. (1987). Endothelium and the vasodilator action of rat calcitonin gene-related peptide (CGRP). *Br J Pharmacol*, *91*, 729-733.

Grant, A. D., Tam, C. W., Lazar, Z., Shih, M. K., & Brain, S. D. (2004). The calcitonin gene-related peptide (CGRP) receptor antagonist BIBN4096BS blocks CGRP and adrenomedullin vasoactive responses in the microvasculature. *British Journal of Pharmacology*, *142*(7), 1091-1098.

Graves, J. E., Greenwood, I. A., & Large, W. A. (2000). Tonic regulation of vascular tone by nitric oxide and chloride ions in rat isolated small coronary arteries. *American Journal of Physiology - Heart and Circulatory Physiology*, *279*(6), 2604-2611.

Gray, D. W., & Marshall, I. (1992a). Human α-calcitonin gene-related peptide stimulates adenylate cyclase and guanylate cyclase and relaxes rat thoracic aorta by releasing nitric oxide. *British Journal of Pharmacology*, *107*(3), 691-696.

Gray, D. W., & Marshall, I. (1992b). Nitric oxide synthesis inhibitors attenuate calcitonin gene-related peptide endothelium-dependent vasorelaxation in rat aorta. *European Journal of Pharmacology*, *212*(1), 37-42.

Gulbenkian, S., Edvinsson, L., Saetrum Opgaard, O., Wharton, J., Polak, J. M., & David-Ferreira, J. F. (1990). Peptide-containing nerve fibres in guinea-pig coronary arteries: immunohistochemistry, ultrastructure and vasomotility. *Journal of the Autonomic Nervous System*, *31*, 153-168.

Gulbenkian, S., Saetrum Opgaard, O., Ekman, R., Costa Andrade, N., Wharton, J., Polak, J. M., Queiroz E Melo, J., & Edvinsson, L. (1993). Peptidergic innervation of human epicardial coronary arteries. *Circulation Research*, *73*(3), 579-588.

Gupta, S., Mehrotra, S., Villalon, C. M., Garrelds, I. M., de Vries, R., van Kats, J. P., Sharma, H. S., Saxena, P. R., & Maassenvandenbrink, A. (2006). Characterisation of CGRP receptors in human and porcine isolated coronary arteries: evidence for CGRP receptor heterogeneity. *Eur J Pharmacol*, *530*(1-2), 107-116.

Gutterman, D. D. (1999). Adventitia-dependent influences on vascular function. *Heart and Circulatory Physiology*, *277*(4), 1265-1272.

Haegerstrand, A., Dalsgaard, C.-J., Jonzon, B., Larsson, O., & Nilsson, J. (1990). Calcitonin gene-related peptide stimulates proliferation of human endothelial cells. *Neurobiology*, *87*, 3299-3303.

Hagner, S., Haberberger, R., Kummer, W., Springer, J., Fischer, A., Bohm, S., Goke, B., & McGregor, G. P. (2001). Immunohistochemical detection of calcitonin gene-related peptide receptor (CGRPR)-1 in the endothelium of human coronary artery and bronchial blood vessels. *Neuropeptides*, *35*(1), 58-64.

Han, S. P., Naes, L., & Westfall, T. C. (1990). Calcitonin gene-related peptide is the endogenous mediator of nonadrenergic-noncholinergic vasodilation in rat mesentery. *Journal of Pharmacology and Experimental Therapeutics*, *255*(2), 423-428.

Hansted, A. K., Jensen, L. J., Olesen, J., & Jansen-Olesen, I. (2020). Localization of TRPA1 channels and characterization of TRPA1 mediated responses in dural and pial arteries in vivo after intracarotid infusion of Na(2)S. *Cephalalgia*, *40*(12), 1310-1320.

Hasbak, P., Eskesen, K., Lind, H., Holst, J., & Edvinsson, L. (2006). The vasorelaxant effect of adrenomedullin, proadrenomedullin N-terminal 20 peptide and amylin in human skin. *Basic Clin Pharmacol Toxicol*, *99*(2), 162-167.

Hasbak, P., Opgaard, O. S., Eskesen, K., Schifter, S., Arendrup, H., Longmore, J., & Edvinsson, L. (2003a). Investigation of CGRP receptors and peptide pharmacology in human coronary arteries. Characterization with a nonpeptide antagonist. *Journal of Pharmacology and Experimental Therapeutics*, *304*(1), 326-333.

Hasbak, P., Saetrum Opgaard, O., Eskesen, K., Schifter, S., Arendrup, H., Longmore, J., & Edvinsson, L. (2003b). Investigation of CGRP receptors and peptide pharmacology in human coronary arteries. Characterization with a nonpeptide antagonist. *J Pharmacol Exp Ther*, *304*(1), 326-333.

Hay, D. L., Chen, S., Lutz, T. A., Parkes, D. G., & Roth, J. D. (2015). Amylin: Pharmacology, Physiology, and Clinical Potential. *Pharmacol Rev*, *67*(3), 564-600.

Hay, D. L., Christopoulos, G., Christopoulos, A., Poyner, D. R., & Sexton, P. M. (2005). Pharmacological discrimination of calcitonin receptor: receptor activity-modifying protein complexes. *Mol Pharmacol*, *67*(5), 1655-1665.

Hay, D. L., Garelja, M. L., Poyner, D. R., & Walker, C. S. (2018). Update on the pharmacology of calcitonin/CGRP family of peptides: IUPHAR Review 25. *British Journal of Pharmacology*, *175*(1), 3-17.

Hay, D. L., Howitt, S. G., Conner, A. C., Doods, H., Schindler, M., & Poyner, D. R. (2002). A comparison of the actions of BIBN4096BS and CGRP8-37 on CGRP and adrenomedullin receptors expressed on SK-N-MC, L6, Col 29 and Rat 2 cells. *British Journal of Pharmacology*, *137*(1), 80-86.

Hay, D. L., Poyner, D. R., Quirion, R., & International Union of, P. (2008). International Union of Pharmacology. LXIX. Status of the calcitonin gene-related peptide subtype 2 receptor. *Pharmacol Rev*, *60*(2), 143-145.

Hong, Y., Hay, D. L., Quirion, R., & Poyner, D. R. (2012). The pharmacology of adrenomedullin 2/intermedin. *British Journal of Pharmacology*, *166*(1), 110-120.

Ignarro, L. J., Buga, G. M., Wood, K. S., Byrns, R. E., & Chaudhuri, G. (1987). Endothelium-derived relaxing factor produced and released from artery and vein is nitric oxide. *Proc Natl Acad Sci U S A*, *84*, 9265-9269.

Irvine, J. C., Favaloro, J. L., & Kemp-Harper, B. K. (2003). NO- activates soluble guanylate cyclase and Kv channels to vasodilate resistance arteries. *Hypertension*, *41*(6), 1301-1307.

Iwatani, Y., Kosugi, K., Isobe-Oku, S., Atagi, S., Kitamura, Y., & Kawasaki, H. (2008). Endothelium removal augments endothelium-independent vasodilatation in rat mesenteric vascular bed. *Br J Pharmacol*, *154*(1), 32-40.

Jansen-Olesen, I., Jorgensen, L., Engel, U., & Edvinsson, L. (2003). In-depth characterization of CGRP receptors in human intracranial arteries. *Eur J Pharmacol*, *481*(2-3), 207-216.

Jepps, T. A., Barrese, V., & Miceli, F. (2021). Editorial: Kv7 Channels: Structure, Physiology, and Pharmacology. *Front Physiol*, *12*, 679317.

Jepps, T. A., Chadha, P. S., Davis, A. J., Harhun, M. I., Cockerill, G. W., Olesen, S. P., Hansen, R. S., & Greenwood, I. A. (2011). Downregulation of Kv7.4 channel activity in primary and secondary hypertension. *Circulation*, *124*(5), 602-611.

Jones, C. J. H., Kuo, L., Davis, M. J., DeFily, D. V., & Chilian, W. M. (1995). Role of Nitric Oxide in the Coronary Microvascular Responses to Adenosine and Increased Metabolic Demand. *Circulation*, *91*(6), 1807-1813.

Kageyama, M., Yanagisawa, T., & Taira, N. (1993). Calcitonin gene-related peptide relaxes porcine coronary arteries via cyclic AMP-dependent mechanisms, but not activation of ATP-sensitive potassium channels. *Journal of Pharmacology and Experimental Therapeutics*, *265*(2), 490-497.

Kark, T., Bagi, Z., Lizanecz, E., Pasztor, E. T., Erdei, N., Czikora, A., Papp, Z., Edes, I., Porszasz, R., & Toth, A. (2008). Tissue-specific regulation of microvascular diameter: opposite functional roles of neuronal and smooth muscle located vanilloid receptor-1. *Mol Pharmacol*, *73*(5), 1405-1412.

Katayama, M., Nadel, J. A., Bunnett, N. W., Di Maria, G. U., Haxhiu, M., & Borson, D. B. (1991). Catabolism of calcitonin gene-related peptide and substance P by neutral endopeptidase. *Peptides*.

Kawasaki, H., Takasaki, K., Saito, A., & Goto, K. (1988). Calcitonin gene-related peptide acts as a novel vasodilator neurotransmitter in mesenteric resistance vessels of the rat. *Nature*, *335*, 164-167.

Kawasaki, H., Takenaga, M., Akari, H., Futagami, K., & Gomita, Y. (1998). Angiotensin Inhibits Neurotransmission of Calcitonin Gene- Related Peptide-Containing Vasodilator Nerves in Mesenteric Artery of Spontaneously Hypertensive Rats. *The Journal of Pharmacology and Experimental Therapeutics*, *284*(2), 508-515.

Kee, Z., Kodji, X., & Brain, S. D. (2018). The Role of Calcitonin Gene Related Peptide (CGRP) in Neurogenic Vasodilation and Its Cardioprotective Effects. *Front Physiol*, *9*, 1249.

Khammy, M. M., Kim, S., Bentzen, B. H., Lee, S., Choi, I., Aalkjaer, C., & Jepps, T. A. (2018). 4-Aminopyridine: a pan voltage-gated potassium channel inhibitor that enhances K(v) 7.4 currents and inhibits noradrenaline-mediated contraction of rat mesenteric small arteries. *Br J Pharmacol*, *175*(3), 501-516.

Khanamiri, S., Soltysinska, E., Jepps, T. A., Bentzen, B. H., Chadha, P. S., Schmitt, N., Greenwood, I. A., & Olesen, S. P. (2013). Contribution of Kv7 channels to basal coronary flow and active response to ischemia. *Hypertension*, *62*(6), 1090-1097.

King, C. T., Gegg, C. V., Hu, S. N., Sen Lu, H., Chan, B. M., Berry, K. A., Brankow, D. W., Boone, T. J., Kezunovic, N., Kelley, M. R., Shi, L., & Xu, C. (2019). Discovery of the Migraine Prevention Therapeutic Aimovig (Erenumab), the First FDA-Approved Antibody against a G-Protein-Coupled Receptor. *ACS Pharmacol Transl Sci*, *2*(6), 485-490.

Kita, T., & Kitamura, K. (2022). Translational studies of adrenomedullin and related peptides regarding cardiovascular diseases. *Hypertens Res*, *45*(3), 389-400.

Kitazono, T., Heistad, D. D., & Faraci, F. M. (1993). Role of ATP-sensitive K+ channels in CGRP-induced dilatation of basilar artery in vivo. *American Journal of Physiology - Heart and Circulatory Physiology*, *265*(2 34-2), 581-585.

Kraenzlin, M. E., Ch'ng, J. L. C., Mulderry, P. K., Ghatei, M. A., & Bloom, S. R. (1985). Infusion of a novel peptide, calcitonin gene-related peptide (CGRP) in man. Pharmacokinetics and effects on gastric acid secretion and on gastrointestinal hormones. *Regul Pept*, *10*, 189-197.

Krapivinsky, G., Kennedy, M. E., Nemec, J., Medina, I., Krapivinsky, L., & Clapham, D. E. (1998). Gbetagamma binding to GIRK4 subunit Is critical for G protein-gated K+? channel activation. *The Journal of Biological Chemistry*, *273*(27), 16946-16952.

Kristiansen, S. B., Sheykhzade, M., Edvinsson, L., & Haanes, K. A. (2017). Changes in vasodilation following myocardial ischemia/reperfusion in rats. *Nitric Oxide*, *70*, 68-75.

Kubota, M., Moseley, J. M., Butera, L., Dusting, G. J., MacDonald, P. S., & Martin, T. J. (1985). Calcitonin gene-related peptide stimulates cylic AMP formation in rat aortic smooth muscle cells. *Biochemical and Biophysical Research Communications*, *132*(1), 88-94.

Kumar, A., Potts, J. D., & DiPette, D. J. (2019). Protective Role of alpha-Calcitonin Gene-Related Peptide in Cardiovascular Diseases. *Front Physiol*, *10*, 821.

Labruijere, S., Compeer, M. G., van den Bogaerdt, A. J., van den Brink, A. M., De Mey, J. G. R., Danser, A. H., & Batenburg, W. W. (2013). Long-lasting physiological antagonism of calcitonin gene-related peptide towards endothelin-1 in rat mesenteric arteries and human coronary arteries. *Eur J Pharmacol*, *720*(1-3), 303-309.

Lacza, Z., Horvath, E. M., Pankotai, E., Csordas, A., Kollai, M., Szabo, C., & Busija, D. W. (2005). The novel red-fluorescent probe DAR-4M measures reactive nitrogen species rather than NO. *J Pharmacol Toxicol Methods*, *52*(3), 335-340.

Larsson, J. E., Frampton, D. J. A., & Liin, S. I. (2020). Polyunsaturated Fatty Acids as Modulators of K(V)7 Channels. *Front Physiol*, *11*, 641.

Lassen, L. H., Haderslev, P. A., Jacobsen, V. B., Iversen, H. K., Sperling, B., & Olesen, J. (2002). CGRP may play a causative role in migraine. *Cephalagia*, *22*, 54-61.

Laufer, R., & Changeux, J.-P. (1989). Calcitonin gene-related peptide and cyclic AMP stimulate phosphinositide turnover in skeletal muscle cells. *The Journal of Biological Chemistry*, *264*(5), 2683-2689.

Lawton, P. F., Lee, M. D., Saunter, C. D., Girkin, J. M., McCarron, J. G., & Wilson, C. (2019). VasoTracker, a low-cost and open source pressure myograph system for vascular physiology. *Frontiers in Physiology*, *10*(FEB), 1-17.

Le, T. L., Grell, A. S., Sheykhzade, M., Warfvinge, K., Edvinsson, L., & Sams, A. (2020). CGRP in rat mesenteric artery and vein - receptor expression, CGRP presence and potential roles. *Eur J Pharmacol*, *875*, 173033.

Lemmey, H. A. L., Garland, C. J., & Dora, K. A. (2020). Intrinsic regulation of microvascular tone by myoendothelial feedback circuits. *Curr Top Membr*, *85*, 327-355.

Li, J., Levick, S. P., DiPette, D. J., Janicki, J. S., & Supowit, S. C. (2013). Alpha-calcitonin gene-related peptide is protective against pressure overload-induced heart failure. *Regul Pept*, *185*, 20-28.

Li, J. Z., Peng, J., Xiao, L., Zhang, Y. S., Liao, M. C., Li, X. H., Hu, C. P., Deng, H. W., & Li, Y. J. (2010). Reversal of isoprenaline-induced cardiac remodeling by rutaecarpine via stimulation of calcitonin gene-related peptide production. *Can J Physiol Pharmacol*, *88*(10), 949-959.

Lim, M. H. (2007). Preparation of a copper-based fluorescent probe for nitric oxide and its use in mammalian cultured cells. *Nature Protocols*, *2*(2), 408-415.

Lipton, R. B., Croop, R., Stock, D. A., Madonia, J., Forshaw, M., Lovegren, M., Mosher, L., Coric, V., & Goadsby, P. J. (2023). Safety, tolerability, and efficacy of zavegepant 10 mg nasal spray for the acute treatment of migraine in the USA:

a phase 3, double-blind, randomised, placebo-controlled multicentre trial. *The Lancet Neurology*, *22*, 209-217.

Liu, X., Miller, M. J. S., Josh, M. S., Sadowska-Krowicka, H., Clark, D. A., & Lancaster Jr., J. R. (1998). Diffusion limited reaction of free nitric oxide with erythrocytes. *The Journal of Biological Chemistry*, *273*(30), 18709-18713.

Loesch, A., Maynard, K. I., & Burnstock, G. (1992). Calcitonin gene-related peptide- and neuropeptide Y-like immunoreactivity in endothelial cells after long-term stimulation of perivascular nerves. *Neuroscience*, *48*(3), 723-726.

Logothetis, D. E., Kurachi, Y., Galper, J., Neer, E. J., & Clapham, D. E. (1987). The Gbetagamma subunits of GTP-binding proteins activate the muscarinic K+ channel in heart. *Nature*, *325*, 321-326.

Lou, H., & Gagel, R. F. (1998). Alternative RNA processing - its role in regulating expression of calcitonin/calcitonin gene-related peptide. *Journal of Endocrinology*, *156*, 401-405.

Ludman, P. F., Maseri, A., Clark, P., & Davies, G. J. (1991). Effects of calcitonin gene-related peptide on normal and atheromatous vessels and on resistance vessels in the coronary circulation in humans *Circulation*, *84*(5).

Luksha, L., Agewall, S., & Kublickiene, K. (2009). Endothelium-derived hyperpolarizing factor in vascular physiology and cardiovascular disease. *Atherosclerosis*, *202*(2), 330-344.

Lundberg, J., Franco-Cereceda, A., Hua, X., Hökfelt, T., & Fischer, J. (1985). Co-existence of substance P and calcitonin gene-related peptide-like immunoreactivities in sensory nerves in relation to cardiovascular and bronchoconstrictor effects of capsaicin. *European Journal of Pharmacology*, *108*, 315-319.

Luo, D., Zhang, Y. W., Peng, W. J., Peng, J., Chen, Q. Q., Li, D., Deng, H. W., & Li, Y. J. (2008). Transient receptor potential vanilloid 1-mediated expression and secretion of endothelial cell-derived calcitonin gene-related peptide. *Regul Pept*, *150*(1-3), 66-72.

Lüscher, T. F., Richard, V., Tschudi, M., Yang, Z., & Boulanger, C. (1990). Endothelial control of vascular tone in large and small coronary arteries. *Journal of the American College of Cardiology*, *15*, 519-527.

MaassenVanDenBrink, A., Meijer, J., Villalon, C. M., & Ferrari, M. D. (2016). Wiping Out CGRP: Potential Cardiovascular Risks. *Trends Pharmacol Sci*, *37*(9), 779-788.

Mani, B. K., Robakowski, C., Brueggemann, L. I., Cribbs, L. L., Tripathi, A., Majetschak, M., & Byron, K. L. (2016). Kv7.5 Potassium Channel Subunits Are the Primary Targets for PKA-Dependent Enhancement of Vascular Smooth Muscle Kv7 Currents. *Mol Pharmacol*, *89*(3), 323-334.

Marshall, I., Al-Kazwini, S., Holman, J., & Craig, R. (1986). Human and rat α-CGRP but not calcitonin cause mesenteric vasodilation in rats. *European Journal of Pharmacology*, *123*, 217-222.

Matteoli, M., Haimann, C., Torri-Tarelli, F., Polak, J. M., Ceccarelli, B., & De Camilli, P. (1988). Differential effect of ci-latrotoxin on exocytosis from small synaptic vesicles and from large dense-core vesicles containing calcitonin gene-related peptide at the frog neuromuscular junction. *Proc Natl Acad Sci U S A*, *85*, 7366-7370.

McLatchie, L. M., Fraser, N. J., Main, M. J., Wise, A., Brown, J., Thompson, N., Solari, R., Lee, M. G., & Foord, S. M. (1998). RAMPS regulate the transport and ligand specificity of the calcitonin- receptor-like receptor. *Nature*, *393*(6683), 333-339.

McNeish, A. J., Sandow, S. L., Neylon, C. B., Chen, M. X., Dora, K. A., & Garland, C. J. (2006). Evidence for involvement of both IKCa and SKCa channels in hyperpolarizing responses of the rat middle cerebral artery. *Stroke*, *37*(5), 1277-1282.

McQuade, L. E., Ma, J., Lowe, G., Ghatpande, A., Gelperin, A., & Lippard, S. J. (2010). Visualization of nitric oxide production in the mouse main olfactory bulb by a cell-trappable copper(II) fluorescent probe. *Proc Natl Acad Sci U S A*, *107*(19), 8525-8530.

Mederos y Schnitzler, M., Storch, U., Meibers, S., Nurwakagari, P., Breit, A., Essin, K., Gollasch, M., & Gudermann, T. (2008). Gq-coupled receptors as mechanosensors mediating myogenic vasoconstriction. *EMBO J*, *27*(23), 3092-3103.

Meens, M., Mattheij, N. J. A., van Loenen, P. B., Spijkers, L. J. A., Lemkens, P., Nelissen, J., Compeer, M. G., Alewijnse, A. E., & De Mey, J. G. R. (2012). G-protein βγ subunits in vasorelaxing and anti-endothelinergic effects of calcitonin gene-related peptide. *British Journal of Pharmacology*, *166*(1), 297-308.

Meininger, G. A., & Davis, M. J. (1992). Cellular mechanisms involved in the vascular myogenic response. *Heart and Circulatory Physiology*, *263*(3), 647-659.

Michell, B. J., Griffiths, J. E., Mitchelhill, K. I., Rodriguez-Crespo, I., Tiganis, T., Bozinovski, S., Ortiz de Montellano, P. R., Kemp, B. E., & Pearson, R. B. (1999). The Akt kinase signals directly to endothelial nitric oxide synthase. *Current Biology*, *9*(15), 846-848.

Moller, M. N., Rios, N., Trujillo, M., Radi, R., Denicola, A., & Alvarez, B. (2019). Detection and quantification of nitric oxide-derived oxidants in biological systems. *J Biol Chem*, *294*(40), 14776-14802.

Moncada, S., & Higgs, E. A. (2006). The discovery of nitric oxide and its role in vascular biology. *Br J Pharmacol*, *147 Suppl 1*(Suppl 1), S193-201.

Moncada, S., & Vane, J. R. (1979). Pharmacology and endogenous roles of prostaglandin endoperoxides, thromboxane A_2, and prostacyclin. *Pharmacol Rev*, *30*(3), 293-331.

Moore, D. H., & Ruska, H. (1956). The fine structure of capillaries and small arteries. *J Biophysic & Biochem Cytol*, *3*(3), 457-475.

Morales-Cano, D., Moreno, L., Barreira, B., Pandolfi, R., Chamorro, V., Jimenez, R., Villamor, E., Duarte, J., Perez-Vizcaino, F., & Cogolludo, A. (2015). Kv7 channels critically determine coronary artery reactivity: left-right differences and down-regulation by hyperglycaemia. *Cardiovasc Res*, *106*(1), 98-108.

Moreira, L. M., Takawale, A., Hulsurkar, M., Menassa, D. A., Antanaviciute, A., Lahiri, S. K., Mehta, N., Evans, N., Psarros, C., Robinson, P., Sparrow, A. J., Gillis, M. A., Ashley, N., Naud, P., Barallobre-Barreiro, J., Theofilatos, K., Lee, A., Norris, M., Clarke, M. V., . . . Reilly, S. (2020). Paracrine signalling by cardiac calcitonin controls atrial fibrogenesis and arrhythmia. *Nature*, *587*(7834), 460-465.

Moreno, M. J., Abounader, R., Hérbert, E., Doods, H., & Hamel, E. (2002). Efficacy of the non-peptide CGRP antagonist BIBN4096BS in blocking CGRP-induced dilations in human and bovine cerebral arteries: potential implications in acute migraine treatment. *Neuropharmacology*, *42*, 568-576.

Mulderry, P. K., Ghatei, M. A., Spokes, R. A., Jones, P. M., Pierson, A. M., Hamid, Q. A., Kanse, S., Amara, S., Burrin, J. M., Legon, S., Polak, J. M., & Bloom, S. R. (1988). Differential expression of alpha-CGRP and beta-CGRP by primary sensory neurons and enteric autonomic neurons of the rat. *Neuroscience*, *25*(1), 195-205.

Mulvany, M. J., & Halpern, W. (1976). Contractile properties of small arterial resistance vessels in spontaneously hypertensive and normotensive rats. *Circulation Research*, *41*(1), 19-26.

Nelson, M., Huang, Y., Brayden, J., Hescheler, J., & Standen, N. (1990a). Arterial dilations in response to calcitonin gene-related peptide

involve activation of K + channels. *Nature*, *344*, 770-773.

Nelson, M. T., Huang, Y., Brayden, J. E., Hescheler, J., & Standent, N. B. (1990b). Arterial dilations in response to calcitonin gene-related peptide involve activation of K+ channels. *344*(APRIL).

Nightingale, T., & Cutler, D. (2013). The secretion of von Willebrand factor from endothelial cells; an increasingly complicated story. *J Thromb Haemost*, *11 Suppl 1*(Suppl 1), 192-201.

Nishikawa, Y., & Ogawa, S. (1997). Importance of nitric oxide in the coronary artery at rest and during pacing in humans. *Journal of the American College of Cardiology*, *29*(1), 85-92.

Norton, C. E., Boerman, E. M., & Segal, S. S. (2021). Differential hyperpolarization to substance P and calcitonin gene-related peptide in smooth muscle versus endothelium of mouse mesenteric artery. *Microcirculation*, *28*(8), e12733.

Norton, C. E., & Segal, S. S. (2018). Calcitonin gene-related peptide hyperpolarizes mouse pulmonary artery endothelial tubes through KATP channel activation. *American Journal of Physiology - Lung Cellular and Molecular Physiology*, *315*(2), L212-L226.

Ozaka, T., Doi, Y., Kayashima, K., & Fujimoto, S. (1997). Weibel-palade bodies as a storage site of calcitonin gene-related peptide and endothelin-1 in blood vessels of the rat carotid body. *The Anatomical Record*, *247*, 388-394.

Padilla, B. E., Cottrell, G. S., Roosterman, D., Pikios, S., Muller, L., Steinhoff, M., & Bunnett, N. W. (2007). Endothelin-converting enzyme-1 regulates endosomal sorting of calcitonin receptor-like receptor and beta-arrestins. *J Cell Biol*, *179*(5), 981-997.

Parsons, S. J. W., Hill, A., Waldron, G. J., Plane, F., & Garland, C. (1994). The relative importance of nitric oxide and nitric-oxide independent mechanisms in acetylcholine-evoked dilation of the rat mesenteric bed. *Br J Pharmacol*, *113*, 1275-1280.

Peng, J., Lu, R., Ye, F., Deng, H. W., & Li, Y. J. (2001). Induction of alpha-calcitonin gene-related peptide mRNA expression in rat dorsal root ganglia by heat stress involves the heme oxygenase-1/carbon monoxide pathway. *Neuropeptides*, *35*(5-6), 297-302.

Perera, D., Berry, C., Hoole, S. P., Sinha, A., Rahman, H., Morris, P. D., Kharbanda, R. K., Petraco, R., Channon, K., & Group, U. K. C. M. D. W. (2022). Invasive coronary physiology in patients with angina and non-obstructive coronary artery disease: a consensus document from the coronary microvascular dysfunction workstream of the British Heart Foundation/National Institute for Health Research Partnership. *Heart*, *109*(2), 88-95.

Phan, T. X., Ton, H. T., Gulyas, H., Porszasz, R., Toth, A., Russo, R., Kay, M. W., Sahibzada, N., & Ahern, G. P. (2020). TRPV1 expressed throughout the arterial circulation regulates vasoconstriction and blood pressure. *J Physiol*, *598*(24), 5639-5659.

Phan, T. X., Ton, H. T., Gulyas, H., Porszasz, R., Toth, A., Russo, R., Kay, M. W., Sahibzada, N., & Ahern, G. P. (2022). TRPV1 in arteries enables a rapid myogenic tone. *J Physiol*, *600*(7), 1651-1666.

Pinkney, A. M. H., Lemmey, H. A. L., Dora, K. A., & Garland, C. J. (2017). Vasorelaxation to the Nitroxyl Donor Isopropylamine NONOate in Resistance Arteries Does Not Require Perivascular Calcitonin Gene-Related Peptide. *Hypertension*.

Poblete, I. M., Orliac, M. L., Briones, R., Adler-Graschinsky, E., & Huidobro-Toro, J. P. (2005). Anandamide elicits an acute release of nitric oxide through endothelial TRPV1 receptor activation in the rat arterial mesenteric bed. *J Physiol*, *568*(Pt 2), 539-551.

Potocnik, S. J., Murphy, T. V., Kotecha, N., & Hill, M. A. (2000). Effects of mibefradil and nifedipine on arteriolar myogenic responsiveness and intracellular Ca2+. *British Journal of Pharmacology*, *131*(6), 1065-1072.

Poyner, D. R. (1992). Calcitonin gene-related peptide: multiple actions, multiple receptors. *Pharmacology and Therapeutics*, *56*(1), 23-51.

Poyner, D. R., Sexton, P. M., Marshall, I., Smith, D. M., Quirion, R., Born, W., Muff, R., Fischer, J. A., & Foord, S. M. (2002). International Union of Pharmacology. XXXII. The mammalian calcitonin gene-related peptides, adrenmedullin, amylin, and calcitonin receptors. *Pharmacological Reviews*, *54*(2), 233-246.

Pries, A. R., & Reglin, B. (2017). Coronary microcirculatory pathophysiology: Can we afford it to remain a black box? *European Heart Journal*, *38*(7), 478-488.

Prieto, D., Benedito, S., & Nyborg, N. C. B. (1991). Heterogeneous involvement of endothelium in calcitonin gene-related peptide-induced relaxation in coronary arteries from rat. *British Journal of Pharmacology*, *103*(3), 1764-1768.

Pugsley, M. K., & Tabrizchi, R. (2000). The vascular system: an overview of structure and function. *Journal of Pharmacological and Toxicological Methods*, *44*, 333-340.

Qing, X., Svaren, J., & Keith, I. M. (2001). mRNA expression of novel CGRP1 receptors and their activity-modifying proteins in hypoxic rat lung. *Am J Physiol Lung Cell Mol Physiol*, *280*, 547-554.

Quallo, T., Gentry, C., Bevan, S., Broad, L. M., & Mogg, A. J. (2015). Activation of transient receptor potential ankyrin 1 induces CGRP release from spinal cord synaptosomes. *Pharmacol Res Perspect*, *3*(6), e00191.

Rees, T. A., Hendrikse, E. R., Hay, D. L., & Walker, C. S. (2022). Beyond CGRP: The calcitonin peptide family as targets for migraine and pain. *Br J Pharmacol*, *179*(3), 381-399.

Reis, S. E., Holubkov, R., Smith, A. J. C., Kelsey, S. F., Sharaf, B. L., Reichek, N., Rogers, W. J., Merz, C. N. B., Sopko, G., & Pepine, C. J. (2001). Coronary microvascular dysfunction is highly prevalent in women with chest pain in the absence of coronary artery disease: Results from the NHLBI WISE study. *American Heart Journal*, *141*(5), 735-741.

Reuveny, E., Siesinger, P. A., Inglese, J., Morales, J. M., Iñiguez-Lluhl, J. A., Lefkowitz, R. J., Bourne, H. R., Jan, Y. N., & Jan, L. Y. (1994). Activation of the cloned muscarinic potassium channel by G protein betagamma subunits. *Letters to Nature*, *370*, 143-146.

Rosenfeld, M., Mermod, J., Amara, S., Swanson, L. W., Sawchenko, P. E., Rivier, J., Vale, W. W., & Evans, R. M. (1983). Production of a novel neuropeptide encoded by the calcitonin gene via tissue-specific processing. *Nature*, *304*, 129-135.

Russell, F. A., King, R., Smillie, S. J., Kodji, X., & Brain, S. D. (2014). Calcitonin gene-related peptide: physiology and pathophysiology. *Physiol Rev*, *94*(4), 1099-1142.

Sakai, K., & Saito, K. (1998). Reciprocal interactions among neuropeptides and adenosine in the cardiovascular system of rats: A role of K(ATP) channels. *European Journal of Pharmacology*, *345*(3), 279-284.

Sams, A., Knyihár-Csillik, E., Engberg, J., Szok, D., Tajti, J., Bodi, I., Edvinsson, L., Vécsei, L., & Jansen-Olesen, I. (2000). CGRP and adrenomedullin receptor

populations in human cerebral arteries: in vitro pharmacological and molecular investigations in different artery sizes. *European Journal of Pharmacology*, *408*, 183-193.

Sams-Nielsen, A., Orskov, C., & Jansen-Olesen, I. (2001). Pharmacological evidence for CGRP uptake into perivascular capsaicin sensitive nerve terminals. *British Journal of Pharmacology*, *132*.

Sand, C. A., Grant, A. D., & Nandi, M. (2015). Vascular Expression of Transient Receptor Potential Vanilloid 1 (TRPV1). *J Histochem Cytochem*, *63*(6), 449-453.

Sandow, S. L., & Hill, C. E. (2000). Incidence of myoendothelial gap junctions in the proximal and distal mesenteric arteries of the rat is suggestive of a role in endothelium-derived hyperpolarizing factor-mediated responses. *Circ Res*, *86*, 341-346.

Sara, J. D., Widmer, R. J., Matsuzawa, Y., Lennon, R. J., Lerman, L. O., & Lerman, A. (2015). Prevalence of Coronary Microvascular Dysfunction Among Patients With Chest Pain and Nonobstructive Coronary Artery Disease. *JACC: Cardiovascular Interventions*, *8*(11), 1445-1453.

Scotland, R. S., Chauhan, S., Davis, C., De Felipe, C., Hunt, S., Kabir, J., Kotsonis, P., Oh, U., & Ahluwalia, A. (2004). Vanilloid receptor TRPV1, sensory C-fibers, and vascular autoregulation: a novel mechanism involved in myogenic constriction. *Circ Res*, *95*(10), 1027-1034.

Segal, S. S., & Duling, B. R. (1986). Flow control among microvessels coordinated by intercellular conduction. *Science*, *234*(4778), 868-870.

Sekiguchi, N., Kanatsuka, H., Sato, K., & Wang, Y. (2019). Effect of Calcitonin Gene-Related Peptide on Coronary Microvessels and Its Role in Acute Myocardial Ischemia. 366-374.

Sekiguchi, N., Kanatsuka, H., Sato, K., Wang, Y., Akai, K., Komaru, T., & Takishima, T. (1994). Effect of calcitonin gene-related peptide on coronary microvessels and its role in acute myocardial ischaemia. *Circulation*, *89*, 366-374.

Sharif-Naeini, R., Dedman, A., Folgering, J. H. A., Duprat, F., Patel, A., Nilius, B., & Honoré, E. (2008). TRP channels and mechanosensory transduction: Insights into the arterial myogenic response. In (Vol. 456, pp. 529-540).

Sheykhzade, M., Amandi, N., Pla, M. V., Abdolalizadeh, B., Sams, A., Warfvinge, K., Edvinsson, L., & Pickering, D. S. (2017). Binding and functional pharmacological characteristics of gepant-type antagonists in rat brain and mesenteric arteries. *Vascul Pharmacol*, *90*, 36-43.

Sheykhzade, M., & Berg Nyborg, N. (1998). Caliber dependent calcitonin gene-related peptide-induced relaxation in rat coronary arteries: effect of K+ on the tachyphylaxis. *Eur J Pharmacol*, *351*, 53-59.

Sheykhzade, M., & Berg Nyborg, N. C. (2001). Mechanism of CGRP-induced relaxation in rat intramural coronary arteries. *British Journal of Pharmacology*, *132*(6), 1235-1246.

Sheykhzade, M., Lind, H., & Edvinsson, L. (2004). Noncompetitive antagonism of BIBN4096BS on CGRP-induced responses in human subcutaneous arteries. *Br J Pharmacol*, *143*(8), 1066-1073.

Sheykhzade, M., & Nyborg, N. C. (1998). Characterization of calcitonin gene-related peptide (CGRP) receptors in intramural coronary arteries from male and female Sprague Dawley rats. *Br J Pharmacol*, *123*(7), 1464-1470

.

Shimokawa, H., Flavahan, N. A., Lorenz, R. R., & Vanhoutte, P. M. (1988). Prostacylcin releases endothelium-derived relaxing factor and potentiates its actions in coronary arteries of the pig. *Br J Pharmacol*, *95*, 1197-1203.

Shimokawa, H., Yasutake, H., Fujii, K., Owada, M., Nakaike, R., Fukumoto, Y., Takayanagi, T., Nagao, T., Egashira, K., Fujishima, M., & Takeshita, A. (1996). The importance of the hyperpolarizing mechanism increases as the vessel size decreases in endothelium-dependent relaxations in rat mesenteric circulation. *Journal of Cardiovascular Pharmacology*, *28*(5), 703-711.

Shoji, T., Ishihara, H., Ishikawa, T., Saito, A., & Goto, K. (1987). Vasodilating effects of human and rat calcitonin gene-related peptides in isolated porcine coronary arteries. *Naunyn-Schmiedeberg's Archives of Pharmacology*, *336*, 438-444.

Sigrist, S., Franco-Cereceda, A., Muff, R., Henke, H., Lundberg, J., & Fischer, J. (1986). Specific receptor and cardiovascular effects of calcitonin gene-related peptide. *Endocrinology*, *119*(1), 381-389.

Smiljic, S. (2017). The clinical significance of endocardial endothelial dysfunction. *Medicina (Kaunas)*, *53*(5), 295-302.

Smrcka, A. V. (2008). G protein betagamma subunits: central mediators of G protein-coupled receptor signaling. *Cell Mol Life Sci*, *65*(14), 2191-2214.

Sohn, I., Sheykhzade, M., Edvinsson, L., & Sams, A. (2020). The effects of CGRP in vascular tissue - Classical vasodilation, shadowed effects and systemic dilemmas. *Eur J Pharmacol*, *881*, 173205.

Soldovieri, M. V., Miceli, F., & Taglialatela, M. (2011). Driving with no brakes: molecular pathophysiology of Kv7 potassium channels. *Physiology (Bethesda)*, *26*(5), 365-376.

Steiner, T. J., Scher, A. I., Stewart, W. F., Kolodner, K., Liberman, J., & Lipton, R. B. (2003). The prevalence and disability burden of adult migraine in England and their relationships to age, gender and ethnicity. *Cephalagia*, *23*, 519-527.

Storkebaum, E., & Carmeliet, P. (2011). Paracrine control of vascular innervation in health and disease. *Acta Physiol (Oxf)*, *203*(1), 61-86.

Stott, J. B., Barrese, V., & Greenwood, I. A. (2016). Kv7 Channel Activation Underpins EPAC-Dependent Relaxations of Rat Arteries. *Arterioscler Thromb Vasc Biol*, *36*(12), 2404-2411.

Stott, J. B., Barrese, V., Jepps, T. A., Leighton, E. V., & Greenwood, I. A. (2015a). Contribution of Kv7 channels to natriuretic peptide mediated vasodilation in normal and hypertensive rats. *Hypertension*, *65*(3), 676-682.

Stott, J. B., Barrese, V., Suresh, M., Masoodi, S., & Greenwood, I. A. (2018). Investigating the Role of G Protein betagamma in Kv7-Dependent Relaxations of the Rat Vasculature. *Arterioscler Thromb Vasc Biol*, *38*(9), 2091-2102.

Stott, J. B., Povstyan, O. V., Carr, G., Barrese, V., & Greenwood, I. A. (2015b). G-protein betagamma subunits are positive regulators of Kv7.4 and native vascular Kv7 channel activity. *Proc Natl Acad Sci U S A*, *112*(20), 6497-6502.

Straub, A. C., Zeigler, A. C., & Isakson, B. E. (2014). The myoendthelial junction: connections that deliver the message. *Physiology (Bethesda)*, *29*(4), 242-249.

Supowit, S. C., Zhao, H., & DiPette, D. J. (2001). Nerve growth factor enhances calcitonin gene-related peptide expression in the spontaneously hypertensive rat. *Hypertension*, *37*, 728-732.

Szabados, T., Gomori, K., Palvolgyi, L., Gorbe, A., Baczko, I., Helyes, Z., Jancso, G., Ferdinandy, P., & Bencsik, P. (2020). Capsaicin-Sensitive Sensory Nerves and

the TRPV1 Ion Channel in Cardiac Physiology and Pathologies. *Int J Mol Sci*, *21*(12).

Szallasi, A., Cruz, F., & Geppetti, P. (2006). TRPV1: a therapeutic target for novel analgesic drugs? *Trends Mol Med*, *12*(11), 545-554.

Szekeres, M., Nádasy, G. L., Kaley, G., & Koller, A. (2004). Nitric oxide and prostaglandins modulate pressure-induced myogenic responses of intramural coronary arteries. *Journal of Cardiovascular Pharmacology*, *43*(2), 242-249.

Takeda, S., Komaru, T., Takahashi, K., Sato, K., Kanatsuka, H., Kokusho, Y., Shirato, K., Shimokawa, H., Komaru, T., Takahashi, K., Sato, K., Kanatsuka, H., Kokusho, Y., & Shimokawa, H. (2019). Beating myocardium counteracts myogenic tone of coronary microvessels : involvement of ATP-sensitive potassium channels. 3050-3057.

Tamburini, P. P., Koehn, J. A., Gilligan, J. P., Palmesino, R. A., Sharif, R., McMartin, C., Erion, M. D., & Miller, M. J. (1989). Rat vascular tissue contains a neutral endopeptidase capable of degrading atrial natriuretic peptide. *Journal of Pharmacology and Experimental Therapeutics*, *251*(3), 956-961.

Toth, A., Czikora, A., Pasztor, E. T., Dienes, B., Bai, P., Csernoch, L., Rutkai, I., Csato, V., Manyine, I. S., Porszasz, R., Edes, I., Papp, Z., & Boczan, J. (2014). Vanilloid receptor-1 (TRPV1) expression and function in the vasculature of the rat. *J Histochem Cytochem*, *62*(2), 129-144.

Uddman, R., Edvinsson, L., Ekblad, E., Håkanson, R., & Sundler, F. (1986). Calcitonin gene-related peptide (CGRP): perivascular distrubution and vasodilatory effects. *Regul Pept*, *15*, 1-23.

Uddman, R., Edvinsson, L., Ekman, R., Kingman, T., & McCulloch, J. (1985). Innervation of the feline cerebral vasculature by nerve fibers containing calcitonin

gene-related peptide: trigeminal origin and co-existance with substance P. *Neurosci Lett*, *62*, 131-136.

Urakami-Harasawa, L., Shimokawa, H., Nakashima, M., Egashira, K., & Takeshita, A. (1997). Important of endothelium-derived hyperpolarizing factor in human arteries. *J Clin Invest*, *100*(11), 2793-2799.

van der Horst, J., Greenwood, I. A., & Jepps, T. A. (2020). Cyclic AMP-Dependent Regulation of Kv7 Voltage-Gated Potassium Channels. *Front Physiol*, *11*, 727.

Varela-Lopez, E., Del Valle-Mondragon, L., Castrejon-Tellez, V., Perez-Torres, I., Arenas, A. P., Rojas, F. M., Guarner-Lans, V., Vargas-Gonzalez, A., Pastelin-Hernandez, G., & Torres-Narvaez, J. C. (2021). Role of the Transient Receptor Potential Vanilloid Type 1 (TRPV1) in the Regulation of Nitric Oxide Release in Wistar Rat Aorta. *Oxid Med Cell Longev*, *2021*, 8531975.

Waldron, G. J., & Garland, C. J. (1994a). Contribution of both nitric oxide and a change in membrane potential in acetylcholine-induced relaxation in the rat small mesenteric artery. *Br J Pharmacol*, *1994*(112), 831-836.

Waldron, G. J., & Garland, C. J. (1994b). Effect of potassium channel blockers on L-NAME insensitive relaxations in rat small mesenteric artery. *Can J Physiol Pharmacol*, *72*(11).

Walker, C. S., Conner, A. C., Poyner, D. R., & Hay, D. L. (2010). Regulation of signal transduction by calcitonin gene-related peptide receptors. *Trends Pharmacol Sci*, *31*(10), 476-483.

Wallis, L., Donovan, L., Johnston, A., Phillips, L. C., Lin, J., Garland, C. J., & Dora, K. A. (2023). Tracking endothelium-dependent NO release in pressurized arteries. *Front Physiol*, *14*, 1108943.

Wang, H., Pan, Z., Shi, W., Brown, B. S., Wymore, R. S., Cohen, I. S., Dixon, J. E., & McKinnon, D. (1998). KCNQ2 and KCNQ3 potassium channel subunits: molecular correlates of the M-channel. *Science*, *282*, 1890-1893.

Wellman, G. C., Quayle, J. M., & Standen, N. B. (1998). ATP-sensitive K+ channel activation by CGRP and PKA in pig coronary arterial smooth muscle. *Journal of Physiology*, *501*(1), 117-129.

Welsh, D. G., Morielli, A. D., Nelson, M. T., & Brayden, J. E. (2002). Transient receptor potential channels regulate myogenic tone of resistance arteries. *Circ Res*, *90*(3), 248-250.

Wharton, J., Gulbenkian, S., Merighi, A., Kuhn, D. M., Jahn, R., Taylor, K. M., & Polak, J. M. (1988). Immunohistochemical and ultrastructural localisation of peptide-containing nerves and myocardial cells in the human atrial appendage. *Cell Tissue Res*, *254*, 155-166.

Wharton, J., Gulbenkian, S., Mulderry, P. K., Ghatei, M. A., McGregor, G. P., Bloom, S. R., & Polak, J. M. (1986). Capsaicin induces a depletion of calcitonin gene-related peptide (CGRP)-immunoreactive nerves in the cardiovascular system of the guinea-pig and rat. *Journal of the Autonomic Nervous System*, *16*, 289-309.

White, R., Vanessa Ho, W.-S., Bottrill, F., Ford, W. R., & Hiley, C. R. (2001). Mechanisms of anandamide-induced vasorelaxation in rat isolated coronary arteries. *Br J Pharmacol*, *134*, 921-929.

Wolfrum, S., Nienstedt, J., Heidbreder, M., Schneider, K., Dominiak, P., & Dendorfer, A. (2005). Calcitonin gene related peptide mediates cardioprotection by remote preconditioning. *Regul Pept*, *127*(1-3), 217-224.

Woolfson, R. G., & Poston, L. (1990). Effect of N^G-monomethyl-L-arginine on endothelium-dependent relaxation of human subcutaneous resistance arteries *Clinical Science*, *79*, 273-278.

Wu, J., Ding, W. G., & Horie, M. (2016). Molecular pathogenesis of long QT syndrome type 1. *J Arrhythm*, *32*(5), 381-388.

Yallampalli, C., Kondapaka, S. B., Lanlua, P., Wimalawansa, S. J., & Gangula, P. R. R. (2004). Female Sex Steroid Hormones and Pregnancy Regulate Receptors for Calcitonin Gene-Related Peptide in Rat Mesenteric Arteries, but Not in Aorta1. *Biology of Reproduction*, *70*(4), 1055-1062.

Yamamoto, Y., Imaeda, K., & Suzuki, H. (1999). Endothelium-dependent hyperpolarization and intercellular electrical coupling in guinea-pig mesenteric arteries. *Journal of Physiology*, *514*(2), 505-513.

Yao, X., & Garland, C. J. (2005). Recent developments in vascular endothelial cell transient receptor potential channels. *Circ Res*, *97*(9), 853-863.

Ye, F., Deng, P. Y., Li, D., Luo, D., Li, N. S., Deng, S., Deng, H. W., & Li, Y. J. (2007). Involvement of endothelial cell-derived CGRP in heat stress-induced protection of endothelial function. *Vascul Pharmacol*, *46*(4), 238-246.

Yi, X., Liu, M., Luo, Q., Zhuo, H., Cao, H., Wang, J., & Han, Y. (2017). Toxic effects of dimethyl sulfoxide on red blood cells, platelets, and vascular endothelial cells in vitro. *FEBS Open Bio*, *7*(4), 485-494.

Yokomizo, A., Takatori, S., Hashikawa-Hobara, N., Goda, M., & Kawasaki, H. (2015). Characterisation of perivascular nerve distribution in rat mesenteric small arteries. *Biol Pharm Bull*, *38*(11), 1757-1764.

Yoshimoto, R., Mitsui-Saito, M., Ozaki, H., & Karaki, H. (1998). Effects of adrenomedullin and calcitonin gene-related peptide on contractions of the rat

aorta and porcine coronary artery. *British Journal of Pharmacology*, *123*(8), 1645-1654.

Zaidi, M., Bevis, P. J. R., Girgis, S., Lynch, C., Stevenson, J. C., & MacIntyre, I. (1985). Circulating CGRP comes from the perivascular nerves. *European Journal of Pharmacology*, *117*, 283-284.

Zeller, J., Poulsen, K. T., Sutton, J. E., Abdiche, Y. N., Collier, S., Chopra, R., Garcia, C. A., Pons, J., Rosenthal, A., & Shelton, D. L. (2008). CGRP function-blocking antibodies inhibit neurogenic vasodilatation without affecting heart rate or arterial blood pressure in the rat. *Br J Pharmacol*, *155*(7), 1093-1103.

Zhang, H., Craciun, L. C., Mirshahi, T., Rohács, T., Lopes, C. M. B., Jin, T., & Logothetis, D. E. (2003). PIP_2 activates KCNQ channels, and its hydrolysis underlies receptor-mediated inhibition of M currents. *Neuron*, *37*, 963-975.

Zou, Y., Akazawa, H., Qin, Y., Sano, M., Takano, H., Minamino, T., Makita, N., Iwanaga, K., Zhu, W., Kudoh, S., Toko, H., Tamura, K., Kihara, M., Nagai, T., Fukamizu, A., Umemura, S., Iiri, T., Fujita, T., & Komuro, I. (2004). Mechanical stress activates angiotensin II type 1 receptor without the involvement of angiotensin II. *Nat Cell Biol*, *6*(6), 499-506.

Zygmunt, P. M., Petersson, J., Andersson, D. A., Chuang, H., Sørgård, M., Di Marzo, V., Julius, D., & Högestätt, E. D. (1999). Vanilloid receptors on sensory nerves mediate the vasodilator action of anandamide. *Letters to Nature*, *400*, 452-457.